2014

Trypanosoma Brucei Telomere Functions in Antigenic Variation

Unnati M. Pandya
Cleveland State University

TRYPANOSOMA BRUCEI TELOMERE FUNCTIONS IN ANTIGENIC VARIATION

UNNATI M. PANDYA

Bachelor in Zoology

The Maharaja SayajiRao University

April, 2005

Master in Microbiology

The Maharaja SayajiRao University

June, 2007

Submitted in partial fulfillment of requirements for the degree

DOCTOR OF PHILOSOPHY IN REGULATORY BIOLOGY

at the

CLEVELAND STATE UNIVERSITY

May, 2014

This dissertation has been approved for the

Department of Biological, Geological, and Environmental Sciences

and

CLEVELAND STATE UNIVERSITY

College of Graduate Studies by

_____Date:_____
Dr. Bibo Li, BGES / CSU
Major Advisor

_____Date:_____
Dr. Valentin Boerner, BGES / CSU
Advisory Committee Member

_____Date:_____
Dr. Roman Kondratov, BGES / CSU
Advisory Committee Member

_____Date:_____
Dr. Alexandru Almasan,
Lerner Research Institute, Cleveland Clinic
Advisory Committee Member

_____Date:_____
Dr. Sailen Barik, BGES / CSU
Internal Examiner

_____Date:_____
Dr. Kausik Chakrabarti
Department of Chemistry, Carnegie Mellon University
External Examiner

DEDICATION

To the Almighty and my loving family.

ACKNOWLEDGMENTS

I would like to express my deepest gratitude towards my advisor and my mentor Dr. Bibo Li. Her constant guidance, rigorous training and motivation have been instrumental in molding my character as a scientist. Dr. Li's passion for science and inquisitiveness has inspired and increased my love for research. I am highly indebted to her for providing me with this opportunity and guiding me. I would like to express my deepest appreciation towards Dr. Valentin Boerner whose valuable suggestions and critiques enriched my research. His intense scientific discussions will be always cherished. I am thankful to Dr. Roman Kondratov and Dr. Alexandru Almasan for their constant guidance throughout the course of my Ph.D. I would like to thank Dr. Girish Shukla for guiding me in my research and for providing me with tremendous moral support. I am very grateful to Dr. Sailen Barik and Dr. Kausik Chakrabarti for providing their valuable time and agreeing to be a part of my dissertation defense committee. Ph.D was impossible without guidance and persistent help from all the departmental faculty and staff members. Many thanks to my lab members and my great friends Dr. Xiaofeng Yang, Imaan Benmerzouga, Ranjodh Sandhu, Vishal Nanavaty, Palak Patel, and Fan Wu for their constant suggestions and discussions. I am thankful to my dear friends Sujata Jha and Sanaa Jehi who gave me their unconditional support and made this journey enjoyable for me. This thesis would have been impossible without the love and support of my family: my parents, my brother and my husband. They bestowed me with their faith and support and gave me strength to surpass difficult times. Words are not enough to thank them.

TRYPANOSOMA BRUCEI TELOMERE FUNCTIONS IN ANTIGENIC VARIATION

UNNATI M. PANDYA

ABSTRACT

Trypanosoma brucei is a protozoan parasite that causes sleeping sickness in humans and Nagana in cattle. They evade the host's immune defense by periodically switching their major surface antigen, variant surface glycoprotein (VSG), a phenomenon termed antigenic variation. Inside its mammalian host, bloodstream form (BF) *T. brucei* monoallelically expresses its major surface molecule VSG from the *VSG* Expression Sites (ESs) located at subtelomeric loci. Monoallelic *VSG* expression ensures effective antigenic variation and maximizes the efficiency of *T. brucei* pathogenesis. In the mid-gut of its insect host (tsetse), procyclic form (PF) *T. brucei* expresses procyclins as the major surface molecules and all *VSGs* are silent. After the migration to the salivary glands of the tsetse fly, *T. brucei* cells differentiate into metacyclic forms and express metacyclic VSGs (mVSGs). Therefore, *VSG* silencing is important for the normal development of *T. brucei*.

Telomeres are important for the regulation of antigenic variation**.** *Tb*RAP1 was previously identified as an intrinsic component of the *T. brucei* telomere complex and was shown to be important for ES-linked *VSG* silencing in BF cells. Our studies further established that *Tb*RAP1 is essential for cell proliferation and required for *VSG* silencing in PF cells. Apart form ES-linked *VSGs*, *Tb*RAP1 also

regulates the silencing of *mVSGs* in both BF and PF cells. The strength of *Tb*RAP1 mediated *VSG* silencing is stronger in PF cells compared to that in the BF cells. In addition, the *Tb*RAP1-mediated *VSG* silencing in PF cells involves chromatin remodeling.

*Tb*TRF, a duplex telomere DNA binding protein that interacts with *Tb*RAP1, does not affect *VSG* silencing but regulates telomere structure. *Tb*TRFH (TRF homology domain) is required for the homodimerization of *Tb*TRF as well as for interaction with *Tb*RAP1. We established several *Tb*TRFH mutants and determined the critical regions required for homodimerization of *Tb*TRF by performing yeast two-hybrid analysis.

TERRA (telomeric repeat- containing RNA) is known to play an important role in the regulation of the higher order chromatin structure at telomeres in mammalian cells. We characterized TERRA in *T. brucei* in order to determine its role in *VSG* silencing. We determined that a significant amount of TERRA is transcribed from the active ES-linked telomere. Also, *Tb*TRF and *Tb*KU80 interact with TERRA *in vivo*. Telomere proteins were found to play an important role in regulating TERRA levels. Most importantly, lower levels of TERRA led to mild de-repression of silent *VSGs* in BF form *T. brucei* cells, indicating that TERRA indeed is involved in *VSG* silencing.

Our study provides insight into various mechanisms of how telomeres contribute to antigenic variation regulation in *T. brucei,* which helps to better understand pathogenesis of *T. brucei* and to achieve its eradication.

TABLE OF CONTENTS

LIST OF TABLES

LIST OF FIGURES

CHAPTER I

INTRODUCTION

African trypanosomiasis: Cause, Clinical features, and Epidemiology

Trypanosomes are a large group of protozoan parasites belonging to the class kinetoplastida and the genus *Trypanosoma* causing diseases in man and animals. *Trypanosoma brucei* is the causative agent of Human African Trypanosomiasis (HAT), more commonly known as 'sleeping sickness'. They also cause Animal African Trypanosomiasis (AAT) or 'nagana' in cattle. *Trypanosoma brucei* is transmitted by a blood-sucking tsetse fly belonging to genus *Glossina.* HAT occurs throughout tropical and sub-tropical sub-Saharan Africa, and 60 million people are estimated to be at risk (Atouguia and Kennedy, 2000, Kennedy 2004 and Brun et al. 2010). Approximately 50 million cattle are at risk of trypanosome infection and the major cause of mortality is due to severe outbreaks leading to depressed productivity and economical set back (Shaw, 2004). HAT is widespread in an area of about 10 million km^2 in Africa (Kennedy,

2004), and it can be fatal if left untreated. The major pathogenic HAT-causing species are *Trypanosoma brucei rhodesiense* and *Trypanosoma brucei gambiense.* They cause East African disease and West African disease, respectively (Brun et al. 2010, Kennedy 2004). 97% of chronic cases of HAT are caused by *Trypanosoma brucei gambiense* and the remaining 3% that are more acute and severe are caused by *Trypanosoma brucei rhodesiense* (Simmaro et al. 2008*). T. b. congolense, T. b. vivax,* and *T. b. brucei* infect cattle, sheep, goat, horse, and donkey. *T. b. simiae* infects pigs (Holmes, 2013).

T. b. brucei that causes African Trypanosomiasis in animals is highly susceptible to lytic factors present in the human serum known as trypanosome lytic factors (TLFs). Due to this reason, animal infecting trypanosomes are non-infective in humans (Capewell et al. 2011). However, *T. b. brucei* is highly similar to *T. b. gambiense*. This property makes it suitable for laboratory research. There are two types of TLFs present in humans: (1) TLF-1 – a high-density lipoprotein particle (Rifkin, 1978) and (2) TLF-2 – a serum protein-binding complex (Raper et al. 1999 and Capewell et al. 2011). *T. b. rhodesiense* expresses serum resistance protein (SRA) encoded by the *SRA* gene. SRA binds TLF-1, making parasite resistant to lysis in humans (Capewell et al. 2011 and Kieft et al. 2012). *T. b. gambiense,* on the other hand, utilizes a different mechanism to prevent lysis. It reduces the expression of haptoglobin-haemoglobin receptor required for binding and uptake of TLF-1 by the parasite (Capewell et al. 2011 and Kieft et al. 2012).

Thousands of people died during the time span when this disease was first discovered (1896-1906) (Brun et al. 2010 and Kennedy, 2010). However, the cases declined in the following years due to strong measures, such as mass sacrifice of animals, eradication of large forested regions, and increased human surveillance for disease and treatment (Peter, 2013). Only a few cases were reported in the 1960s (Brun et al. 2010, Kennedy, 2010 and Simarro et al. 2011). Later, the number of cases grew to 300,000 in 1998 due to the decline in human case surveillance and several other factors such as war, famine and socioeconomic instability (World Health Organization, 1998). These numbers declined eventually due to better vector control and treatment. In 2009, the number of cases reported by the World Health Organization (WHO) fell below 10,000 for the first time (Simarro et al. 2011). However, many cases are unreported due to various infrastructural reasons, and hence there could still be many undetected or undiagnosed cases. There were estimated 12 undetected deaths due to HAT for every one reported in Uganda in 2005 (Odiit et al. 2005). Due to frequent travelling, 94 cases were also reported in non-endemic countries in 2010 (Simmaro et al. 2000-2010). Hence, HAT still remains a major concern in endemic as well as non-endemic countries.

(A)

(B)

Figure 1-1: Trypanosome cells and its insect vector. (A) A blood smear of a patient suffering from African trypanosomiasis. Trypanosome cells can be seen in extracellular fluid. (From Myron G Schultz, Centers for Disease Control Public Health Image Library) (B) A tsetse fly, the insect host of *T. brucei.* (From Anthony Bannister, Encyclopedia Britannica).

Symptoms, diagnosis and treatment

Blood-sucking infected tsetse flies bite humans leading to the onset of HAT. A primary lesion is a painful swelling (Chancres) appearing after 10 to 15 days of the initial bite. After the bite of a tsetse fly, trypanosome cells enter the bloodstream, lymph nodes and several other organs, such as spleen, heart, liver, eyes, and endocrine organs. This leads to the onset of heamolymphatic stage also known as stage one (Kennedy, 2004 and Kennedy, 2013). Wide ranges of symptoms are present such as headache, malaise, arthralgia, weight loss, fatigue and fever. If left untreated, patients can suffer from lymphadenopathy, cardiac failure, endocrine dysfunction, or fertility problems (Duggan and Hutchington 1996, Atouguia and Kennedy 2000, Brun et al. 2010 and Kennedy, 2010). Trypanosome cells cross the blood-brain barrier in humans and invade the brain after a few weeks of infection in the case of *T. b. rhodesiense* infection or after several months in the case of *T. b. gambinese* infection. This is the late stage of HAT known as the encephalitic stage or stage two (Kennedy, 2013). Death could occur within few weeks in the case of *T. b. rhodesiense* infection. This stage is characterized by the occurrence of meningoencephalitis, tremor, abnormal movements, and speech impairment (Blum et al. 2006). Typical symptom of this stage is alteration in the structure of sleep and reversal of the normal sleep/wake cycle. Patient suffers from insomnia during the night and uncontrollable episodes of sleep during the day; hence, the name ‘sleeping sickness’ (Buguet et al. 2005). Untreated patients will deteriorate and eventually die.

Treatment of HAT depends on the stage of the disease. It is, therefore, vital to establish whether the patient is suffering from an early or a late stage of infection. *T. b. rhodesiense* infections are associated with high parasitemia and can be easily detected by blood or lymph smears at the early stage (Kennedy, 2006). *T. b. gambiense* infections are harder to detect using a blood smear due to low parasitemia levels. An antibody test has been developed called the card agglutination Trypanosomiasis test (CATT) for detection of the parasite (Truc et al. 2002). PCR has also been developed to detect the disease at its early stage. However, the approach needs further development, as it cannot be utilized for routine screening in the community (Mugasa et al. 2012). The late stage disease is detected by analyzing the cerebrospinal fluid for the presence of trypanosomes and/or elevated levels of white blood cells (WHO, 1998 and Kennedy, 2008).

Treatment of HAT has been unsatisfactory so far due to the lack of oral and less toxic drugs. Current available drugs could also be ineffective at times (Fairlamb, 2003).

	First-line treatment	Second-line treatment
Early stage		
T b rhodesiense	Suramin (IV)	Pentamidine (IM)
T b gambiense	Pentamidine (IM)	Suramin (IV)
Late stage		
T b rhodesiense	Melarsoprol (IV)	None available
T b gambiense	Eflornithine (IV) plus nifurtimox (oral)	Melarsoprol (IV)

Table 1: Drugs used for treatment of human African trypanosomiasis (Kennedy, 2013). IV= intravenous, IM= intramuscular.

Pentamidine is administered through an intramuscular route as a first line treatment of *T. b. gambiense* infection (Atouguia and Kennedy, 2000, Brun et al. 2010). Life-threatening complications such as hyperglycemia, hypoglycemia, hypotension, and gastrointestinal troubles arise upon administering this drug (Atouguia and Kennedy, 2000, Kennedy, 2004, Brun et al. 2010). Intravenous Suramin is administered to first stage patients with the *T. b. rhodesiense* infection. Complications associated with the drug include renal failure, anaphylactic shock, skin lesions, bone marrow toxicity, and neuropathy (Atouguia and Kennedy, 2000, Kennedy, 2004, Brun et al. 2010). Trivalent organic arsenical Melarsoprol is the only drug available for treatment of the late stage *T. b. rhodesiense* infection. It acts on a parasite molecule called typanothione that maintains an intracellular reducing environment (Fairlamb et al. 1989). Drug resistance has been observed in Melarsoprol along with toxic side effects, such as encephalopathy, skin rashes, peripheral neuropathy, and cardiac arrhythmia (Legros et al. 1999, Kennedy, 2004, Brun et al. 2010). Eflornithine (an ornithine decarboxylase inhibitor) is administered for the late-stage treatment of *T. b. gambiense* infection (Burri and Brun 2003, Kennedy, 2008). Eflornithine has many drawbacks such as bone marrow toxicity, seizures, and gastrointestinal issues (Burri and Brun 2003, Kennedy, 2004). Hence, development of less toxic and better medication is required for ultimate elimination of this disease.

Life cycle of T. brucei

The *T. brucei* is an obligate parasite and requires a host for its survival. It is transmitted to the mammalian host via tsetse fly.

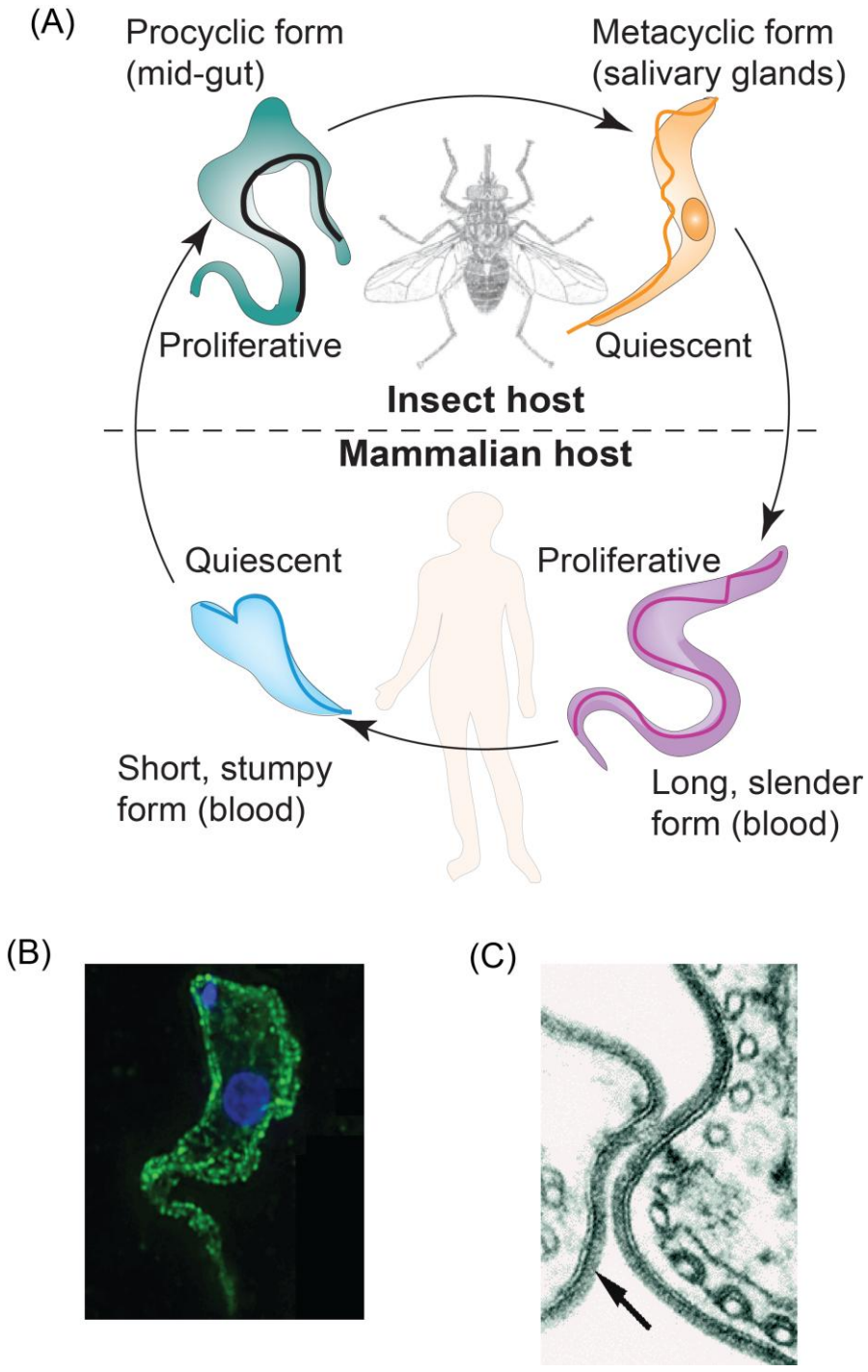

Figure 1-2: Life cycle of the *T. brucei.* (A) Schematic representation of the *T. brucei* life cycle (Dreesen et al. 2007). (B) An immunofluorescence image of a bloodstream form *T. brucei* cell stained with *VSG* specific antibody (green). DAPI staining depicts nucleus and kinetoplast. (C) High magnification electron microscope image depicting surface coat protein of *T. brucei* (black arrow) (Image was obtained from Rockefeller University Laboratory of Medical Parasitology).

Trypanosome parasites enter the mammalian host when an infected tsetse fly bites the host. In the mammalian host, the bloodstream form (BF) *T. brucei* expresses a dense layer of ~10 million surface coat protein molecules called variant surface glycoproteins (VSG) (figure 1-2). These VSGs are rod shaped molecules anchored to the membrane through a glycosylphosphatidylinositol (GPI) anchor, and they cover the entire cell surface including the flagellum (Ferguson, 1999, Schwede and Carrington, 2010). The parasite remains extracellular and survives in the bloodstream of the host by evading its immune response through periodically changing VSGs, a phenomenon termed antigenic variation (McCulloch, 2004, Pays et al. 2004). These proliferative BF *T. brucei* are morphologically slender and long; and eventually differentiated to a short and stumpy form (Matthews et al. 2004). This serves two purposes: (1) the parasitemia levels is controlled ensuring prolonged host survival and (2) the stumpy form *T. brucei* cells uniformly arrest in the G1 phase, which allows them to have coordinated morphological changes upon re-entry into the tsetse fly (Matthews, 2005).

Upon re-entry into the tsetse fly, the stumpy form metamorphoses into a more proliferative form called procyclic form (PF). At this stage all *VSG* genes are silenced (Kooter and Borst, 1984, Kooter et al. 1987) and a different but a less dense surface coat of procyclic acidic repetitive protein (PARP, also known as Procyclin) is expressed (Roditi et al. 1989, Dorn et al. 1991, pays et al. 1993). Procyclins, unlike VSGs, are resistant to tsetse fly gut proteases, allowing parasite to survive in the gut of the insect host (Gruszynski et al. 2006). PF cells

proliferate in the mid-gut of tsetse fly and eventually migrate towards the salivary glands of the fly. They attach to the fly's salivary glands by elaboration of the flagellar membrane and become quiescent. This quiescent metacyclic form *T. brucei* expresses a surface coat consisting of metacyclic VSGs (mVSGs). Metacyclic form cells remain in the lumen of the salivary gland and are transferred to a new mammalian host when the tsetse fly takes a bite of the host. After infection mVSGs are silenced in the mammalian host and BF VSGs are expressed. Expressing metacyclic VSG is important for parasite survival and proliferation after *T. brucei* cells are transferred back into the mammalian host (Vickerman, 1985).

Hence, the regulation of the expression of the life cycle stage-specific coat protein as well as the silencing of the other surface coat is crucial for *T. brucei* survival and pathogenesis. Elucidating the mechanism of this regulation is important for understanding the pathogenesis of this parasite.

Genome of T. brucei

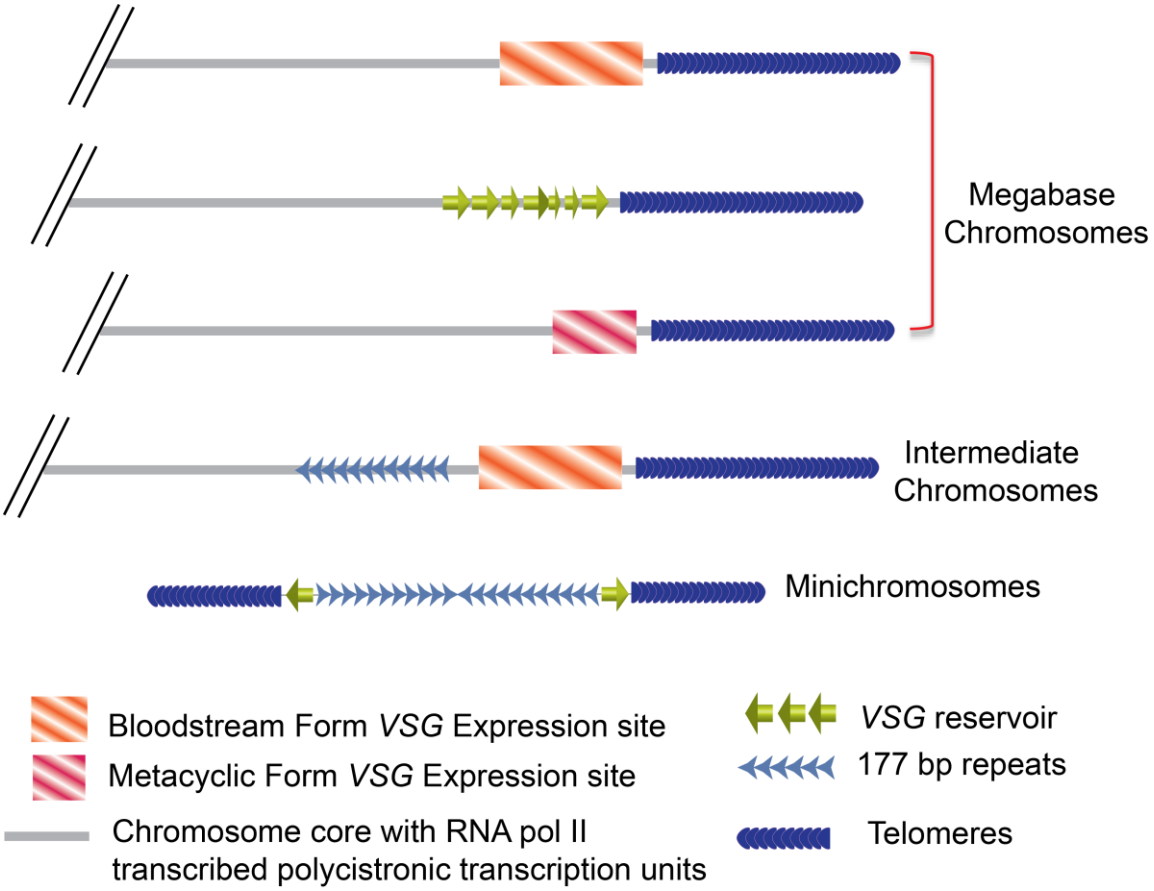

Figure 1-3: Schematic representation of chromosomes of *T. brucei*. Sequencing of intermediate chromosome is not yet complete, and hence the representation is partially hypothetical (Ersfeld, 2011).

The *T. brucei* genome consists of 11 pairs of megabase chromosomes, ~5 intermediate chromosomes, and ~100 minichromosomes (figure 1-3). Intermediate chromosomes, and minichromosomes are usually haploid. The sizes of diploid megabase chromosomes vary greatly, ranging from 5.5 Mbp (chromosome XI) to 0.9 Mbp (chromosome I) (Berriman et al. 2005, Melville et al. 1998, Melville et al. 2000). Megabase chromosomes can be divided into two large regions: (1) The chromosome internal core region consisting of housekeeping genes transcribed by RNA polymerase II and (2) the subtelomeric region consisting of *VSG* expression sites where *VSG* genes are transcribed by RNA polymerase I (Berriman et al. 2002, Hertz-Fowler et al. 2008). Heterogeneity in the size of megabase chromosomes is mostly due to the subtelomeric chromosomal regions (Callejas et al. 2006). Not every megabase chromosome and every telomere has the *VSG* expression site at the subtelomeric region, resulting in these chromosomes being partially hemizygous (Melville et al.1999).

There are approximately 9,000 predicted genes in the *T. brucei* genome (Berriman et al. 2005). ~1,500 genes among them are *VSG* genes and they are usually organized in large subtelomeric arrays (figure 1-3, megabase chromosomes) (Barry et al. 2005, Berrimen et al. 2005). Many of these genes are *VSG* pseudogenes that are used by the parasite for assembling functional mosaic genes through DNA recombination (Marcello and Barry, 2007). *T. brucei* genes lacks introns and are transcribed in polycistronic transcription units (Mair et al. 2000).

There are ~5 intermediate chromosomes ranging in size from 200 to 900 Kbp in each cell (Van der Ploeg et al. 1984a). They consist of non-repetitive DNA cores, subtelomeric 177 bp repeats, and telomeric repeats (Wickstead et al. 2004). Few of the Intermediate chromosomes can also carry subtelomeric *VSG* expression sites (Van der Ploeg et al. 1984b). Similar to the megabase chromosome, not every intermediate chromosome carries ESs at their subtelomeric loci.

The *T. brucei* genome consists of ~100 minichromosomes ranging in size from 30 to 150 kbp; this comprises approximately 10% of the nuclear DNA (Gibson and Borst, 1986, Van der Ploeg et al. 1984a). Minichromosomes consist of palindromic 177 bp repeats in the core and non-repetitive elements including *VSG* genes towards the telomeric ends (Weiden et al. 1991, Zomerdijk et al. 1992, Alsford et al. 2001, Wickstead et al. 2004). It is thought that the *VSGs* on minichromosomes are never expressed. They serve as an important *VSG* reservoir for *VSG* switching (Borst, 1986).

Surface molecules of T. brucei and their expression

T. brucei expresses different major surface coat proteins at various stages of its life cycle. In the mammalian host, it expresses the bloodstream form *VSGs.* In the mid-gut of the insect host, it expresses procyclins and all bloodstream form *VSGs* are silent. After reaching the salivary glands of the fly, it changes its surface coat and expresses metacyclic *VSGs.* All these coat proteins are expressed from different sites (some being in specialized expression sites) on chromosomes, and their expression is tightly regulated.

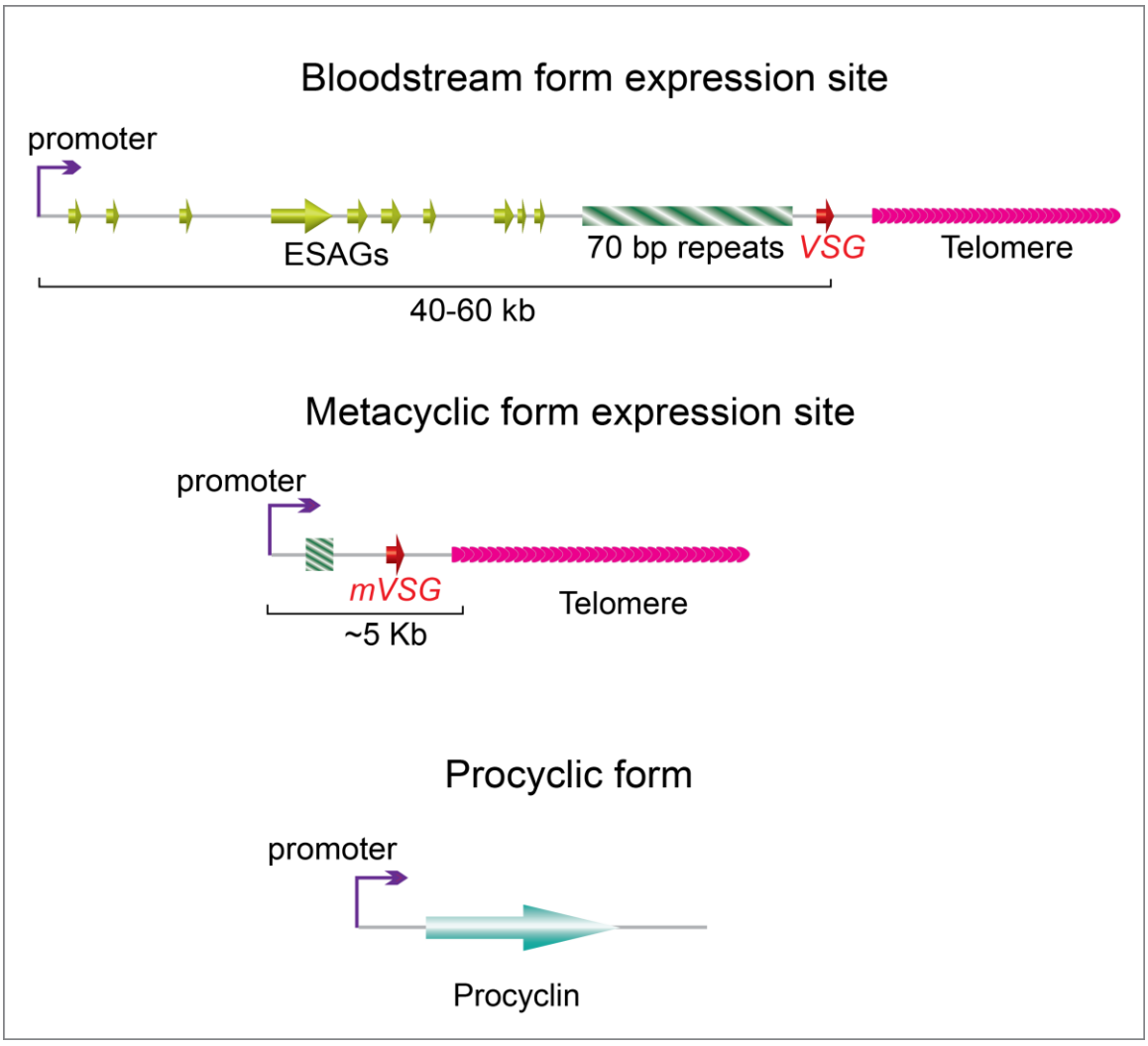

Figure 1-4: Loci of *VSGs* and procyclin expression sites in *T. brucei.*

In the bloodstream form, *VSGs* are exclusively expressed from the subtelomeric bloodstream form *VSG* expression sites (ESs) (de Lange and Borst 1982). In total there are 15 different ESs present on the megabase and intermediate chromosomes in the *T. brucei* 427 strain (Hertz-Fowler et al. 2008). Along with *VSG*, ESs also consist of other genes known as Expression Site-Associated Genes (ESAGs) (Pays et al. 2001) and a stretch of repeats with TAA-rich sequence known as 70-bp repeats. *VSG* is located at the end of the ES and next to the telomeres. These expression sites are polycistronically transcribed by RNA polymerase I, and the promoter is located 40-60 kb upstream of the *VSG* gene (Gunzl et al. 2003, Hertz-Fowler et al. 2008). Only one ES promoter is fully active, resulting in a single type of VSG being expressed and present on the surface of the trypanosome cell. The silent archives of *VSGs* are present in long tandem arrays on the megabase chromosomes or as a single gene on the minichromosomes. These *VSGs* can only be expressed after they are recombined into the active ES (Horn and Barry 2005).

When *T. brucei* cells are in the metacyclic form, metacyclic VSGs (mVSGs) are expressed from metacyclic *VSG* expression sites (MESs) located on a few of the megabase chromosomes. MESs are monocistronic transcription units located at subtelomeres with the promoter being located ~5 kb upstream of the telomeres (Lenardo et al. 1984, Cornelissan et al. 1985, Alarcon et al. 1994). MESs are also transcribed by RNA polymerase I (Ginger et al. 2002). The *VSG* genes in these sites are rarely replaced. The parasite population injected into the mammalian host expresses many different mVSGs; however, each cell

expresses only one type of mVSG (Tetley et al. 1987). This diversity in the population allows the parasite to easily establish successful infection in the mammalian host (Barry et al. 1998).

Unlike VSGs, procyclin is expressed from a chromosomal-internal locus. Procyclin genes are organized in tandem arrays of two or three copies on two pairs of megabase chromosomes (Mowatt and Clayton, 1987, Koenig et al. 1989). In total there are four types of loci expressing procyclins (Ruepp et al. 1997). Three of these loci express proteins with extensive glutamic acid-proline dipeptide repeats (EP repeats) and can be distinguished by a presence or an absence of glycosylation sites, while the fourth type of locus encodes proteins with pentapeptide repeat (GPEET) and no glycosylation site (Roditi et al. 1998). Similar to *VSGs* and *mVSGSs*, procyclins are also transcribed by RNA polymerase I (Gunzl et al. 2003). However, in contrast to ESs and MESs, procyclins can be simultaneously expressed from two or more loci (Mowatt and Clayton, 1987, Mowatt and Clayton, 1988).

In the mammalian host, *T. brucei* is able to evade the attack from the host immune system through regular switching of *VSG* through a phenomenon called antigenic variation. Antigenic variation allows the parasite to establish persistent infection in the host.

Antigenic variation in T. brucei and its regulation

Antigenic variation comprises of two main aspects:

(1) *VSG* switching – This involves periodic switching of the expressed *VSG* and changing the surface coat to an immunologically distinct VSG.

(2) Monoallelic *VSG* expression – *VSGs* are exclusively expressed from only one of the 15 ESs while the rest are kept silent. This monoallelic expression ensures effective *VSG* switching and provides the parasite with an inexhaustible reservoir of surface molecules when challenged by the host's immune system.

T. brucei megabase chromosomes carry a large array of *VSG* genes located at the subtelomeres. Minichromosomes also carry *VSGs* at their subtelomeric loci. All these silent *VSGs* serve as a reservoir for antigenic variation (Marcello and Barry, 2007). Activation of these *VSGs* occurs primarily through recombination into the ESs located on the megabase chromosomes. There are fundamentally two main mechanisms used during *VSG* switching: (a) a transcriptional switch and (b) recombination (reviewed in Horn and McCulloch, 2010 and Rudenko, 2011).

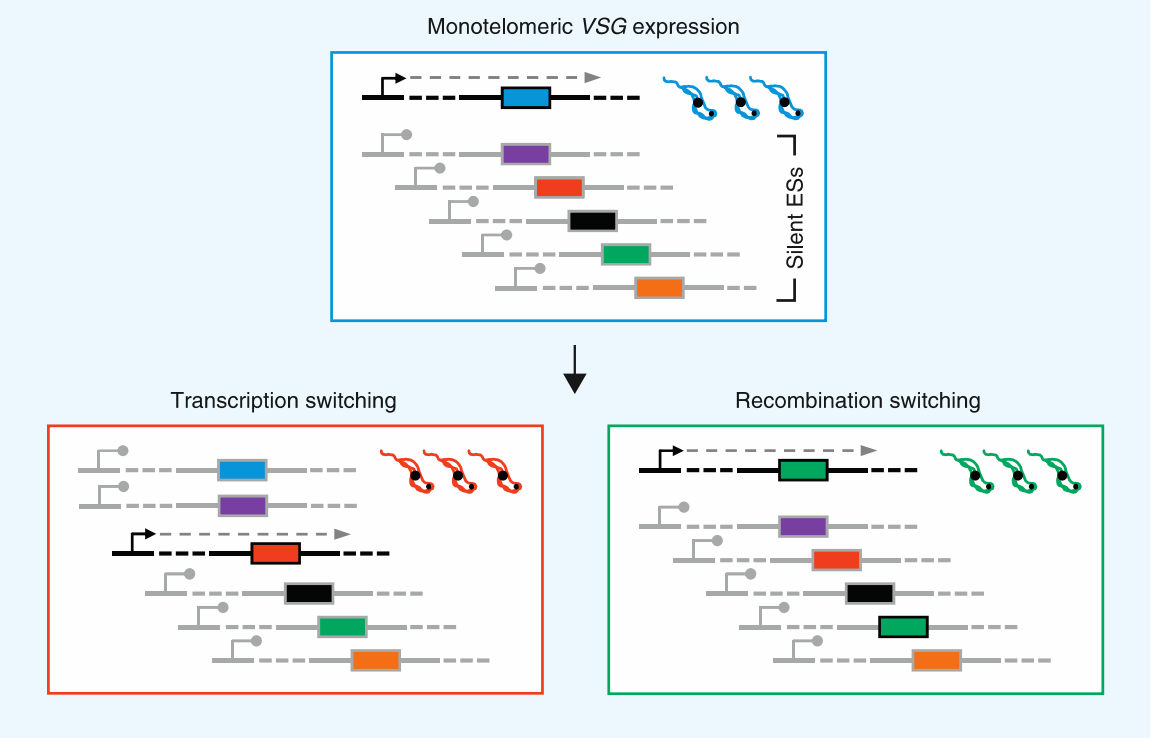

Figure 1-5: Mechanism of *VSG* switching in *T. brucei.* Two main mechanisms of *VSG* switching are schematically depicted. Different color rectangular boxes depict different *VSGs* (figure adapted from Horn and McCulloch, 2010).

As seen in figure 1-5, during transcriptional switching, a new ES is expressed and the originally active ES is silenced. Another mechanism involves DNA recombination, which primarily occurs through a gene conversion process (Barry and McCulloch, 2001). During the duplicative *VSG* gene conversion process, a silent *VSG,* usually from a silent ES, is duplicated and copied into the active ES by replacing the old *VSG* gene (which is lost). Another mechanism is ES gene conversion, where an entire ES is copied into the active ES resulting in its duplication and loss of the previously active ES. Switching can also occur through crossovers where *VSG* crossover occurs between two telomeric ends carrying *VSG* genes, resulting in a new *VSG* gene (present on minichromosomes or a silent ES) inserted into the active ES. Such crossovers may or may not include telomeric sequences. Finally, a less frequent process can generate a novel mosaic *VSG* gene in the active ES. This is achieved by copying the sequence from multiple *VSGs* genes that are normally nonfunctional (Kamper and Barbet, 1992). Such a mechanism is thought to be important for maintaining a persistent late-stage infection.

Many factors regulating *VSG* switching have been identified. DNA damage repair factors BRCA2, RAD51, and its paralogue RAD51-3 have been shown to affect the *VSG* switching frequency. Knockout cells for these factors displayed lower switching frequencies (McCulloch and Barry, 1999, Proudfoot and McCulloch, 2005, Hartley and McCulloch, 2008, Dobson et al. 2011). On the contrary, deletion of the factors, such as TOPO3α topoisomerase and RMI1 (usually involved in DNA recombination) led to an increased *VSG* switching

frequencies (Kim and Cross, 2010, Kim and Cross, 2011). The cohesin subunit SCC1 was shown to be required for faithful inheritance of the active *VSG* to the daughter cell and its depletion led to an increase in the *VSG* switching frequency (Landeira et al. 2009). Depletion of the DNA replication factor ORC1 (origin recognition complex) displayed an elevated *VSG* switching frequency (Benmerzouga et al. 2013). Finally, telomeres play an important role in regulating the *VSG* switching. Telomerase reverse trancriptase (TERT) null cells carrying extremely short telomeres had a higher *VSG* switching frequency, where most *VSG* switchers arose through gene conversion events (Hovel-Miner et al. 2012). Also, the depletion of telomeric proteins, such as *Tb*TRF (Jehi et al., reviewed and currently in revision), *Tb*RAP1 (Nanavaty and Li, unpublished data), and *Tb*TIF2 (Jehi et al. 2014) affect the *VSG* switching frequencies.

For a successful *VSG* switching, it is extremely important to have a tightly regulated monoallelic *VSG* expression.

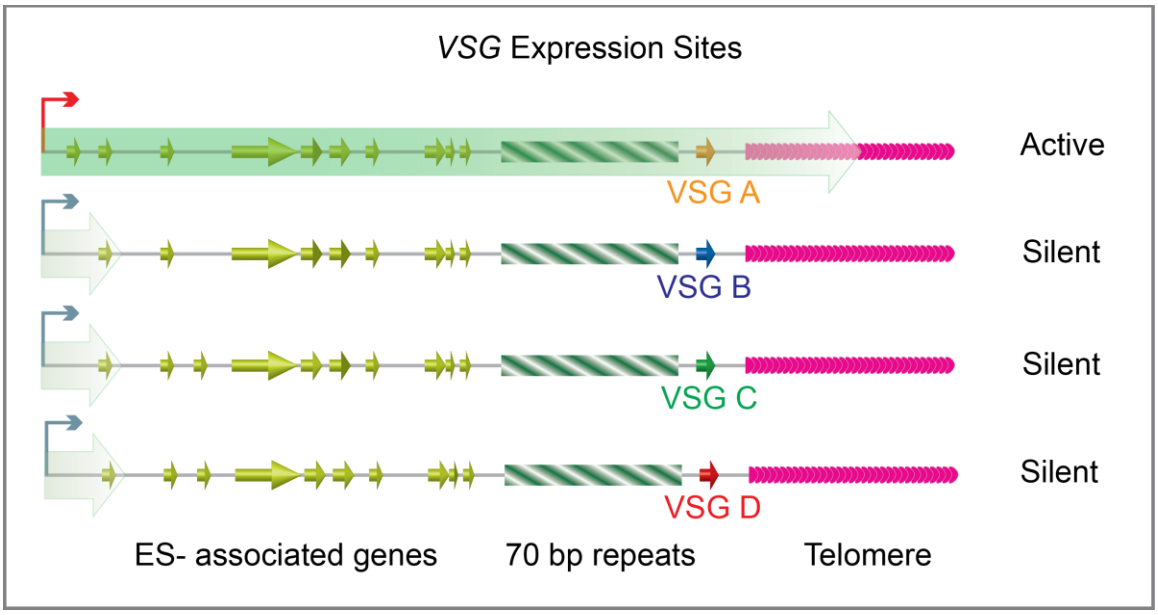

Figure 1-6: Monoallelic expression of *VSG* in *T. brucei.* Multiple ESs carrying different *VSGs* are depicted.

Only one ES is fully active at any time in a *T. brucei* cell (Cross, 1975). Although transcription initiates at all ES promoters, only one promoter is fully active, resulting in a single type of VSG being expressed. Multiple mechanisms have been identified that play roles in regulating monoallelic *VSG* expression: (1) restricted transcription elongation, (2) a unique subnuclear locus for *VSG* transcription, (3) chromatin remodeling, (4) replication machinery, and (5) telomeric silencing.

Transcription initiates at multiple ES promoters, but transcription elongation quickly attenuates in all but one ES, resulting in only one ES being fully transcribed. This is proposed to happen due to selective recruitment of the RNA elongation/processing machinery (Vanhamme et al. 2000). Another interesting feature observed in *T. brucei* is the presence of an extranucleolar polymerase I containing focus. It has been determined that only the active ES is associated with this extranucleolar focus called ES body (ESB) (Navarro and Gull, 2001). An ESB is required for stable inheritance of the active *VSG,* thus suggesting its role in the monoallelic expression (Landeira et al. 2009).

The chromatin structure has been shown to play an important role in regulating ES transcription. It was determined that silent ESs have regularly spaced nucleosomes while the active ES is highly devoid of nucleosomes (Figueiredo and Cross, 2010, Stanne and Rudenko, 2010). However, it still needs to be determined whether such nucleosome occupancy in the active ES is a cause or a consequence of RNA polymerase I transcription. Many chromatin-remodeling factors have been identified that affect ES promoter activities. The

depletion of histone H3 (Alsford and Horn, 2012), linker histone H1 (Povelones et al. 2012), and histone chaperones, such as FACT (Denninger et al. 2010), NLP (Narayanan et al. 2011), and ASF1A or CAF-1b (Alsford and Horn, 2012) led to the derepression of the silent ES promoter without affecting *VSG* silencing. Similar effects on the ES promoter were also observed upon the depletion of chromatin remodeler ISWI (Stanne et al. 2011). Depletion of SIR2rp1 (homolog of yeast Sir2) (Alsford et al. 2007), MYST-family histone acetyltransferase HAT1 (Kawahara et al. 2008), and histone deacetylase DAC1 or DAC3 (Wang et al. 2010) led to the derepression of telomere proximal reporter genes without affecting *VSG* silencing. Interestingly, depletion of the histone methyltransferase DOT1B led to an ~10 fold derepression of the silent *VSGs* suggesting that it is required for monoallelic *VSG* transcription (Figueiredo et al. 2008).

The DNA replication machinery is suggested to have a link with antigenic variation in *T. brucei.* The depletion of ORC1 (origin recognition complex) led to a 4-12 fold derepression of the silent *VSGs* (Benmerzouga et al. 2013). The knockdown of MCM-BP (MCM binding protein, a component of replication complex) also led to a 12-30-fold derepression of silent *VSGs* (Kim et al. 2013). However, the detailed mechanisms are unknown.

Finally and most importantly, telomeres have been shown to play important roles in maintaining *VSG* silencing. *Tb*RAP1, a telomeric protein, is known to be important for maintaining *VSG* silencing. Depletion of *Tb*RAP1 led to a 10-100-fold derepression of all the silent *VSGs* tested (Yang et al. 2009). Such high derepression is not observed when other factors were examined, suggesting that

telomeres are crucial in *VSG* expression regulation. Our lab focuses on characterizing and elucidating functions of telomere in antigenic variation of *T. brucei*.

Telomeres and the telomere complex

Telomeres are the ends of linear chromosomes. They contain telomeric DNA and telomere-associated proteins. Telomeric DNA consist of G-rich repetitive sequences, such as $TG_{2-3}(TG)_{1-6}$ in budding yeast, $TTACAG_{2-5}$ in fission yeast, TTTAGGG in plants and, TTAGGG in humans (Shampay et al. 1984, Sugawara et al. 1986, Moyzis et al. 1988, McKnight et al. 1997). Most of the telomere DNA is duplex except for a single-stranded 3'-overhang present at the end of telomeres known as G-overhang. Protein-free DNA ends are susceptible to degradation by nucleases and illegitimate repair by DNA damage repair machineries, which leads to genome instability. Telomeric proteins form a protective cap and ensure chromosome stability and genome integrity. Linear DNA molecules require additional mechanisms to complete the replication of their extreme termini. Attrition of sequences from the ends of chromosomes occurs after every round of semi-conservative DNA replication. This is known as the end replication problem. Without alternative mechanism such attrition would lead to loss of genetic information and prevent cells from multiplying. This end replication problem is solved by telomerase (Greider and Blackburn 1985). Telomerase is a ribonucleoprotein complex with a reverse transcriptase activity that can synthesize telomeric DNA *de novo*, and solve the telomere end replication problem.

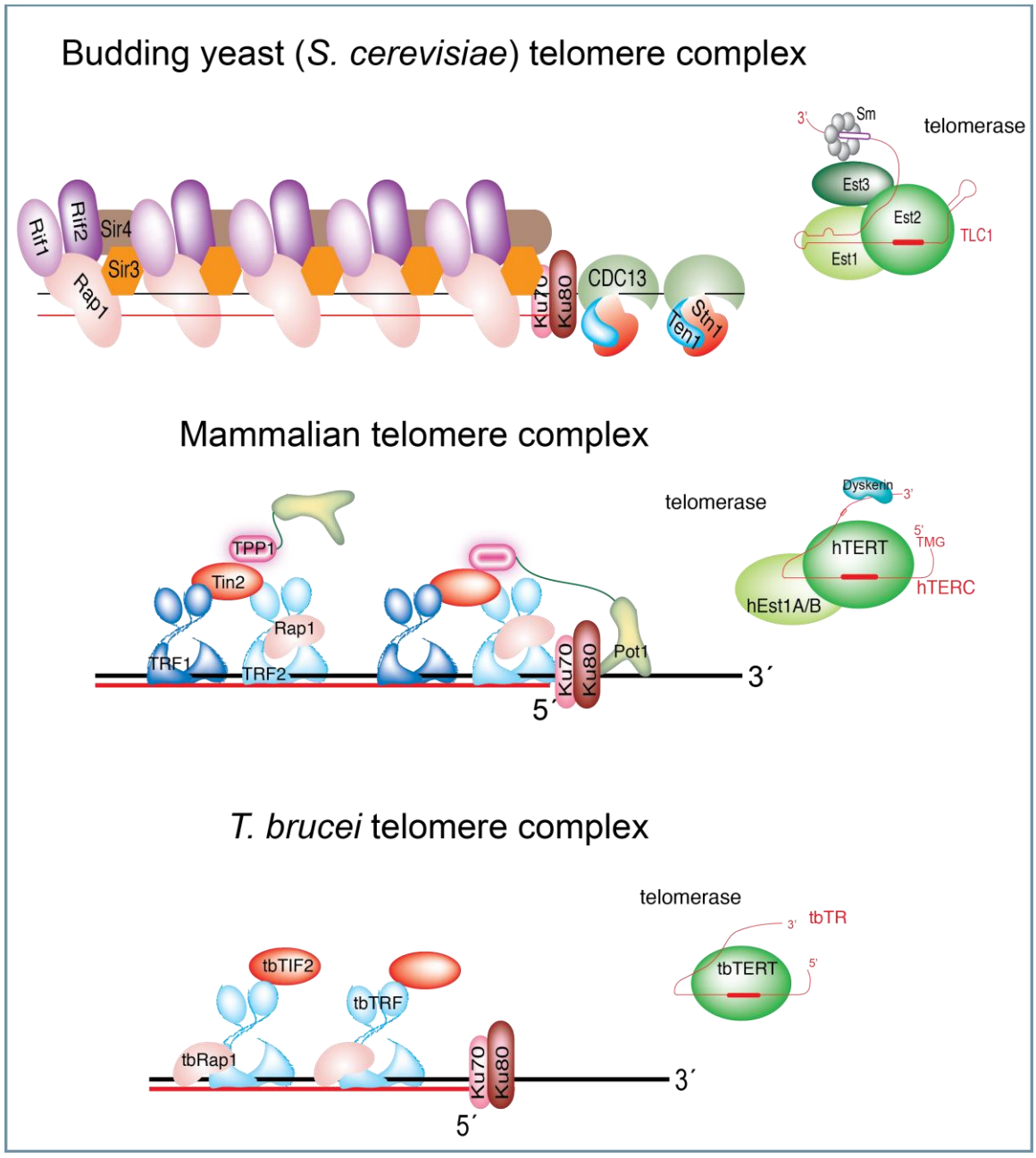

Figure 1-7: Telomere complexes in different organisms. Core components of telomere complex identified so far along with telomerase in budding yeast, mammals, and *T. brucei* are depicted.

Telomeric DNA in budding yeast consists of a G-rich imperfect repeat sequence, such as $TG_{2-3}(TG)_{1-6}$ (Shampay et al. 1984). The distal end of telomeres contains G-rich 3' single-stranded overhang called G-overhang (McElligott and Wellinger, 1997, Klobutcher et al. 1981, Shampay et al. 1984, Moyzis et al. 1988). *Sc*RAP1 is a component of the budding yeast telomere complex and is the predominant duplex telomere DNA binding factor (Konig et al. 1996). *Sc*RAP1 interacts with two groups of telomeric proteins. One group consisting of *Sc*Rif1 and *Sc*Rif2 is primarily involved in telomere length regulation (Hardy et al. 1992, Wotton and Shore, 1997). The other group consists of Sir3 and Sir4 and is primarily involved in heterochromatin formation/maintenance and silencing of subtelomeric gene transcription (Moretti et al. 1994, Cockell et al. 1995). Sir3 and Sir4 recruits Sir2, which deacetylates histones on neighboring nucleosomes and provides further binding sites for Sir3 and Sir4, thereby allowing propagation of heterochromatic structure (Rusche et al. 2002). Cdc13 binds to the single-stranded G-overhang along with two other factors called Stn1 and Ten1, and mutations in this complex lead to abnormally elongated or shortened telomeres (Nugent et al. 1996, Grandin et al. 1997, Grandin et al. 2001). The Ku heterodimer, consisting of yku70 and yku80 subunits, binds to the distal end of the telomeres and is known to be important for regulating telomere length and silencing (Boulton and Jackson 1998, Gravel et al. 1998, Polotnianka et al. 1998). Finally, telomeres in budding yeast are maintained by telomerase, consisting of Tlc1 (the RNA subunit of telomerase), Est2 (the catalytic protein

subunit of telomerase), Est1, and Est3 (Singer and Gottschling 1994, Zhou et al. 2000,Timothy et al. 2000).

The human telomeric DNA consists of TTAGGG repeats (Moyzis et al. 1988). The core telomere protein complex in humans is known as the Shelterin and consists of six subunits. TRF1 and TRF2 bind directly to the duplex telomeric DNA as homodimers (Broccoli et al. 1997). Overexpression of a dominant negative mutant of TRF1 leads to removal of TRF1 from the telomere and abnormally elongated telomeres. Overexpression of a dominant negative mutant of TRF2 leads to removal of TRF2 from the telomere and chromosome end fusions (Van Steensel and de Lange 1997, Van Steensel et al. 1998). It has been shown that human telomeres fold back and the single stranded telomere G-overhang invade the double stranded telomeric DNA region to form a lasso-like structure, known as the T-loop (Griffith et al. 1999). TRF2 is required for the formation and/or maintenance of the T-loop (Dokasani et al. 2013). TIN2 is localized to telomeres through interaction with both TRF1 and TRF2, and its truncation leads to abnormally elongated telomeres (Kim et al. 1999). RAP1 was identified as a TRF2-interacting factor, and overexpression of RAP1 or some domain deletion mutants leads to elongation of telomeres (Li et al. 2000, Li and de Lange 2003). POT1 is another component of Shelterin and binds to the single-stranded telomeric DNA (Lei et al. 2002, Loayza and de Lange 2004, Lei et al. 2004). POT1 protects telomere ends from nucleolytic degradation and also regulates telomerase-dependent telomere elongation (Loayza and de Lange 2003, Liu et al. 2004, Hockemeyer et al. 2005, Yang et al. 2005). Recent work

also showed that POT1 protects the telomere by preventing RPA-mediated activation of the ATR signaling pathway (Denchi and de Lange 2007). TPP1 interacts with POT1 and is required for the telomere localization of POT1 (Liu et al. 2004). TPP1 binds to POT1 and increases its affinity for telomeric ssDNA. It also interacts with the telomerase for its recruitment to telomeres (Xin et al. 2007, Wang et al. 2007). The Ku heterodimer is known to bind DNA ends in a sequence independent manner and is a key player in the Non-homologous end joining pathway (NHEJ). At telomeres, the Ku70/Ku80 heterodimer is known to interact with TRF1 or TRF2 and prevent end joining (Hsu and Gilley 2000, Song et al. 2000). The telomerase consists of a protein subunit called TERT and its RNA component called TERC (Nakamura et al. 1997). However, these are just minimal components and additional accessory factors are required for its function *in vivo*. Other telomerase-associated factors include hEST1A, hEST1B, and dyskerin (Mitchell et al. 1999, Reichenbach et al. 2003, Snow et al. 2003).

The *T. brucei* telomere sequence is the same as the one for the vertebrate telomere and consists of TTAGGG repeats (Blackburn and Challoner 1984). The *T. brucei* telomere can be more than 10 kb long and comprises 10% of the total DNA (Dreesen and Cross 2008). Similar to human telomeres, but comparatively much smaller (~1 kb), t-loops have been observed in *T. brucei* (Munoz-Jordan et al. 2001). At the end of the telomeres there is a short single stranded 3' G-rich overhang. *Tb*TRF is a component of the core telomere complex, and it directly binds to the duplex telomere DNA (Li et al. 2005). *Tb*TRF is required for telomere end protection, and its depletion leads to loss of the telomere G-overhang

structure (Li et al. 2005). *Tb*RAP1 was identified as a *Tb*TRF-interacting factor and it plays an important role in regulating *VSG* silencing at *T. brucei* telomeres (Yang et al. 2009). *Tb*TIF2 (TRF interacting factor) was recently identified as a component of the telomere complex, and it is required for maintaining subtelomere/telomere integrity and stability. Depletion of *Tb*TIF2 leads to an increased *VSG* switching frequency (Jehi et al. 2014). *Tb*TRF and *Tb*RAP1 also play roles in regulating *VSG* switching in *T. brucei* (Jehi et al., reviewed and currently in revision, Nanavaty and Li, unpublished data). Ku80 has been characterized in *T. brucei*, and it is required for telomere length maintenance as its deletion leads to telomere shortening (Conway et al. 2002, Janzen et al. 2004). The telomerase complex in *T. brucei* consists of a protein subunit called *Tb*TERT and an RNA component called *Tb*TR (Cano et al. 1999, Dreesen et al. 2005, Sandhu et al. 2013, Gupta et al. 2013). Deletion of *Tb*TERT and *Tb*TR leads to the shortening of telomeres. This shortening of telomeres led to an increased *VSG* switching frequency (Dreesen and Cross, 2006, Hovel-Miner et al. 2012, Sandhu et al. 2013).

Recent studies have shown that the *T. brucei* telomeres and its integral components play a key role in regulating antigenic variation (*VSG* silencing and *VSG* switching). Hence, it is crucial to understand the telomere biology and elucidate its role in pathogenesis of *T. brucei.*

Telomere transcription and heterochromatin formation

Long non-coding RNAs are involved in epigenetic regulation of gene expression by either forming euchromatic or heterochromatic structures.

Chromatin associated long non-coding RNAs, such as XIST and rox regulate dosage compensation in mammals and *Drosophila melanogaster*, respectively (Deng and Meller, 2006, Payer and Lee, 2008). Air or Kcnq1ot1 are long non-coding RNAs involved in genomic imprinting (Pauler et al. 2007, Pandey et al. 2008). Hence, it is increasingly evident that long non-coding RNAs play important roles in epigenetic regulation of gene transcription.

Contrary to popular belief that telomeres are transcriptionally silent due to their repressive chromatin state, it has been established that telomeres are transcriptionally active and produce long non-coding RNA molecules called TERRA (telomere repeat containing RNA) (Azzalin et al. 2007, Schoeftner and Blasco, 2008). TERRA ranges in size from 100 bp to 9 kb in mammals and is transcribed from the C-rich strand giving rise to UUAGGG repeats (Azzalin et al. 2007, Schoeftner and Blasco, 2008). TERRA forms discrete nuclear foci and is associated with telomeres *in vivo* (Azzalin et al. 2007). It is known to interact with the telomeric proteins TRF1 and TRF2 (Deng et al. 2009).

Not all TERRA foci are colocalized with telomeres. Interestingly, in mouse embryonic fibroblasts, an intense TERRA focus co-localizes with XIST RNA that coat inactive X chromosomes (Schoeftner and Blasco, 2008). Also, TERRA associates with mouse sex chromosomes in a development specific manner. Upon development, it is only associated with telomeres of heterochromatinzed (inactive) sex chromosome of each sex (Ogawa et al. 2008). This suggests that the possible role of TERRA is to establish/maintain heterochromatin at inactive sex chromosomes.

Open chromatin structure favors transcription of TERRA. TERRA levels are increased when human cells are treated with an inhibitor of Class I and II histone deacetylases (Azzalin et al. 2007). Mouse cell lines deficient in histone methyltransferases Suv3-9h and Suv4-20h also displayed elevated levels of TERRA (Schoeftner and Blasco 2008). On the contrary, the knock-out of telomerase RNA component in mouse cells led to shortened telomere sand decreased levels of TERRA (Schoeftner and Blasco 2008). These shortened telomeres also had an open chromatin structures with decreased levels of telomeric histone methylation and increased histone acetylation (Benetti et al. 2007). In addition, overexpression of TRF2 in mouse cells led to the telomere shortening with an open chromatin structure but with decreased levels of TERRA (Benetti et al. 2008). Hence, TERRA levels are intricately balanced *in vivo*, and the telomere length can affect TERRA levels.

Not much is known about functions of TERRA. SiRNA mediated depletion of TERRA affected cell viability, telomere aberrations, decreased recruitment of ORC to telomeres, and decreased H3K9 trimethylation at telomeres in human cells (Deng et al. 2009). TERRA is known to facilitate ORC recruitment to telomeres via binding to TRF2 (Deng et al. 2009). These results collectively suggest that TERRA may play a role in forming the heterochromatin structure at telomeres.

TERRA is also proposed to negatively regulate telomerase-mediated telomere elongation (Schoeftner and Blasco 2008). Telomerase-positive cells display higher methylation of TERRA promoters and lower level of TERRA compared to

telomerase-negative cell lines (Ng et al. 2009). Also, high-grade tumors have diminished levels of TERRA compared to low-grade tumors (Schoeftner and Blasco 2008). During embryonic development of mouse, high telomerase activity is related to lower levels of TERRA (Schoeftner and Blasco, 2008). Finally, TERRA was shown to efficiently inhibit telomerase *in vitro* by base pairing with the RNA component of telomerase (Schoeftner and Blasco, 2008). On the contrary, a recent study in budding yeast showed that TERRA nucleates telomerase molecules and recruits them specifically to short telomeres for their elongation (Cusanelli et al. 2013). Thus, more research needs to be done in order to determine the role of TERRA in regulating telomerase activity.

It is critical to regulate TERRA levels in the cell. The impairment of non-sense-mediated RNA decay machinery in human cells or the deletion of 5'-3' exonuclease Rat1p in budding yeast interferes with the decay of TERRA molecules and leads to its eventual accumulation (Azzalin et al. 2007, Luke et al. 2008). These elevated levels of TERRA led to the dramatic shortening of telomere tracts by rapid truncations (Azzalin et al. 2007, Luke et al. 2008). Forced transcription of yeast telomeres led to the shortening of its telomeric tracts (Sandell et al. 1994). Using transcriptionally induced telomeres, it was proven that high levels of TERRA lead to telomere shortening in a DNA-replication dependent manner and also cellular senescence in the absence of telomere maintenance mechanisms (Maicher et al. 2012). TERRA forms RNA-DNA hybrids with telomeric DNA and their accumulation promotes telomeric recombination (Balk et al. 2013). Collectively, these results suggest that it is

extremely important to regulate TERRA levels in cells as it can lead to an early senescence and a deleterious effect. However, deregulating TERRA transcription can be beneficial when fighting against pathogens such as *T. brucei.*

TERRA has been identified in *T. brucei*; however, nothing is known about its function or regulation (Rudenko and Ploeg 1989). It ranges in size from ~200 bp to 9 kb and is transcribed by polymerase insensitive to α-aminitin treatment (Rudenko and Ploeg 1989). From the results mentioned above, it is likely that TERRA plays a role in forming a heterochromatic structure at telomeres and also regulates telomere length and recombination in *T. brucei*. Hence, it will be imperative to determine the functions of TERRA in regulating *VSG* silencing at *T. brucei* telomeres. Due to its role in suppressing telomere recombination, it can be hypothesized that TERRA may additionally regulate *VSG* switching in *T. brucei*.

Significance of the study

The *T. brucei* undergoes antigenic variation and evades host immune responses. Genes encoding its surface antigen are located at subtelomeric loci, and it is proven that telomeres play important roles in the regulation of *VSG* expression. Importantly, telomeric proteins of *T. brucei*, although functionally conserved, have very low sequence homology with the human telomeric proteins. This makes telomeric proteins potential drug targets for therapeutic purposes, as they are essential for survival of the parasite. Understanding the functions of telomeres in regulating antigenic variation will provide means to disrupt its regulation. Disruption of antigenic variation will facilitate the host's

immune system to combat *T. brucei* infection. In addition, since telomere proteins are essential for the survival of the parasite; targeting these telomere proteins will have deleterious effects.

CHAPTER II

MATERIAL AND METHODS

Growth analysis

Uninduced and induced cells were grown in parallel to compare their growth. Cells were counted at regular intervals and population doublings was calculated. Population doubling = log2 (total number of cell, n/total number cells, (n-1)) + PD (n-1), where n is the hour or day when cells are counted and n-1 is the immediate time-point preceding it.

Western blot analysis

Cells were lysed in 2X laemmli buffer (0.1 M Tris-Cl, pH 6.8, 6% SDS, 20% glycerol, 0.004% bromophenol blue) and boiled at 100ºC for ten minutes in order to collect total cell lysate (Laemmli 1970). Samples were separated on 6-10% Tris-Glycine polyacrylamide gel at 100 V for ~2 hours. After separation, proteins were transferred onto 0.45 µm nitrocellulose membrane (GE healthcare life sciences) by electrophoresis at 70 V for 2 hours at 4ºC. The membrane was stained with Ponseau dye (2% w/v Ponseau S in 30% w/v Tri-chloroacetic acid)

for about a minute and rinsed with Ponseau destaining buffer (2.3 liters of ddH20 + 4ml of concentrated HCl) to ensure proper transfer of proteins. The membrane was blocked with 10% milk/ 0.5% Tween20/ 1x PBS (phosphate-buffer saline) at room temperature for ~1 hour. The membrane was rinsed twice for ~5 minutes each using 0.1% milk/0.1% Tween 20/ 1x PBS. The membrane was hybridized overnight in a plastic bag using appropriate primary antibody and dilution, in 5%milk/ 0.1% Tween 20/ 1x PBS. Next day, the membrane was washed twice for ~5 minutes using 0.1% milk/ 0.1% Tween 20/ 1x PBS and hybridized with appropriate secondary antibody in 5%milk/ 0.1% Tween 20/ 1x PBS at room temperature for one hour. Followed by hybridization membrane was washed 4 times for ~5 minutes each using 0.1% milk/ 0.1% Tween 20/ 1x PBS. Final wash was given for 5 minutes using 1x PBS. Membrane was rinsed with water and incubated with Amersham ECL western blotting reagent (GE Healthcare Life Sciences) for ~2 minutes. The blot was exposed to X-ray films for various lengths of time and the films were developed.

For detection of endogenous *Tb*RAP1 protein, rabbit polyclonal antibodies 597 or 598 were used (Yang et al. 2009). Rabbit polyclonal antibodies 1260 or 1261 were used to detect *T*bTRF (Li et al. 2005). TAT-1 (gift from Dr. keith Gull) was used to detect tubulin. A commercially available goat antibody against EF-2 (elongation factor 2) (Santa Cruz Biotechnology Inc.) was used. Rabbit anti-VSG2 (CRD-depleted) antibody was used to detect VSG2 (Figueiredo et al. 2008). BB2 antibody (MSKCC, AB core facility) was used to detect Ty1-*Tb*RAP1. Rabbit GFP antibody was used to detect GFP tagged *Tb*TRF, *Tb*KU80, and

hygromycin-GFP-TK. Commercially available HA antibody (F-7) (Santa Cruz Biotechnology Inc.) was used to detect F2H (Flag-HA-HA) tagged *Tb*RAP1 and *Tb*TIF2. Rabbit polyclonal antibody was used to detect histone H3 (AbCam). Histone H2A was detected using a rabbit polyclonal antibody (Millipore Corporation).

Southern blot analysis

Genomic DNA was isolated either using DNAzol (Life Science Inc.) or the DNA spooling method (de Lange et al. 1990). The DNA concentration was measured using NanoDrop 2000 (Thermo Fisher Scientific Inc.). 2-5 µg of digested genomic DNA (using appropriate restriction enzymes) were separated on a 0.7% agarose gel prepared in 0.5xTAE at 100 V until the orange G dye reaches the bottom of the gel. The gel was scanned on Typhoon FLA 9140 (GE Healthcare Life Sciences) by placing a ruler next to it. DNA was depurinated (0.25 M HCL) for 30 minutes followed by denaturation (1.5 M NaCl; 0.5 M NaOH) for one hour (buffer was changed after 30 minutes). Finally the DNA was neutralized (1 M Tris 7.4; 1.5 M NaCl) for one hour and blotted onto hybond nylon membrane (GE healthcare life sciences) in 20x SSC (3 M NaCl, 0.3 M sodium citrate). After overnight blotting, the membrane was cross-linked (Stratalinker UV crosslinker) and pre-hybridized for ~1 hour in CHURCH mix (0.5 M NaPi pH 7.2, 4 mM EDTA pH 8.0, 7% SDS, 1% BSA) at 65ºC. Hybridization was done at 65ºC overnight using the CHURCH mix and appropriate radiolabeled probe. The blot was washed three times using CHURCH wash (40 mM NaPi pH 7.2, 1 mM EDTA pH 8.0, 1% SDS) for ~15 minutes each at 65ºC,

wrapped, and exposed to a phosphorimager screen (GE Healthcare Life Sciences).

Probe labeling

For labeling of the probe, a desired DNA fragment of around 600-800 bp was generated. 200 ng of this DNA fragment was mixed with 5 ng of random hexamer and the total volume was brought up to 39 µl with double distilled water. The mixture was incubated at 100ºC for 5 minutes and immediately moved on ice after boiling. 5 µl of 10X nucleotide mixture (containing dATP, dGTP, dTTP) without dCTP was added to the tube. Klenow polymerase (New England Biolabs) and 5 µl of ^{32}P-alpha-dCTP (3000 Ci/mmol) were added. The reaction was incubated at room temperature for 90 minutes followed by adding 50 µl of TNES (10 mM Tris pH7.4, 10 mM EDTA, 100 mM NaCl, 1%SDS) buffer. The probe was purified on a 3 ml of G-50 beads column and eluted using TNES buffer. After monitoring with a Geiger counter, the probe was heated at 100ºC for 5 minutes and added to 10-25 ml of CHURCH mix. This mixture was filtered using a 0.22 µm syringe filter and added directly onto the blot.

End labeling of oligonucleotide probe was done for telomere in-gel hybridization. 50 ng of TELC4 oligo ($(CCCTAA)_4$) or TELG4 oligo ($(TTAGGG)_4$) was mixed with ^{32}P-gamma-ATP, Kinase buffer, and Polynucleotide kinase (New England Biolabs). The reaction was incubated at 37ºC for 45 minutes followed by adding 80 µl of TES (Tris-HCl/EDTA/SDS) buffer to the mixture. The probe was purified using a 3 ml Sepharose G-25 column and elution with TNES buffer. The

purified probe was mixed with 25 ml of CHURCH mix, filtered through a 0.22 µm syringe filter, and added to the blot for hybridization.

RNA collection

Total RNA was isolated from *T. brucei* cells using RNAstat (TEL-TEST, Inc). Briefly, 140 million cells were harvested by centrifugation at 580 g for 10 minutes at 4ºC. The pellet was resuspended and evenly homogenized in 1 ml of RNAstat reagent. After incubation at room temperature for 5 minutes, 200 µl of chloroform was added to the tube and mixed vigorously by vortexing for 15-30 seconds. After another 5 min incubation, the sample was centrifuged at 15,682 g for 15 minutes at 4ºC to collect the aqueous phase. 600 µl of isopropanol was added to the aqueous phase and mixed thoroughly. Samples were stored at -20ºC. When ready to use, samples were centrifuged at 15,682g for 15 minutes at 4ºC. The RNA pellet was washed with 70% ethanol, air-dried, and dissolved using ddH_2O.

Reverse transcription and quantitative Real time PCR

RNA samples were cleaned using QIAGEN RNeasy kit and treated with DNase (QIAGEN). Reverse transcription was performed using M-MLV (Promega) according to the manufacturer's protocol. Quantitative RT-PCR was carried out using Bio-Rad iTaq SYBR Green supermix with ROX according to the manufacturer's protocol. The amount of DNA was quantified using DNA Engine Opticon 2 (Bio-Rad). The following formula was used to calculate normalized increase in mRNA levels: $(mRNA_{V,\ n}/mRNA_{V,\ 0})/(mRNA_{T,\ n}/\ mRNA_{T,\ o})$, where $mRNA_{V,\ n}$ represents mRNA level for particular *VSG* at n hour after induction and $mRNA_{V,\ 0}$ represents mRNA levels at 0 hour. $mRNA_{T,\ n}$ and $mRNA_{T,\ o}$ represent

the mRNA levels for β-tubulin at 0 hour (pre-induction) and n hours (post-induction).

Flow cytometry

~20 million cells were harvested by centrifugation at 208 g for 10 minutes at 4ºC. Cells were washed twice with 1xPBS/2 mM EDTA for PF cells or with 1xTDB (5 mM KCl, 80 mM NaCl, 1 mM MgSO4, 20 mM Na2HPO4, 2 mM NaH2PO4, 20 mM glucose pH 7.4), with 2 mM EDTA for BF cells. Cells were resuspended in 200 µl of 1xPBS/2mM EDTA (for PF cells) or in 1xTDB/2mM EDTA (for BF cells). Cells were fixed by adding 2 ml of ice-cold 70% ethanol drop wise while vortexing. After fixing, cells were stored for at least overnight at 4ºC. Storage never exceeded more than one week. For performing FACS analysis, cells were harvested by centrifugation at 208 g for 10 minutes at 4ºC. The cell pellet was resuspended in 0.5 ml of staining solution (1xPBS, 2mM EDTA, 200 µg/ml RNAse A and 50 µg/ml propidium iodide). Cells were collected in a tube by passing them through a cell-strainer cap and incubated in dark at 37ºC for 30 minutes. FACS was performed on BD FACSCanto II cytometer (BD Biosciences) using the BD FACS DIVA software (BD Biosciences). Data were analyzed using the FlowJo software.

Chromatin Immunoprecipitation (ChIP)

Dynabead protein G beads (Life Sciences Inc.) were prepared for the immunoprecipitation. 50 µl of beads were washed and resuspended in 200 µl of antibody binding and washing buffer (1xPBS, 0.02% Tween 20) with appropriate antibody. Pre-immune serum of equal amount was used for a negative control.

Beads were kept for antibody coupling at 4ºC on a rotor. $2x10^8$ cells were harvested by centrifugation at 580 g for 10 minutes at 4ºC. Cells were resuspended in 40 ml 1xTDB with proper mixing. Cells were fixed for precisely 20 minutes by adding 4 ml of freshly prepared 11% formaldehyde solution (final concentration 1%). After fixing, 2.75 ml of 2M glycine was added to quench formaldehyde. Cells were centrifuged at 5,000 g for 15 minutes at 4ºC. After discarding supernatant cells were washed with cold 1xPBS. Cells were lysed using lysis buffer containing appropriate protease inhibitors and sonicated using sonic dismembrator (Thermo Fisher Scientific Inc.) at out put ~6 (Scale 4-5) for 4 cycles with 30 second on/ 30 second off for each cycle. After taking out sample to check sonication efficiency, 50 µl of 10% Triton-X100 was added to the tubes and centrifuged at 15,682 g for 10 minutes at 4ºC. After centrifugation the supernatant was carefully transferred to a fresh tube. 50 µl of sample was taken out for Input from each tube. Beads were prepared for binding by placing them on magnetic rack and removing the supernatant. The remaining lysate was equally divided among the control tube (pre-immune serum) and the IP (containing antibody) tube. Tubes were rotated at 4ºC for three hours. After incubation, beads were thoroughly washed three times using 1xPBS and samples were eluted using elution buffer (50 mM Tris-HCl, pH8.0, 10 mM EDTA and 1% Sodium-dodecyl-sulphate). All samples (including input sample) were reverse crosslinked using 5 µl of 5 M Nacl at 65ºC overnight. DNA was extracted by phenol chloroform and purified using the Qiaquick spin PCR purification kit

(Qiagen). Quantitative PCR was performed using appropriate dilutions of the DNA.

10 µg of 598 antibody (rabbit polyclonal) was used for testing differential binding of *Tb*RAP1 to active and silent *VSGs*. 10 µg of 598 pre-immune serum was used for a negative control. 5 µg of 1260 or 1261 antibody (rabbit polyclonal) was used for testing differential binding of *Tb*TRF to the active and silent *VSGs*.

Pull-down of specific DNA was calculated as percentage of input. The following formula was used for calculation after performing quantitative PCR.

$$\% \text{ of input} = (1 + \text{Efficiency})^{\Delta CT} / (\text{dilution factor}) * 100$$

where ΔCT (sample) = ΔCT (untreated sample) - ΔCT (treated sample)

In this case, treated samples were either preimmune control or IP sample. Untreated sample represents input.

Formaldehyde assisted isolation of regulatory elements (FAIRE) analysis

FAIRE analysis was performed according to Giresi et al. 2009. Briefly, $2x10^8$ cells were fixed using 1 ml of 37% formaldehyde for 20 minutes at room temperature. Cells were lysed using lysis buffer and sonicated for 4 cycles (30 seconds on/ 30 seconds off) using Bioruptor®300 (Diagenode Inc.) at high output. Sonication sample (25µl) (to check efficiency of sonication) and input sample (50µl) were taken out after sonication. DNA was extracted from remaining lysate by performing phenol chloroform extraction. Input sample and sonication sample were kept for reverse crosslinking overnight at 65ºC after adding 125 mM NaCl and treated with RNAse A and Proteinase K before extracting DNA. DNA from all samples was precipitated and purified using

Qiaquick spin PCR purification kit (Qiagen). The amount of DNA extracted was measured by quantitative PCR using iTaq SYBR Green Supermix with ROX (Bio-rad) in an Opticon II (Bio-rad). The amount of FAIRE-extracted DNA was normalized to that of the input DNA.

VSG cloning

RNA was collected from $50x10^6$ cells using RNAstat 60 (Tel-Test Inc). RNA samples were treated with DNaseI (Qiagen) and purified using RNeasy column (Qiagen). Reverse transcription was performed using polydT primers. PCR was performed using cDNA as the template. Forward primer was designed to recognize spliced leader sequence (present on each mature mRNA) and backward primer was designed to recognize C-terminal region of VSG (which is similar in all VSGs). PCR products were purified and sent for sequencing. Sequences were compared with the *T. brucei* genome using BLAST to determine the VSGs expressed in each cell line.

Statistical analysis

P-values of unpaired t-tests were calculated using the GraphPad Prism software.

Micrococcal nuclease (MNase) digestion

$5x10^7$ cells were collected and washed with 1xTDB (BF cells) or 1x PBS (PF cells). Cells were permeabilized using 40 mM digitonin. All samples were treated with 1 unit of Micrococcal nuclease (Worthington Biochemicals) for 1, 2.5 or 5 minutes. EDTA and EGTA (final concentration of 10 mM each) were added to terminate the reaction. DNA was subsequently extracted by phenol-chloroform.

Equal amount of DNA (for untreated and treated samples) was loaded and separated by agarose gel electrophoresis. EtBr-stained gel was scanned using Typhoon FLA 9140 (GE healthcare life sciences). After scanning, DNA was treated as described for southern blot analysis and blotted onto the Hybond nylon membrane (GE healthcare life sciences). After UV cross-linking, the blot was hybridized with the appropriate radiolabeled probe at 65ºC overnight. After hybridization, the blot was washed three times with CHURCH wash for 15 minute each and exposed to a phosphorimager screen (GE Healthcare Life Sciences).

Telomere southern blot analysis

Genomic DNA was isolated using the DNA spooling method (de Lange et al. 1990). An appropriate amount of genomic DNA was digested overnight at 37ºC by using frequent cutting enzymes such as AluI and MboI. The DNA concentration was measured. A 0.7% agarose gel with 20x20 cm dimensions was prepared by using 0.5xTAE. 1-2 µg (for telomere blots) or ~12 µg (for single copy genes) of digested genomic DNA was loaded per lane along with an appropriate DNA marker. Initially, the gel was run for 1 hour at 30 volts followed by overnight at 50 volts. In total, the gel was run for ~1,000-1,100 V•hrs. The EtBr-stained gel was scanned using Typhoon FLA 9140 (GE healthcare life sciences) by placing a ruler next to it. The DNA was depurinated, denatured, neutralized, and blotted onto a Hybond nylon membrane (GE Healthcare Life Sciences) in 20xSSC (3 M NaCl, 0.3 M sodium citrate) overnight. The blot was UV cross-linked (Stratalinker UV crosslinker) and hybridized with the appropriate radiolabeled probe.

Pulsed field gel electrophoresis

To prepare DNA plugs, ~150x10^6 cells were harvested and washed with 1xTDB (BF cells) or 1xPBS (PF cells). After centrifugation, cell pellets were resuspended in L-buffer (0.01 M Tris-HCl pH 7.6, 0.02 M NaCl, 0.1 M EDTA pH 8.0) to obtain a final concentration of 4x10^8 cells/ml and incubated at 50ºC for 10 minutes. Equal volume of 1.6% of low melting point agarose (Agarose type VII, Sigma Aldrich) in L-buffer (50ºC) was added to the cells. Cells were mixed and loaded into disposable molds at a concentration of ~1x10^7 cells per plug. Plugs were allowed to solidify at room temperature, subsequently, plugs were incubated in L-buffer with 1% Sarkosyl and 1 mg/ml Proteinase K at 50ºC for 48 hours. After 48 hours, the plugs were washed twice with L-buffer followed by incubation in L buffer with Proteinase K for another 48 hours at 50ºC. DNA plugs were finally washed and stored in L-buffer at 4ºC.

A 1.2 % agarose gel was prepared using 0.5xTris-borate-EDTA (TBE). DNA plugs were loaded on the gel with the appropriate marker (*H. wingei* chromosomal DNA). Intact chromosomes were separated in a CHEF DR II (Bio-Rad) using the following conditions: initial pulse 1,500 seconds, ending pulse 700 seconds, voltage 2.5 volts/cm, at 14ºC for 120 hours. Subsequently, the gel was stained for 1 hour in 0.5xTBE containing 1 µg/ml of Ethidium Bromide and destained in ddH2O for 30 minutes. The EtBr-stained gel was scanned using Typhoon FLA 9140. DNA was depurinated, denatured, and neutralized using southern blot analysis conditions. DNA was blotted onto the Hybond nylon membrane in 20X SSC followed by UV cross-linking. The blot was hybridized

with appropriate radiolabeled probe at 65ºC overnight, washed, and exposed to a PhosphorImager screen (GE healthcare life sciences).

G-overhang analysis

Pulsed field gel electrophoresis followed by in-gel hybridization was performed to quantify the telomere G-overhang signal. The same DNA sample was run in duplicates and after electrophoresis the gel was dried overnight in a gel dryer (Bio-rad). The DNA-containing gel was prehybridized at 50ºC for 30 minutes in a CHRUCH mix. TELC4 oligo ((CCCTAA)4) and TELG4 oligo ((TTAGGG)4) were end-labeled by Polynucleotide kinase with ATP (γ-32 P). One gel was hybridized with the TELC4 oligo to detect the G-strand overhang and the other gel with the TELG4 oligo to detect the C-stand overhang. The latter serves as a negative control. Both gels were hybridized overnight at 50ºC in CHURCH mix. After hybridization, gels were washed three times for 30 minutes each with 4xSSC (0.6 M NaCl and 0.06 M sodium citratre) at 50ºC followed by a final wash in 4xSSC with 0.1%SDS for 30 minutes at 50ºC. Gels were wrapped in plastic wrap and exposed to PhosphorImager screens. After overnight exposure, signals were quantified using Typhoon FLA 9140. Subsequently, both gels were denatured (1.5 M NaCl and 0.5 M NaOH) for 30 minutes and neutralized for 30 minutes (3 M NaCl and 0.5 M Tris-HCl, pH 7.0). After rinsing with ddH_2O, the gels were prehybridized in CHURCH mix at 55ºC for 1 hour. Hybridization was done using the same TELC4 and TELG4 probes at 55ºC for overnight. Gels were washed the same as described above and exposed to PhosphorImager screens

for 2 hours. Signals were quantified using Typhoon FLA 9140. This signal was used as a loading control.

The following formula was used to calculate the telomere G-overhang signal:

G-overhang signal for any given sample = (Native TelC4 signal)/ (Denatured TelC4 signal)

The change in the G-overhang signal was calculated by normalizing G-overhang levels at different time points (induced samples) with that at the zero time point (uninduced samples).

In vitro transcription and translation of TbRAP1

The *Tb*RAP1 ORF containing the Kozak sequence was cloned after the T3 promoter in the pBlueScript SK vector. pSK-*Tb*RAP1 (Kozak) was linearized using PvuI and purified using the Qiaquick spin PCR purification kit (Qiagen). 1µg of digested and purified plasmid was used as the template to for *in vitro* transcription using the mMESSAGE mMACHINE® T3 transcription kit (Thermo Fisher Scientific Inc.) according to the manufacturer's protocol. After completing transcription, the product was treated with DNaseI and RNA was precipitated using Lithium chloride. The resulting RNA pellet was washed once with cold 70% ethanol and resuspended in ddH_2O. RNA was electrophoresed in a formaldehyde gel to determine the quality and the yield of transcribed RNA.

1 µg of the transcript was used for *in vitro* translation using the TNT® T7/T3 Coupled Reticulocyte Lysate System (Promega) with S^{35} labeled Methionine according to the manufacturer's protocol. Lysate containing translated *Tb*RAP1 was separated on a 10% polyacrylamide gel, which was subsequently fixed in

5% methanol and 7% acetic acid for 30 minutes followed by drying for 30 minutes at 80ºC using a Gel dryer (Bio-Rad). The dried gel was exposed to a PhosphorImager screen overnight.

Electrophoretic mobility shift assay (EMSA)

The $(TTAGGG)_{12}$ probe was prepared as previously discussed (Zhong et al. 1992). Purified GST-*Tb*TRF was available in the lab (Li et al. 2005). *Tb*RAP1 was obtained by performing *in vitro* transcription and translation as described above (lysate containing *Tb*RAP1). Proteins were incubated with 80% glycerol, 1 µg/µl of sheared *E. coli* DNA, 200 mM Glycine pH 7.6, 100 ng/µl β-casein, 10 mM dithiothreitol, 1 ng/µl of probe, and cold competitor (non radiolabeled $(TTAGGG)_5$ probe) for 20 minutes at room temperature. Antibody was added when necessary and incubated for another 20 minutes at room temperature. All samples were loaded onto a 0.6% agarose gel and separated in 0.1x Tris-borate-EDTA. Gel was dried at 80ºC for 2 hours by placing a DE-81 membrane underneath. After drying, the gel was exposed overnight to a PhosphorImager screen (GE Healthcare Life Sciences).

Cloning of TbTRFH domain mutants

The N-terminal half of the *Tb*TRFH domain upstream of the helix to be deleted along with the N-terminal region of *Tb*TRF was PCR-amplified using primers containing the EcoRI and HindIII sites. The *Tb*TRFH region downstream of the helix to be deleted to the end of the *Tb*TRF was PCR-amplified using primers containing the HindIII and BamHI sites. The wild type *Tb*TRF gene previously cloned in the pBTM116 vector (lex A-fusion bait vector) was used as the template

in the PCR reactions. Hence, the two fragments flanking the helix to be deleted were generated by PCR. After digestion and purification, the two fragments were simultaneously ligated with the pBTM116 vector that was digested with EcoRI and BamHI to obtain the lexA-fused *Tb*TRF with the helix-deletion mutation. This procedure was repeated to delete each helix in the *Tb*TRFH domain. For helix 1 deletion, the N-terminal region upstream of helix is very short. Hence annealed oligo pairs with appropriate restriction sites instead of the PCR product was used for ligation.

All seven helix mutants were subsequently cloned into the pACT2 (GAD) vector. Specifically, each mutant was PCR-amplified using primers having the BamHI and XhoI restriction sites and cloned into pACT2 vector.

Yeast transformation

Single colony from a freshly streaked L40 cells was inoculated in YPD medium for overnight at 30ºC with rotation. OD600 was measured to determine the cell concentration. The overnight yeast culture was used to inoculate appropriate amount of YPD medium (10 ml/transformation) so that the OD600 of the new culture was ~0.1. The new yeast culture was grown till OD600 reaches ~0.5. Yeast cells were harvested by centrifugation at 6,446 g for 5 minutes and the cell pellet was resuspended in 10 ml sterile water. Cells were centrifuged at 6,446g for 5 minutes again, and the cell pellet was resuspended in freshly prepared lithium solution (1xTBE pH7.5/1x lithium acetate (0.1M, pH7.5)). For each transformation 5 µg of plasmid DNA was fully mixed with 200 µl of yeast cells and 1.2 ml of freshly prepared Polyethylene glycol solution (40% PEG,/1x

Tris-EDTA buffer pH 7.5/1x lithium acetate). The DNA/yeast cell mixure was rotated at 100 rpm at 30ºC for 30 minutes. Cells were heat shocked for precisely 15 minutes at 42ºC and centrifuged for 15 seconds to obtain the cell pellet. Cells were resuspended in 200 µl of 1x Tris-EDTA buffer and plated on Tryptophan and Leucine dropout plates. Plates were incubated at 30ºC for ~3-4 days to obtain yeast transformants.

Yeast two-hybrid analysis

pBTM116-based LexA binding domain (LexABD)-fused protein and pACT2-based Gal4 activation domain (GAD)-fused protein were co-expressed in yeast L40 transformants. The interaction between LexABD and GAD fusion proteins was represented as the *LacZ* reporter gene expression. β-galactosidase activity was measured using ONPG (*o*-nitro-phenyl-β-D-galactopyranoside) as the substrate . Single colonies of yeast transformants were inoculated in Tryptophan and Leucine dropout medium and allowed to grow for ~18-20 hours at 30ºC with constant rotation. OD600 was measured to determine the cell concentration of the overnight yeast culture. Yeast cells were centrifuged and the cell pellet was washed with 1 ml ddH_2O then resuspended in 200 µl Z buffer (60mM $Na_2HPO_4 \cdot 7H_2O$, 40mM $NaH_2PO_4.H_2O$, 10mM KCl and 1mM $MgSO_4 \cdot 7H_2O$). 100 µl of this cell suspension was transferred to a fresh Eppendorf tube along with two tubes containing only z buffer (for blank purpose). Cells were quickly frozen using liquid nitrogen and subsequently thawed by incubating at 37ºC. 900 µl of z buffer containing β-mercaptoethanol and 200 µl of z buffer containing 4 mg/ml ONPG was added to the cells and immediately incubated at 30ºC. 500 µl of 1 M

Na_2CO_3 was added to stop the reaction after the sample turned yellow. The time required for each sample to turn yellow was noted. At the end of experiment, cells were pelleted and the supernatant was used to measure OD 420.

The final β-glactosidase activity was calculated using the following formula:

Unit = 1000*OD420/(OD600 * time * dilution factor/10)

Dilution factor = Volume of cells used (4 ml in this case)/volume of Z buffer used to resuspend the cell pellet (200 µl in this case)

Northern blot analysis

A 1.5% agarose gel containing formaldehyde was prepared in MOPS buffer (0.4 M MOPS, 0.1 M NaOAc and 0.01 M EDTA). 2-5 µg (to detect *VSGs* and other transcripts) or 10 µg (to detect TERRA transcript) of RNA was mixed with premix (1.5 µl 10xMOPS, 2.6 µl 37% formaldehyde, 7.5 µl Formamide, 3 µl 5x loading buffer and Ethidium bromide). 5 µg of RNA marker was also mixed with premix. Samples were mixed and incubated at 65ºC for 10 minutes. After heating, samples were immediately loaded onto the gel. Gel was run at ~5V/cm (50 volts in this case) using 1xMOPS buffer. The EtBr stained gel was scanned using a Typhoon FLA 9140 on the completion of running and washed in ddH_2O for one hour by gentle rotation. The gel was blotted onto a nylon hybond membrane (GE healthcare life sciences) for overnight in 20x SSC (3 M NaCl, 0.3 M sodium citrate). UV crosslinking was performed and the blot was prehybridized at 55ºC for one hour using the CHURCH mix. Hybridization was performed overnight at 55ºC using the appropriate radiolabeled probe. The blot was washed

three times for 15 minutes each at 55ºC using the CHURCH wash, wrapped, and exposed overnight to a Phosphorimager screen (GE healthcare life sciences).

To detect the TERRA transcript, hybridization was performed at 55ºC overnight and the blot was washed twice for 15 minutes each at 65ºC using 0.1xSSC (15 mM NaCl, 1.5mM sodium citrate)/0.1% SDS followed by exposure to a phosphorimager screen overnight.

RNA Immunoprecipitation (RNA IP)

Dynabead protein G beads (Thermo Fisher Scientific Inc.) were prepared for the immunoprecipitation. 50 µl of beads were washed and resuspended in 200 µl of antibody binding and washing buffer (1xPBS/0.02% Tween 20). An appropriate antibody was added to the beads and the mixture was kept for antibody coupling at 4ºC on a rotor. $2x10^8$ cells were harvested and washed once with 1xTDB. The cell pellet was resuspended in 1 ml NET-5 buffer (40 mM Tris-HCl, pH 7.5, 420 mM NaCl, 0.5% Nonidet P-40, 2 mg/ml aprotinin A, 1 mg/ml leupeptin, 1mg/ml pepstatin A and 10 units of RNAsin). Cells were lysed by repeated freezing/thawing technique by freezing them in -80ºC. Repeated freezing and thawing was done three times and lysate was cleared by centrifugation at 1,5682 g for 10 minutes at 4ºC. The lysate was transferred to a fresh tube.100 µl of input sample was taken out and the rest of the lysate was equally divided between the control IP (no antibody) and the desired IP. Tubes were rotated at 4ºC for three hours. After incubation beads were thoroughly washed thrice using 1xPBS and samples were eluted using elution buffer (50 mM Tris-HCl, pH8.0, 10 mM EDTA and 1% SDS). RNA was extracted from all

samples including the input sample by phenol/chloroform. 50 µl of 5 M ammonium acetate, 15 µl of 7.5 M lithium chloride, 1 µl of 20 mg/ml glycogen and 850 µl of 100% ethanol was added to 300 µl of aqueous phase for precipitating RNA. Samples were stored overnight at -20ºC. All the samples were treated with DNaseI before performing a RNA slot blot experiment.

RNA slot blot

The slot blot manifold was treated with 0.1 M NaOH before assembly and rinsed with distilled water. The Hybond nylon membrane was pre-treated with 10xSSC for 10 minutes before assembly into the manifold. Each slot of manifold was filled with 10xSSC. RNA samples were treated with DNaseI at room temperature for precisely 20 minutes. At the completion of incubation, 3 volumes of denaturing solution (500 µl formamide, 162 µl of 37% formaldehyde, 100 µl of MOPS buffer) was added to the RNA samples and samples were incubated at 65ºC for 15 minutes. At the end of incubation all the samples were kept on ice and 2volumes of ice-cold 20xSSC was added. Samples were allowed to pass through manifold. 1 ml of 10xSSC was allowed to filter through manifold after loading the samples. The apparatus was disassembled, the blot was allowed to dry and UV-crosslinked (Stratalinker UV cross-linker).

Blots were pre-hybridized for one hour at 55ºC using the CHURCH mix. Hybridization was done at 55ºC overnight using an appropriate radiolabeled probe. Blots were washed twice for 15 minutes each at 65ºC using 0.1X SSC and 0.1% SDS and exposed overnight onto a PhosphorImager screen (GE Healthcare Life Sciences). .

CHAPTER III

*Tb*RAP1-MEDIATED *VSG* SILENCING IN *T. BRUCEI*

INTRODUCTION

RAP1 (Repressor/Activator Protein 1) is one of the intrinsic and well-characterized components of the telomere complex in mammalian cells, budding yeast, fission yeast, and *T. brucei* (Conrad et al. 1990, Li et al. 2000, Kanoh and Ishikawa 2001, Yang et al. 2009). It plays various roles in telomere end protection, telomere length regulation, and telomeric silencing.

(A)

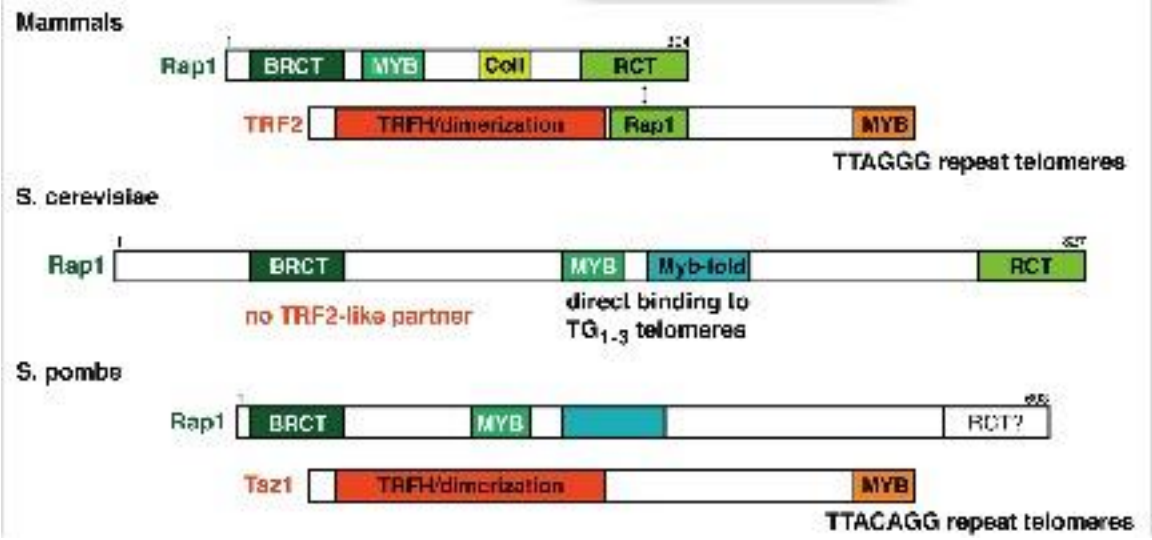

(B)

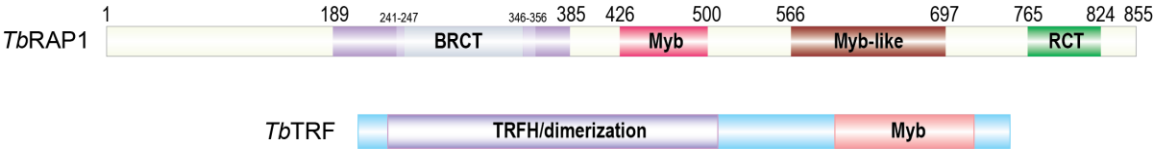

Figure 3-1: The domain structure of RAP1 in various organisms (Kabir et al. 2010). (A) A diagram depicting the conserved protein motifs of RAP1 in mammals and yeasts. Its TRF2 like interacting partners are depicted as well. The empty cyan box in *S. pombe* indicates that it has a sequence similarity with *S. cerevisiae* myb-fold; however, the structure has not yet been determined. It is not known whether *S. pombe* RAP1 contains RCT domain. (B) Conserved motifs of *Tb*RAP1 along with its protein interacting partner *Tb*TRF.

*Sc*RAP1 directly binds to the telomeric DNA through its myb and myb-like domains (Konig et al. 1996), while hRAP1 and *Sp*RAP1 do not seem to directly bind to the telomeric DNA *in vivo*. Instead, they depend on TRF2 and TAZ1 for their recruitment to telomeres, respectively (Li et al. 2000, Kanoh and Ishikawa 2001). Recently, an *in vitro* study using EM analysis showed that hRAP1 could bind to the telomeric DNA sequence (Arat and Griffith 2012). However, the proof of DNA binding *in vivo* is still lacking. The *Tb*RAP1 domain structure is very similar to that of *Sc*RAP1 and hRAP1. However, it is still not clear whether *Tb*RAP1 can interact with telomeric DNA by itself or solely depends on *Tb*TRF for its recruitment. The RCT (RAP1 C-terminus) domain present in RAP1 is thought to be required for protein-protein interaction (Kabir et al. 2010), while the functions of the RAP1 BRCT domain are unknown.

Genes present on the subtelomeric region are often silenced due to the heterochromatic nature of telomeres. This phenomenon is known as telomere position effect (TPE) or telomeric silencing. So far, TPE has been identified in *Drosophila melanogaster*, yeast, human, mouse, *T. brucei,* and *Plasmodium falciparum* (Hazelrigg et al. 1984, Gottschling et al. 1990, Horn and Cross 1995, Baur et al. 2001, Frietas-Junior et al. 2005, Duraisingh et al. 2005, Pedram et al. 2006). RAP1 is known to play an important role in TPE and in expression of subtelomerically located genes.

In *S. pombe,* the deletion of *Sp*RAP1 led to a loss of telomere silencing as well as a loss in telomere clustering towards spindle pole body, and increased telomere length (Kanoh and Ishikawa 2001). In human cells a telomere position

effect has been identified. However, the proteins involved in TPE are currently unknown (Baur et al. 2001).

*Sc*RAP1 plays an important role in TPE. It recruits Sir3/Sir4 to the telomere to regulate telomeric silencing and heterochromatin formation/maintenance (Moretti et al. 1994, Cockell et al. 1995), and the mechanism is well characterized. Sir3 and Sir4 together recruit Sir2, an NAD^+-dependent histone deacetylase that can remove the acetyl group from histone H3 at K9 and K14 residues, and from histone H4 at K16 (Moazed et al. 1997, Bourn et al. 1998, Imai et al. 2000, Moretti et al. 2001). Sir3 in turn recognizes the unacetylated H4K16 (Hect et al. 1995). Therefore, binding of Sir3 and Sir4 recruits Sir2, which deacetylates neighboring histone tails and allows the subsequent binding of Sir3 and Sir4 to neighboring nucleosomes, allowing the propagation of the heterochromatin structure from telomere to subtelomeric region (Rusche et al. 2002). The loss of the RCT domain of *Sc*RAP1 leads to de-repression of subtelomeric genes, indicating that *Sc*RAP1 is required for proper telomeric silencing (Kyrion et al. 1993). In *T. brucei,* homologs of Sir3 and Sir4 are not known. However, homologs of Sir2 have been identified (Garcia-salcedo et al. 2003). *Tb*Sir2rp1 (the only homolog located in the nucleus) is required for silencing a reporter gene targeted to a subtelomeric locus but not *VSG* (Alsford et al. 2007).

The proper regulation of *VSG* silencing is of the utmost importance for parasite survival and pathogenesis. *Tb*RAP1 (Tb11.03.0760) was identified as a *Tb*TRF-interacting protein in a yeast 2-hybrid screen using *Tb*TRF as bait (Yang et al. 2009). *Tb*RAP1 is an essential protein. It was confirmed using ChIP, CO-

ImmunoPrecipitation (CO-IP), and Immunofluorescence (IF) that *Tb*RAP1 localizes to the telomere. Most importantly, *Tb*RAP1 is required for *VSG* silencing in BF form *T. brucei* (Yang et al. 2009). Upon depletion of *Tb*RAP1, multiple *VSGs* were expressed as confirmed by qRT-PCR and western blot analysis. IF confirmed that more than one silent *VSG*s were expressed on the surface of *Tb*RAP1-depleted *T. brucei* cells. However, the observed *VSG* de-repression was not at the same level as the fully activated *VSG*, suggesting that *Tb*RAP1 independent mechanisms are also involved in ES expression regulation. Telomere proximal genes were more strongly de-repressed compared to telomere distal genes upon depletion of *Tb*RAP1. Thus, finding confirmed that in *T. brucei* *Tb*RAP1 plays an important role in *VSG* silencing. However, the mechanism of *Tb*RAP1-mediated silencing is not fully understood.

In PF cells, *T. brucei* growing in the mid-gut of tsetse fly, all *VSGs* are silent, and a different surface protein called procyclin is expressed. Metacyclic *VSGs* (*mVSGs*) expressed during the metacyclic stage (in the salivary glands of fly) are silent in both BF and PF cells. We hypothesized that *Tb*RAP1 may also be required in silencing ES-linked *VSGs* in PF cells as well as *mVSGs* in both BF and PF cells.

RESULTS

TbRAP1 is essential for PF T. brucei survival

In order to study the role of *Tb*RAP1 in PF cells, various independent clones carrying inducible *Tb*RAP1 RNAi vector were established. The *Tb*RAP1 RNAi

vector was inserted in the rDNA spacer of 29-13 cells. 29-13 (PF) cells express the tet repressor and the T7 polymerase, which allow inducible expression of a double stranded *Tb*RAP1 RNAi fragment (Wirtz et al. 1999). The RNAi construct contains the *Tb*RAP1 sequence encoding its C-terminal domain. RNAi is induced upon adding doxycycline. We obtained a pool (PRi-Pool) of transfected cells as well as various independent clones (PRi-B2, PRi-C1 and PRi-C2) by limiting dilution. Upon adding doxycycline (2µg/ml), depletion of *Tb*RAP1 was achieved and growth arrest was observed (Figure 3-2).

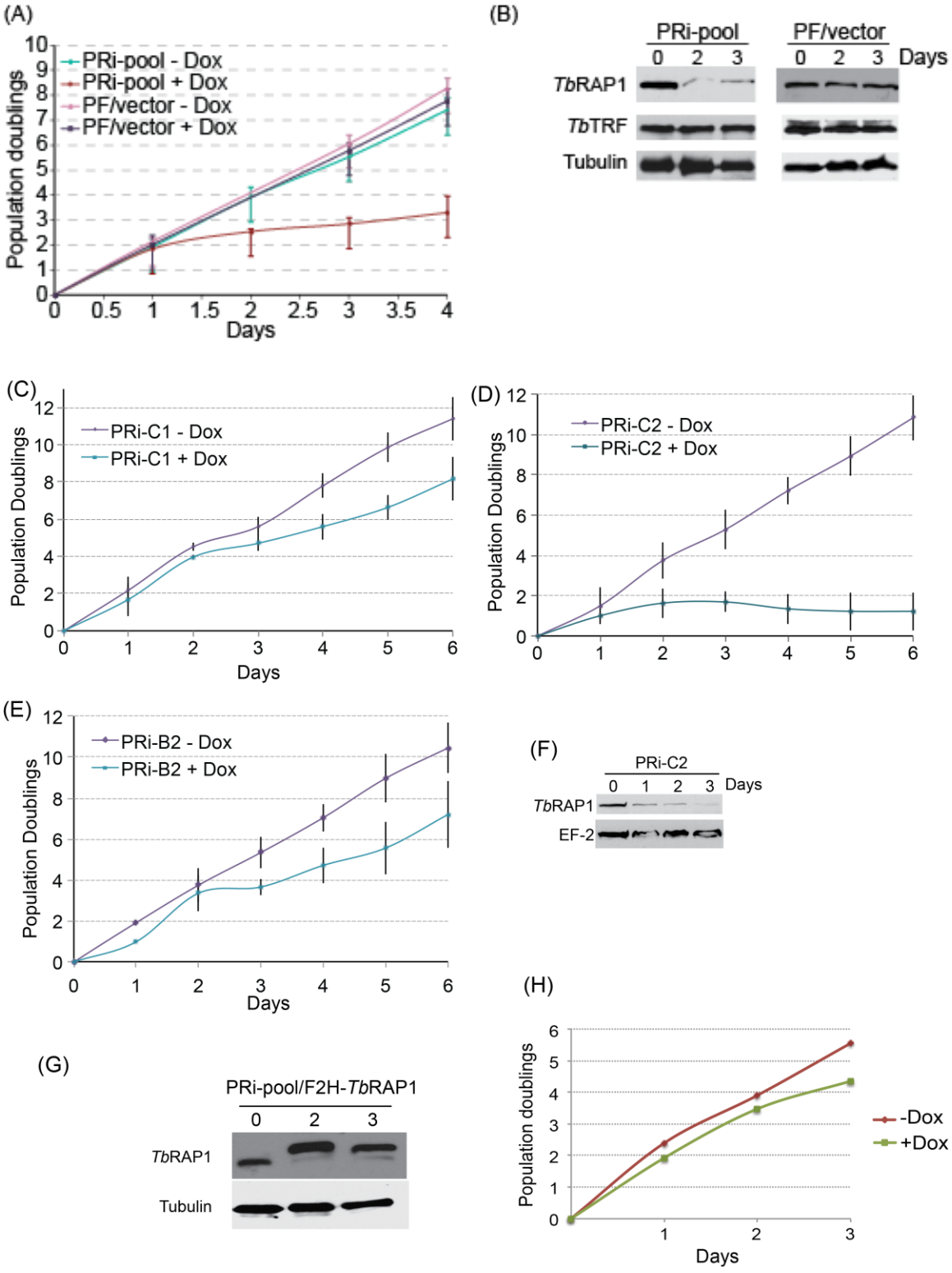

Figure 3-2: Depletion of *Tb*RAP1 in the PF cells. (A) Growth curve analysis for the PRi-pool and control cells carrying empty vector under induced (+Dox) or uninduced (-Dox) conditions. Y-axis depicts population doubling calculated as average from six independent experiments. Error bars represent standard

deviation. (B) Western blot analysis to detect knockdown of *Tb*RAP1 in PRi-pool and empty vector cells. Whole cell lysate was collected before (Day 0) and after induction (Day 2 & 3) to detect *Tb*RAP1 and *Tb*TRF using antibodies against endogenous proteins. Tubulin was used as a loading control. (C), (D) and (E) Growth curves of independent *Tb*RAP1 RNAi clones (PRi-C1, PRi-C2, and PRi-B2, respectively). Population doubling was calculated as an average from three independent experiments. Error bars represent standard deviation. (F) Whole cell lysate was collected before and after induction of clone PRi-C2 to detect *Tb*RAP1. EF-2 (elongation factor 2) was used as a loading control. (G) Complementation of *Tb*RAP1 by ectopically expressing F2H-*Tb*RAP1 in PRi-pool cells. Western blot analysis depicts ectopically tagged *Tb*RAP1 (running slightly higher at day 2 & 3) as well as endogenous *Tb*RAP1 before and after induction. (H) Growth curve of PRi-pool/F2H-*Tb*RAP1 cells after adding doxycycline. The population doubling was plotted for a single growth analysis.

Upon depletion of *Tb*RAP1, we observed a severe growth defect by day 2 in PRi-Pool cells (figure 3-2 A). Control cells carrying empty vector did not have any growth defects. Western analysis confirmed that the *Tb*RAP1 protein was significantly depleted by day 2 of induction. Depletion of *Tb*RAP1 did not have any effect on protein levels of another telomeric protein, *Tb*TRF (figure 3-2 B). *Tb*RAP1 and *Tb*TRF protein levels were unaffected in control cells upon induction with the same amount of doxycycline. We obtained several independent clones that had various degrees of growth defects after depletion of *Tb*RAP1. PRi-C2 had the strongest growth arrest (figure 3-2 D). Western analysis of cell lysate collected from PRi-C2 showed that a significant amount of *Tb*RAP1 was depleted within 24 hours of induction (figure 3-2 F). In order to avoid phenotypic variations associated with the clonal cell lines, we decided to use PRi-Pool cells for further studies and key phenotypes were also verified in PRi-C2 clone. Complementation of *Tb*RAP1 knockdown was achieved by expressing an ectopic F2H (Flag-HA-HA) tagged allele of *Tb*RAP1. Expression of

both vectors (ectopic F2H-*Tb*RAP1 and *Tb*RAP1 RNAi) was under the control of tet operator and is induced simultaneously upon adding doxycycline. After multiple independent transfections and screening several clones, we were able to achieve partial complementation as seen in western analysis (Figure 3-2 G) and growth analysis (Figure 3-2 H). Ectopically tagged *Tb*RAP1 was expressed upon induction (as seen by slightly higher mobility running band), however by day 3 the protein levels were a little lower than at day 2. Similarly, normal growth was restored at day 2 but was a little delayed by day 3. This finding suggests that the complementation was partial and that by day 3 the RNAi was able to deplete even ectopically expressed *Tb*RAP1, possibly due to a stronger expression of the *Tb*RAP1 double stranded RNA than the ectopic wild-type *Tb*RAP1 allele.

Next, flow cytometry analysis was performed to examine the cell cycle profile of PRi-pool cells after depletion of *Tb*RAP1. Cells were collected before and after depletion of *Tb*RAP1 and subjected to propidium iodide staining to measure the DNA content. We observed a mild increase in G2/M and sub G1 population with a decrease in G1 population upon depletion of *Tb*RAP1 (figure 3-3 C). These results are very similar to those observed previously in BF cells upon *Tb*RAP1 depletion (Yang et al. 2009).

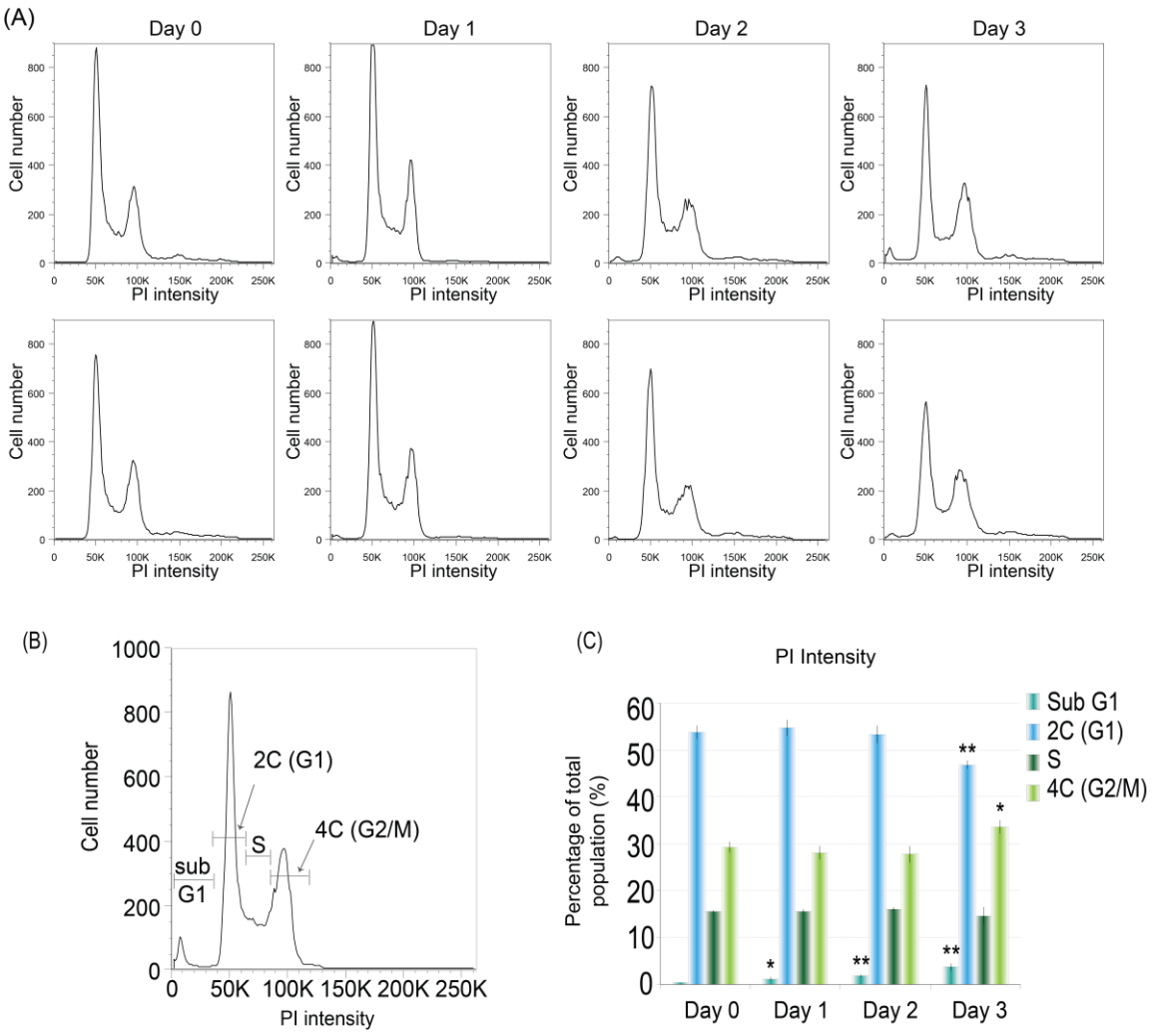

Figure 3-3: Flow cytometry analysis of PRi-pool cells. (A) Results from two independent analyses are shown. Cells were collected before (Day 0) and after (Day1, Day2 and Day3) depletion of *Tb*RAP1. (B) Gating schematics of uninduced PRi-Pool cells in flow cytometry analysis. Sub-G1 population contains DNA content less than 2C and represents cells experiencing DNA degradation. PI, propidium iodide intensity. (C) Quantification of cell population at various cell cycle stages of PRi-pool cells before (Day 0) and after (Day 1, 2 & 3) depletion of *Tb*RAP1. P values were calculated to compare day 1, 2, and 3 with day 0 using unpaired t-test. *, $0.01<P\leq 0.05$; **, $0.001<P\leq 0.01$.

TbRAP1 is required for silencing ES-linked VSGs in PF cells.

We wanted to test whether *Tb*RAP1 plays similar roles in regulating *VSG* silencing in PF cells as it does in BF cells. Total RNA was collected before and

after depletion of *Tb*RAP1 to compare steady state mRNA levels of various ES-linked *VSG*.

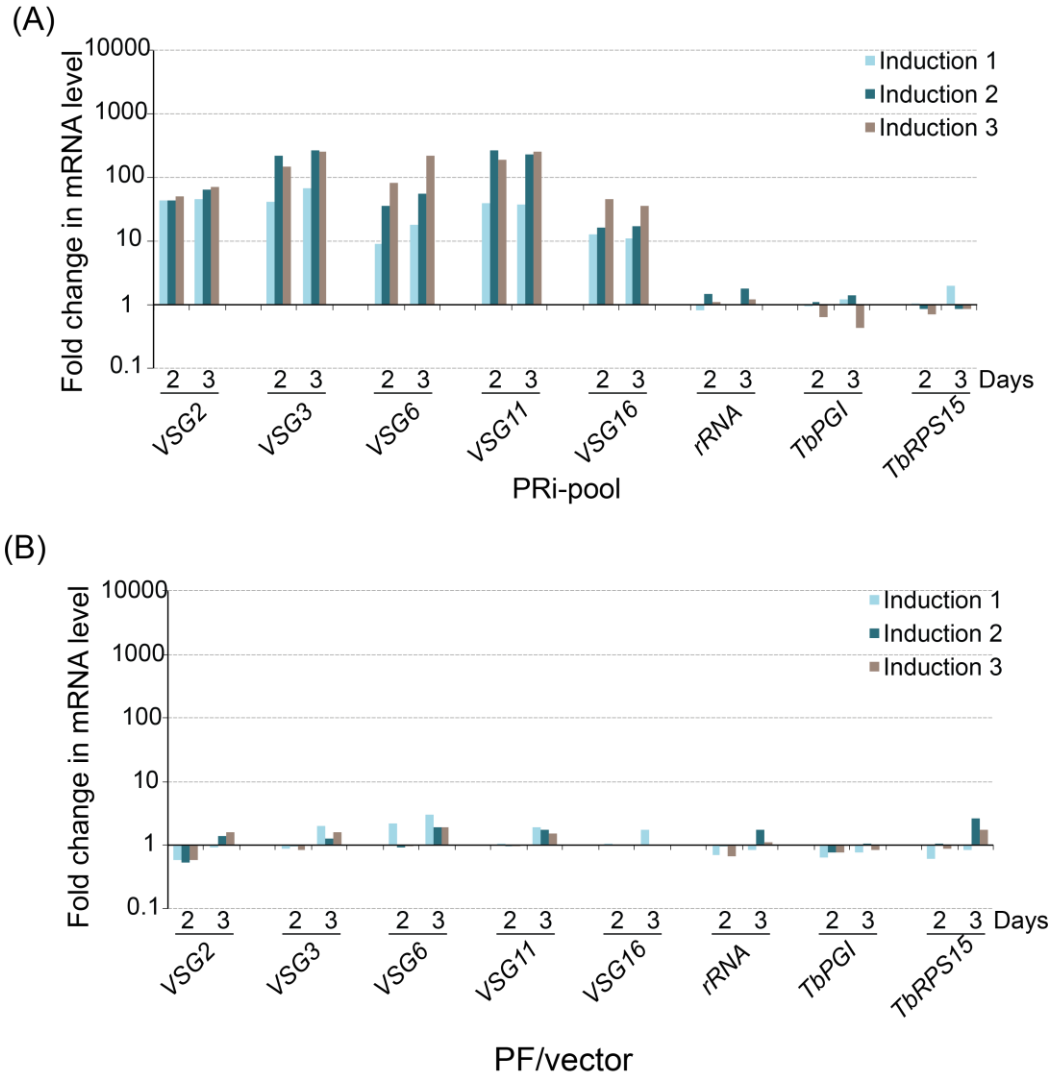

Figure 3-4: ES-linked *VSGs* are de-repressed in PF cells upon depletion of *Tb*RAP1. qRT-PCR analysis was performed to measure steady state mRNA levels of ES-linked *VSGs* and control genes before (day 0) and after depletion (day 2 & 3) of *Tb*RAP1 in PRi-pool cells (A) and control cells (B). Day 0 value was set to 1 but not shown. Fold change in mRNA level was calculated for day 2 & 3 (after depletion) by normalizing against day 0 (before depletion). All samples were normalized with tubulin as an internal loading control. Fold changes in mRNA levels are shown for three independent experiments. (C) Western analysis to determine levels of various proteins in PRi-pool cells (left) and PF/*Tb*TRF RNAi cells (right). Whole cell lysate was collected before (day 0) and after (day 1, 2, & 3) adding doxycycline. (D) qRT-PCR analysis to measure steady state mRNA levels of ES-linked *VSGs* and control gene in PRi-C2 cells. Day 0 value was set to 1 but is not shown. Fold change was calculated by normalizing after *Tb*RAP1 depletion value by before *Tb*RAP1 depletion.

Steady-state mRNA levels were estimated for several ES-linked *VSGs* and control genes before and after depletion of *Tb*RAP1 in PRi-Pool cells by qRT-PCR analysis. 35% of *Tb*RAP1 protein was left by day 1 after induction of RNAi vector, however, by day 2 only 10% of protein was left. Hence we decided to collect RNA samples at day 2 and 3 following induction. Upon depletion of *Tb*RAP1 in PRi-pool cells, mRNA levels of all tested *VSGs* (*VSG 2, 3, 6, 11,* and *16*) increased by several ten- to several hundred-fold (figure 3-4 A). No significant changes in mRNA levels were observed in control cells (figure 3-4 B). We also tested the expression of RNA Pol II-transcribed *Tb*PGI (a glycolytic protein), *Tb*RPS15 (a ribosomal protein), and the RNA Pol I-transcribed rRNA. Expression of these genes was unaffected upon depletion of *Tb*RAP1, suggesting that *Tb*RAP1's effect on *VSGs* is specific. Western analysis confirmed depletion of *Tb*RAP1 and expression of VSG2 protein by day 2 following induction (figure 3-4 C). Levels of *Tb*TRF (*Tb*RAP1-interacting partner and another telomeric protein) remained unchanged upon depletion of *Tb*RAP1. Induction of *Tb*TRF RNAi in PF cells leads to growth arrest by day 2 (Li et al.

2005). We did not detect any VSG2 expression upon depletion of *Tb*TRF (figure 3-4 C right), suggesting that *VSG* derepression is not a consequence of cell growth arrest and that *Tb*RAP1 is required for *VSG* silencing in PF *T. brucei* cells. We also tested steady state mRNA levels of two representative *VSGs* in the PRi-C2 clone to further confirm this phenotype. Several hundred-fold of derepression was observed for both tested *VSGs* while rRNA expression was unaffected (figure 3-4 D). In addition to ES-linked *VSGs*, *VSGs* are also present on subtelomeric regions of minichromosomes. Minichromosomes mostly contain 177 bp repeats and terminal telomere repeats. The *VSGs* located on minichromosomes lack upstream promoters.

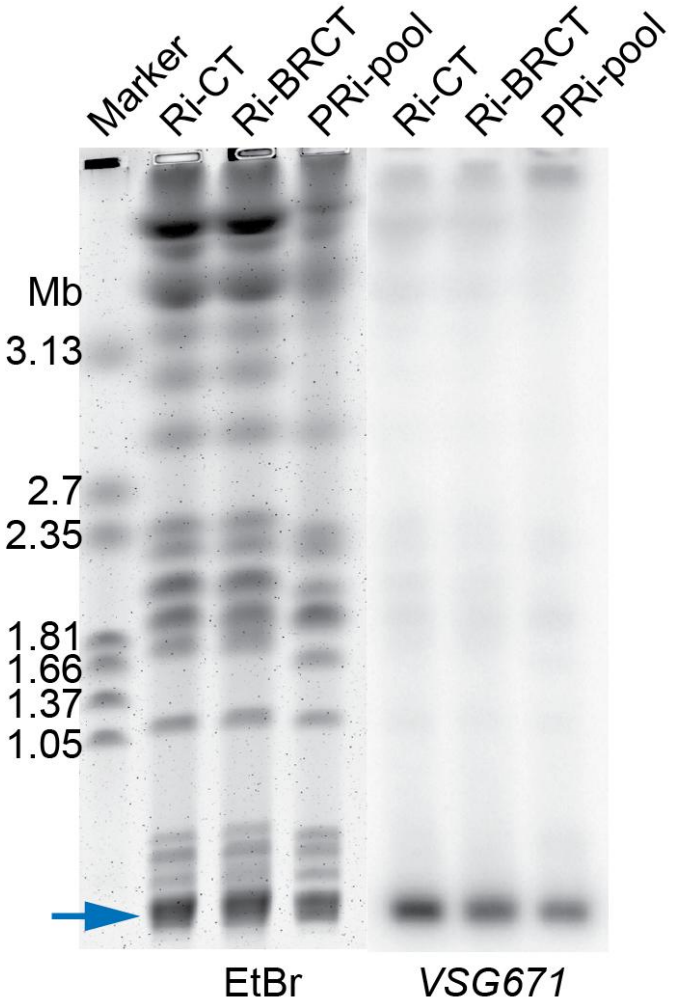

Figure 3-5: Detection of *VSG671* on minichromosomes. Southern blot analysis was performed to test the presence of *VSG*671 on minichromosomes in BF (Ri-CT and Ri-BRCT) and PF (PRi-pool) RAP1 RNAi cells. Pulsed field gel electrophoresis was performed followed by hybridization with *VSG671* probe (right panel). The EtBr stained-gel is depicted on the left. Arrow indicates minichromosome species.

DNA plugs were made from BF and PF *Tb*RAP1 RNAi cells. Pulsed field gel electrophoresis was performed using these plugs under conditions that separate intact *T. brucei* chromosomes (Li et al. 2005). *VSG671* was detected on minichromosomes in all three *Tb*RAP1 RNAi cell lines (figure 3-5). We subsequently tested whether *VSG671* is derepressed upon depletion of *Tb*RAP1 in PRi-pool cells. No *VSG671* mRNA was detected in the northern blot analysis (data not shown) after knockdown of *Tb*RAP1, suggesting that derepression of *VSG* requires functional upstream promoter.

TbRAP1 is required for silencing mVSGs in PF cells.

Metacyclic VSGs (mVSGs) are major surface proteins expressed in the metacyclic form of *T. brucei* in salivary glands of the tsetse fly. The *mVSGs* are expressed from subtelomerically located monocistronic expression sites. The *mVSGs* are silent in both PF and BF forms. However, their silencing mechanisms are not understood. Five *mVSG* genes (*mVSG 397, 531, 639, 653,* and *1954*) were identified in our lab strain (Kolev et al. 2012). We wanted to determine whether *Tb*RAP1 plays a role in silencing *mVSGs* in PF and BF *T. brucei* cells.

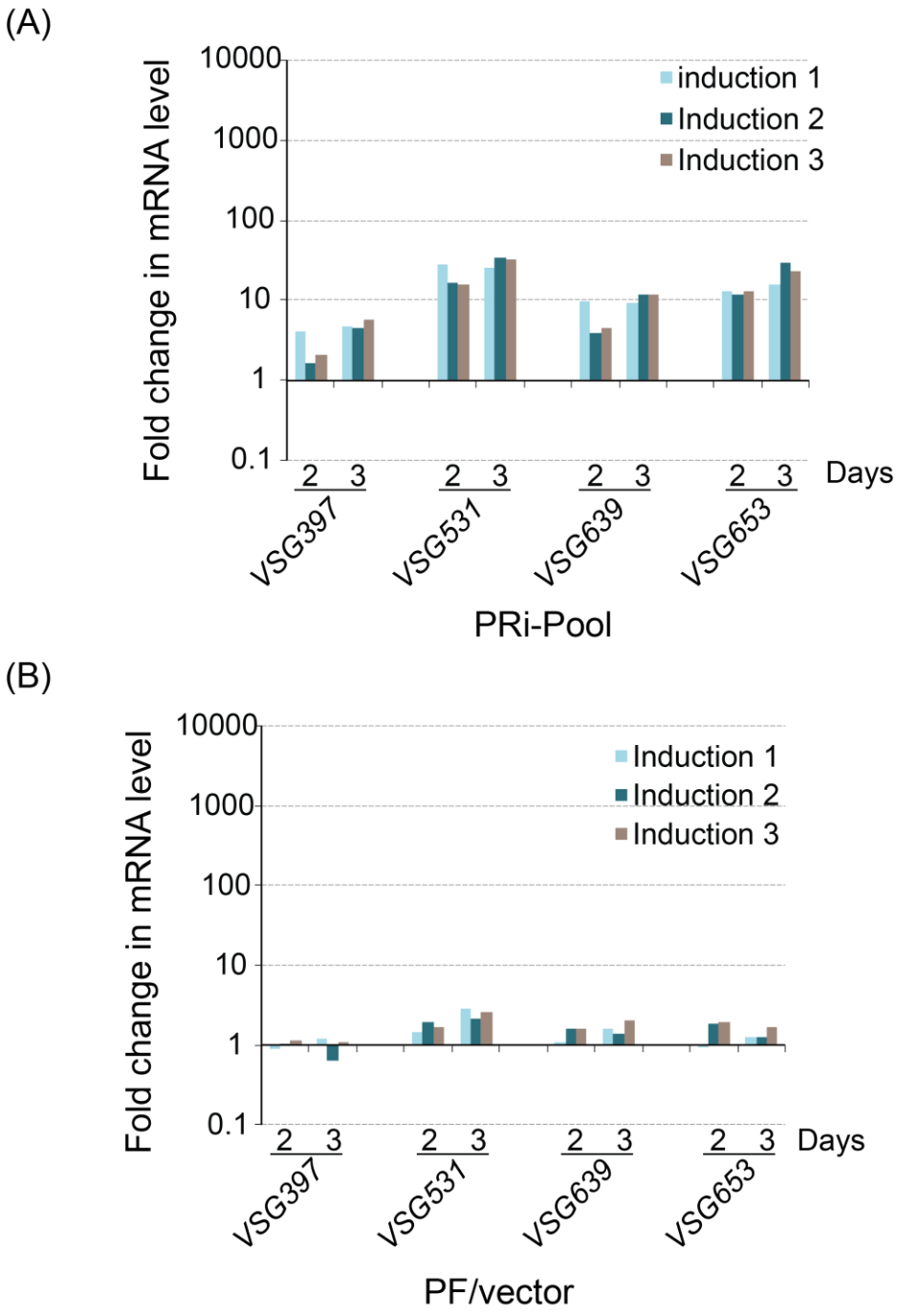

Figure 3-6: Silencing of *mVSGs* in PF cells. (A) Steady state levels of *mVSG* mRNA was measured before (day 0) and after (day 2, 3) depletion of *Tb*RAP1 in PRi-pool (A) and control cells (B) using qRT-PCR analysis. Fold change is calculated for day 2 & 3 compared to that of day 0 value, which is set to 1 but not shown. Values for three independent induction experiments are shown.

Upon depletion of *Tb*RAP1 in PF cells, steady state levels of all tested *mVSGs* increased from several to several 10-fold. In control, no change in steady-state mRNA levels of *mVSGs* was detected. These results indicated that *Tb*RAP1 not only plays a role in silencing ES-linked *VSGs* but also is required for silencing *mVSGs* in PF cells.

TbRAP1 is required for silencing mVSGs in BF cells.

We wanted to test whether *Tb*RAP1 is also required for silencing *mVSGs* in BF *T. brucei* cells. Two BF *Tb*RAP1 RNAi cell lines were generated. One cell line had expressed the pZJMβ-based RNAi construct (Wang et al. 2000) containing the BRCT domain of *Tb*RAP1 (Ri-BRCT) while the other the RCT domain (Ri-CT) inserted into the rDNA spacer region. Since these cell lines were not previously characterized, we decided to confirm critical phenotypes of *Tb*RAP1 depletion in these cell lines first.

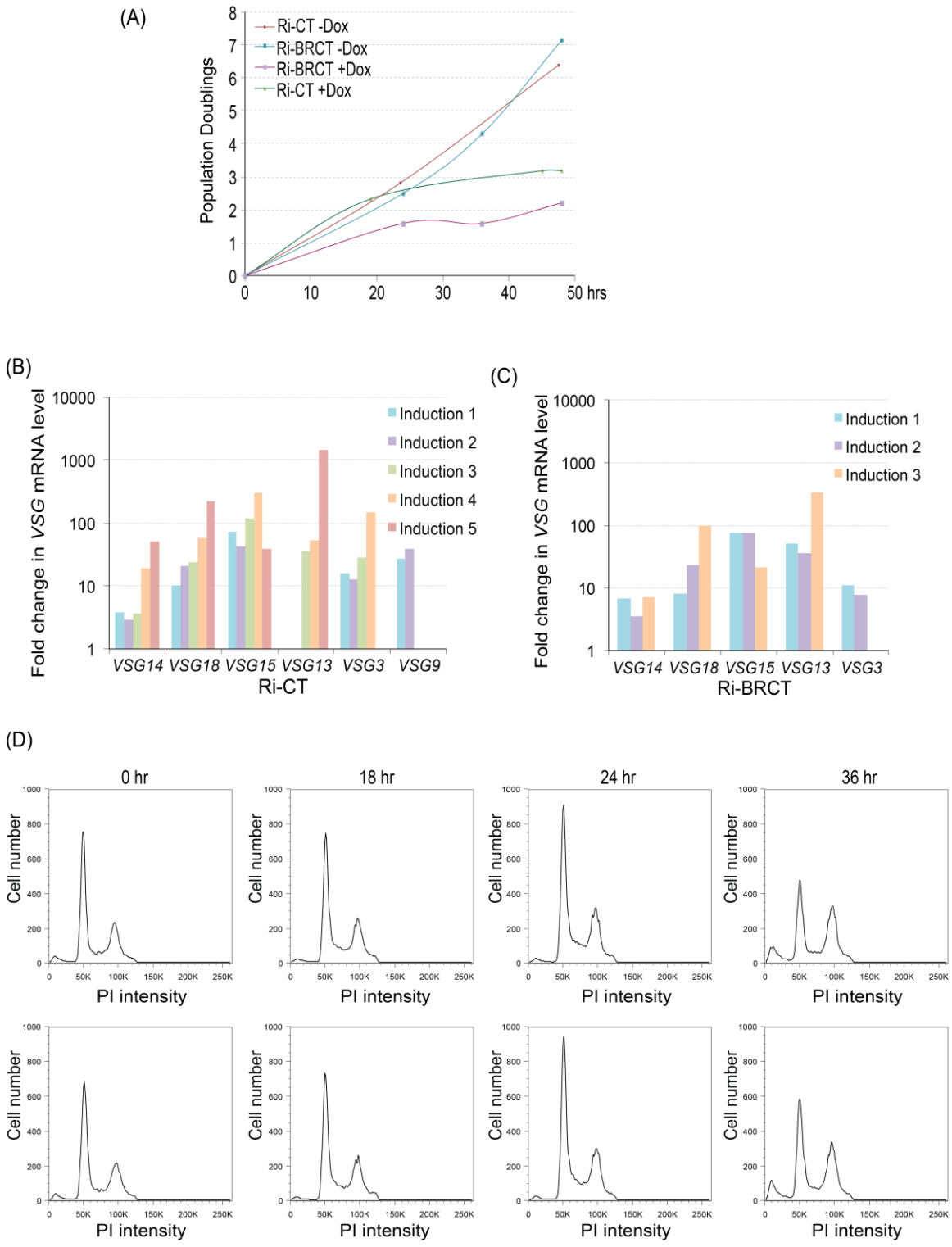
(A)
Ri-CT -Dox
Ri-BRCT -Dox
Ri-BRCT +Dox
Ri-CT +Dox
Population Doublings
0 10 20 30 40 50 hrs
(B)
Fold change in VSG mRNA level
Induction 1
Induction 2
Induction 3
Induction 4
Induction 5
VSG14 VSG18 VSG15 VSG13 VSG3 VSG9
Ri-CT
(C)
Fold change in VSG mRNA level
Induction 1
Induction 2
Induction 3
VSG14 VSG18 VSG15 VSG13 VSG3
Ri-BRCT
(D)
0 hr
18 hr
24 hr
36 hr
Cell number
PI intensity

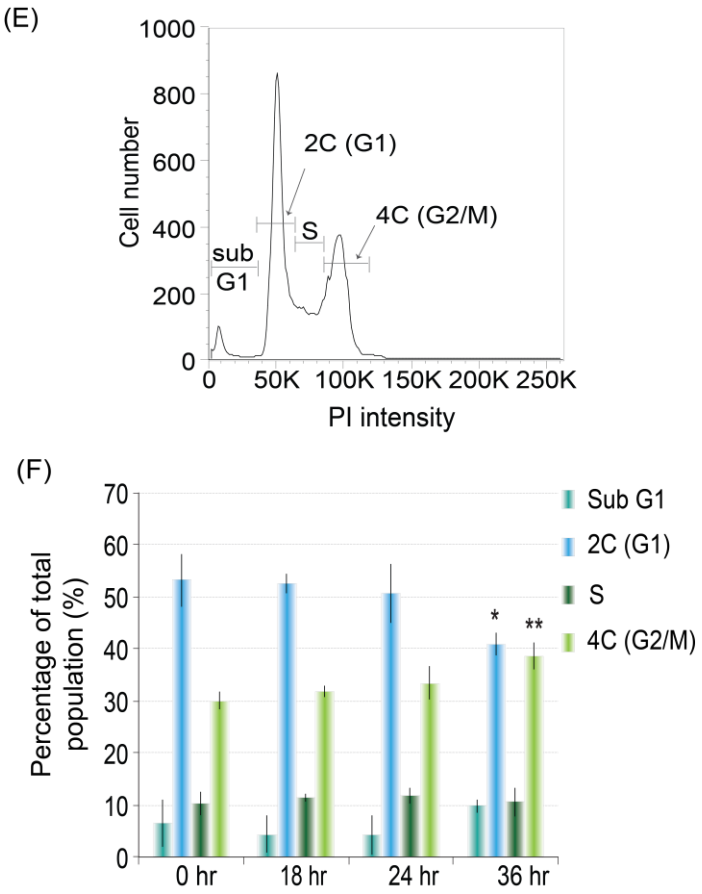

Figure 3-7: Depletion of *Tb*RAP1 in the BF cells. (A) A representative growth curve of the two *Tb*RAP1 RNAi strains (Ri-CT & Ri-BRCT). The population doubling was calculated in the presence (+) or absence (-) of doxycycline (Dox). (B) & (C) qRT-PCR analysis to determine steady state levels of ES-linked *VSGs* in Ri-CT & Ri-BRCT cell lines respectively. Values were calculated before (0 hr) and after (24 hr) depletion of *Tb*RAP1. Fold change in mRNA levels was calculated compared to day 0. Results for 5 (Ri-CT) and 3 (Ri-BRCT) independent experiments are shown. (D) Flow cytometry analysis for the Ri-CT cell line. Results from two independent analyses are shown. Cells were analyzed before (0 hr) and after (18, 24, & 36 hr) depletion of *Tb*RAP1. (E) Gating schematics of uninduced BF cells. The Sub-G1 population refers to cells having DNA content less than 2C, which often experienced DNA degradation. (F) Quantification of the cell population at various cell cycle stages of the Ri-CT cells before (0 hr) and after (18, 24, & 36 hr) depletion of *Tb*RAP1. P values were calculated to compare 18, 24 & 36 hr values with 0 hr value using unpaired t-test. *, $0.01<P\leq 0.05$; **, $0.001<P\leq 0.01$.

Upon depletion of *Tb*RAP1 growth arrest was observed in both strains by 30 hours (figure 3-7 A). Steady state mRNA levels of various ES-linked *VSGs* were tested before and after induction. As previously published (Yang et al. 2009), an increase in *VSG* mRNA levels from several ten- to several hundred-fold was observed after depleting *Tb*RAP1 from both strains (figure 3-7 B & C). FACS analysis showed a slight decrease in the proliferation of cells in G1 phase and, an increase in G2/M and sub G1 phase.

After it was proved that these newly established *Tb*RAP1 RNAi strains give similar phenotypes as previously published, we decided to use them for further experimentation. The role of *Tb*RAP1 in silencing *mVSGs* in BF cells was tested by collecting total RNA before (0 hr) and after (24 hr and 36 hr) depletion of *Tb*RAP1. By 24 hr only 6% *Tb*RAP1 was left in the Ri-CT cells while 26% was left in the Ri-BRCT cells. The RNA collected was then subjected to reverse transcription and steady state mRNA levels of various *mVSGs* were determined using specific primers in qRT-PCR analysis. Derepression of *mVSGs* was observed from several to over 1000-fold upon depletion of *Tb*RAP1 (figure 3-8 A & B). No change in *mVSG* mRNA levels was observed in control cells (figure 3-8 C). Expression of control genes such as rRNA and *Tb*PGI remain unaffected upon depletion of *Tb*RAP1. Thus, these results proved that *Tb*RAP1 is required for ES-linked as well as metacyclic *VSG* silencing in BF cells.

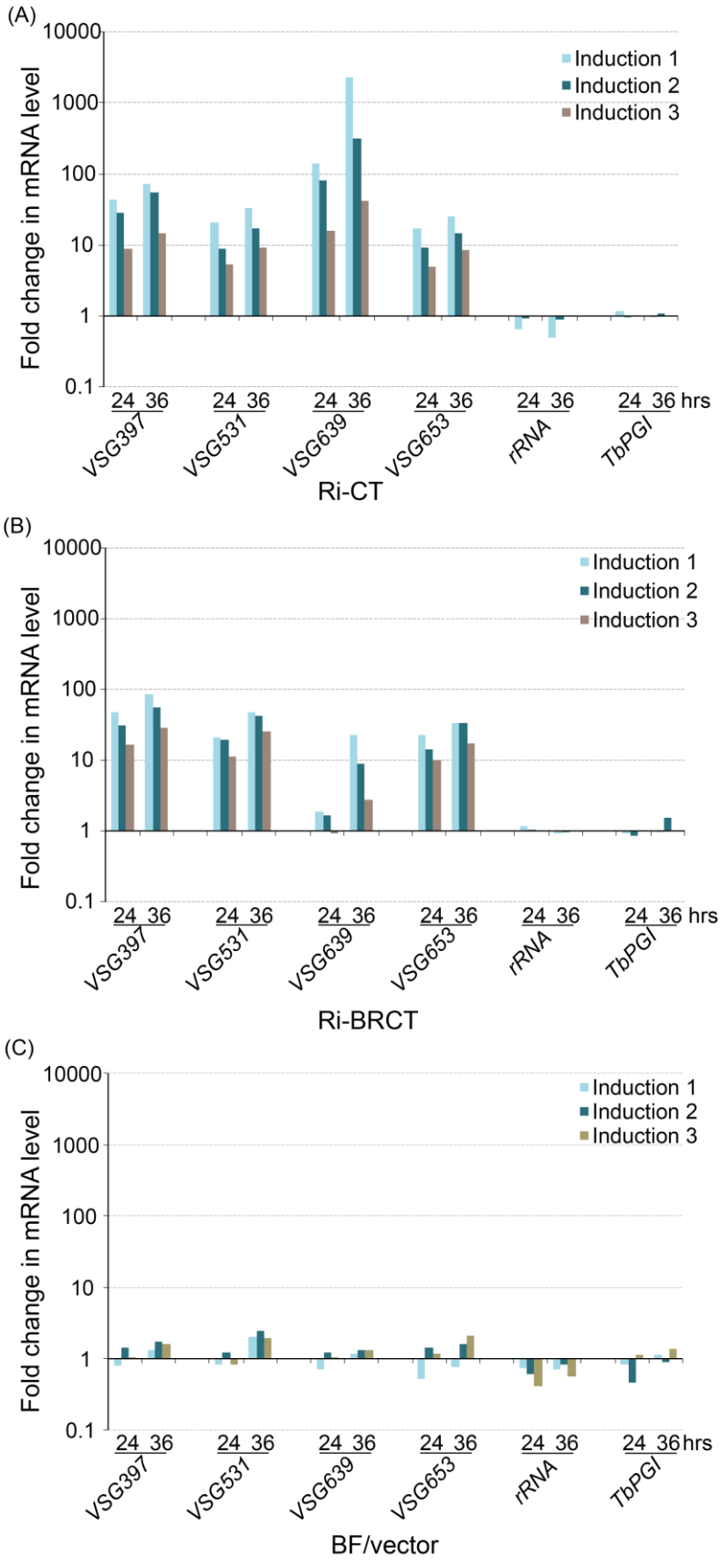
(A)
Fold change in mRNA level
10000
1000
100
10
1
0.1
Induction 1
Induction 2
Induction 3
24 36 hrs
VSG397
VSG531
VSG639
VSG653
rRNA
TbPGI
Ri-CT
(B)
Fold change in mRNA level
Induction 1
Induction 2
Induction 3
Ri-BRCT
(C)
Fold change in mRNA level
Induction 1
Induction 2
Induction 3
BF/vector

Figure 3-8: Silencing of *mVSGs* in BF cells. qRT-PCR analysis to measure steady state mRNA levels of *mVSGs* in (A) Ri-CT, (B) Ri-BRCT & (C) control cells before (0 hr) and after (24 hr and 36 hr) depletion of *Tb*RAP1. Fold change in mRNA level was calculated after depletion compared to that of 0 hr whose value is set to 1 and not shown. Values for three independent experiments are shown.

Comparison of TbRAP1-mediated ES-linked VSG silencing at different life cycle stages

Our results suggest that *Tb*RAP1 is required for silencing ES-linked *VSGs* in both PF and BF cells. However, it seems that derepression of ES-linked *VSGs* in PF is much stronger than that in BF. From our previous studies in BF cells (Yang et al. 2009), we know that *VSG* 3, 6, and 11 were derepressed up to 8-, 23- and 41-fold respectively upon depletion of *Tb*RAP1. Whereas in PF cells, upon depletion of *Tb*RAP1, the same *VSGs* were de-repressed up to 270-, 220-, and 260- fold respectively (figure 3-4 A).

In order to better quantify these differences, we decided to perform a comprehensive qRT-PCR analysis. We wanted to test and compare individual ES-linked *VSG* mRNA level under different conditions: i) at the silent state in WT/PF and WT/BF cells, ii) at the derepressed state in PF and BF *Tb*RAP1 RNAi cells, and at iii) the fully active state in BF cells. Total RNA was collected and subjected to reverse transcription followed by qRT-PCR analysis. *VSG* 2, 3, and 9 were tested owing to availability of all the necessary cell lines in our laboratory.

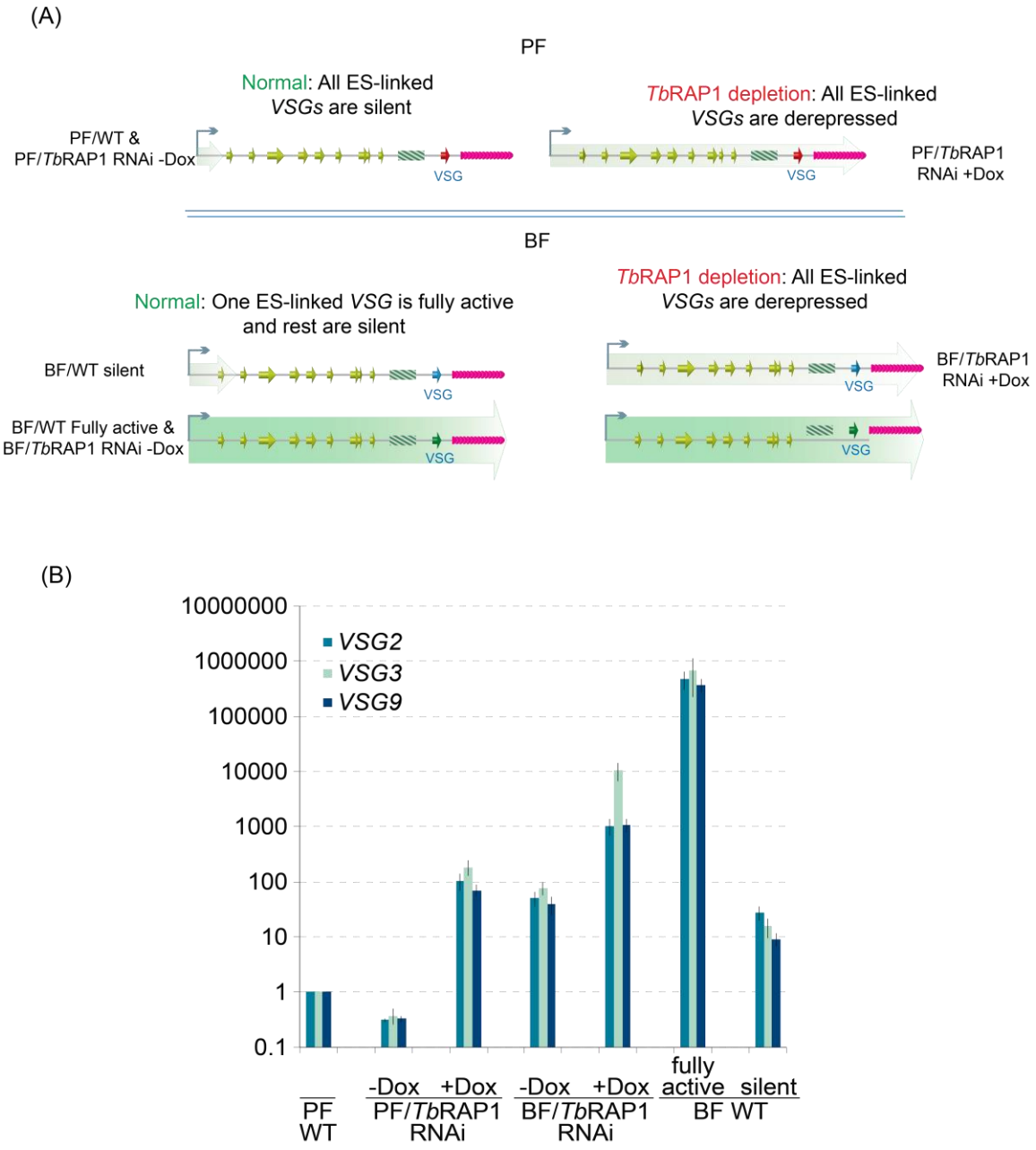

Figure 3-9: Strength of *Tb*RAP1 mediated *VSG* silencing at PF and BF stages. (A) Schematic representation of the status of ES-linked *VSGs* in various scenarios. (B) Quantification of qRT-PCR analysis for relative mRNA levels of the same *VSG* in various backgrounds. All the values were normalized to that of the PF WT silent state, whose value was arbitrarily set to 1. The average value was calculated from five independent experiments. Error bars represent standard deviation. *VSG* derepression was analyzed at day 0 & day 2.5 in PRi-pool cells. Derepression of *VSG* 3 and 9 in BF cells were analyzed at 0 hr & 36 hr in cells originally expressing *VSG2* (Ri-2 cells). While derepression of *VSG2* was analyzed at the same time points in cells originally expressing *VSG9* (Ri-9 cells). For fully active state, three BF WT cells were used: i) *VSG2* expresser (SM cells)

(Wirtz et al. 1999), ii) *VSG9* expresser (PVS3-2/OD1-1 cells) (Yang et al. 2009) and iii) *VSG3* expresser (SM-derived cell lines).

Several conclusions were obtained from qRT-PCR analysis. 1) Steady state mRNA levels of *VSG* were 28-, 16- and 9-fold higher in the WT BF cells compared to the WT PF cells (figure 3-9 B PF/WT and BF/WT silent) respectively. It is known that *VSG* mRNAs are less stable in PF cells than in BF cells where they are prevented from degradation (Berberof et al. 1995). Hence, this could contribute to our observation. 2) *Tb*RAP1 is required for ES-linked *VSG* silencing in both the PF and BF cells since *VSG* derepression was observed upon its depletion. 3) This derepression observed due to depletion of *Tb*RAP1 is significantly stronger in PF than in BF cells. *VSG* mRNA levels were elevated on an average 333-, 527-, and 217-fold, respectively, in PF. In BF cells, proven derepression was on an average 22-, 133-, and 30-fold, respectively (figure 3-9 B, PF/*Tb*RAP1 RNAi -/+Dox, BF/*Tb*RAP1 RNAi -/+Dox). P values were all <0.02 when comparing derepression of *VSG* 2, 3, and 9 in BF to that in PF cells. Thus *Tb*RAP1-mediated *VSG* silencing is stronger in PF cells than that in BF cells. We observed that *VSG* mRNA level is ~3 fold lower for the uninduced PRi-pool cells (PF/*Tb*RAP1 RNAi –Dox) compared to PF WT cells, while theoretically it should be the same. This observation could be due to variations between different cell populations.

In yeast, longer telomere results in stronger telomeric silencing (Kyrion et al. 1993). It is possible that different strength of *Tb*RAP1-mediated *VSG* silencing in the PF and BF could be due to different telomere length. However, the PF and BF strains used in this study have similar length of telomeres (on average ~15

kb) suggesting that telomere length is not the contributing factor. Another possibility is that *Tb*RAP1 might not be equally depleted in PF and BF cells, resulting in different levels of *VSG* derepression in both forms. To rule out this possibility, we tested and compared *Tb*RAP1 protein levels within all the *Tb*RAP1 RNAi cell lines used for this study.

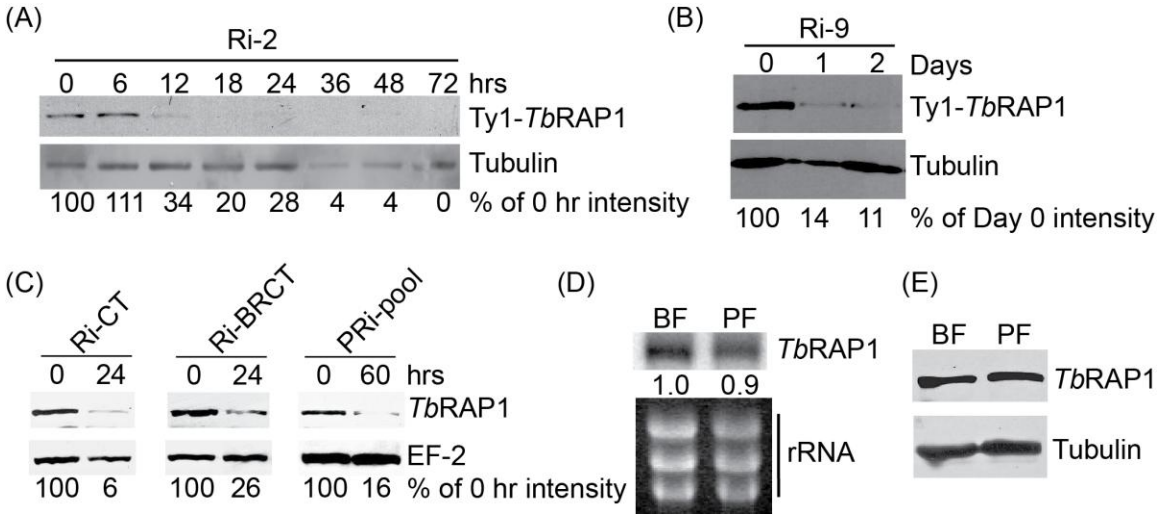

Figure 3-10: Depletion of *Tb*RAP1 in PF and BF cells. (A-C) Representative western blot analysis to determine depletion of *Tb*RAP1. Whole cell lysate was collected before (0 hr) and after depletion of *Tb*RAP1 in Ri-2 (A), Ri-9 (B), Ri-CT, Ri-BRCT and PRi-pool cells (C). Tubulin and EF-2 were used as loading control. Numbers below blots indicate the average relative amount of *Tb*RAP1 protein levels. These numbers were calculated from 2 (Ri-2 and Ri-9) or 3 (Ri-CT, Ri-BRCT, and PRi-pool) independent experiments. (D) Northern analysis to determine the relative mRNA levels of *Tb*RAP1 in BF and PF cells. rRNA is shown as loading control. Numbers indicate relative ratio of *Tb*RAP1 mRNA level. (E) Western blot analysis to determine relative protein levels of *Tb*RAP1 in the BF and PF cells. Tubulin was used as a loading control.

RNA samples were collected at 36 hr (for Ri-2 and Ri-9 cells), and at 60 hr (for PRi-pool cells). From figure 3-10 A-C, it is evident that comparative residual amount of *Tb*RAP1 was left in all the cell lines at respective time points. On an average, 4% *Tb*RAP1 was left in Ri-2 cells, 14-11% in Ri-9 cells, and 16% was left in PRi-pool cells. Thus, it is unlikely that differential derepression of ES-linked *VSGs* in PF and BF cells is due to different levels of *Tb*RAP1 depletion. We further confirmed that *Tb*RAP1 mRNA and protein levels are equal in both life cycle stages (figure 3-10 D and E). Collectively, these results suggest that, indeed, *Tb*RAP1-mediated silencing is stronger in PF compared to that in BF. Such differential strength of silencing was not observed for *mVSGs* between both forms.

TbRAP1 depletion led to more open chromatin structure in PF cells.

Next, we wanted to test whether *Tb*RAP1-mediated *VSG* silencing involves chromatin remodeling. In order to test this, FAIRE (formaldehyde assisted isolation of regulatory elements) was performed (Giresi et al. 2009). In FAIRE, cells are cross-linked, lysed, and sonicated followed by the phenol-chloroform extraction. Protein-free DNA fragments are enriched in the aqueous phase, while protein-bound DNA is retained at interphase. DNA from aqueous phase is subsequently isolated. PCR analysis can then be done to estimate enrichment of protein-free DNA fragments of interest. We were interested in testing whether chromatin of subtelomeric ES-linked *VSGs* is more opened up (hence devoid of bound protein) upon depletion of *Tb*RAP1. FAIRE was performed to isolate protein-free DNA before and after depletion of *Tb*RAP1. Quantitative PCR using

primers specific for various *VSGs* was performed to calculate the amount extracted. Fold change was calculated by dividing values obtained post-*Tb*RAP1 depletion by those obtained before depletion.

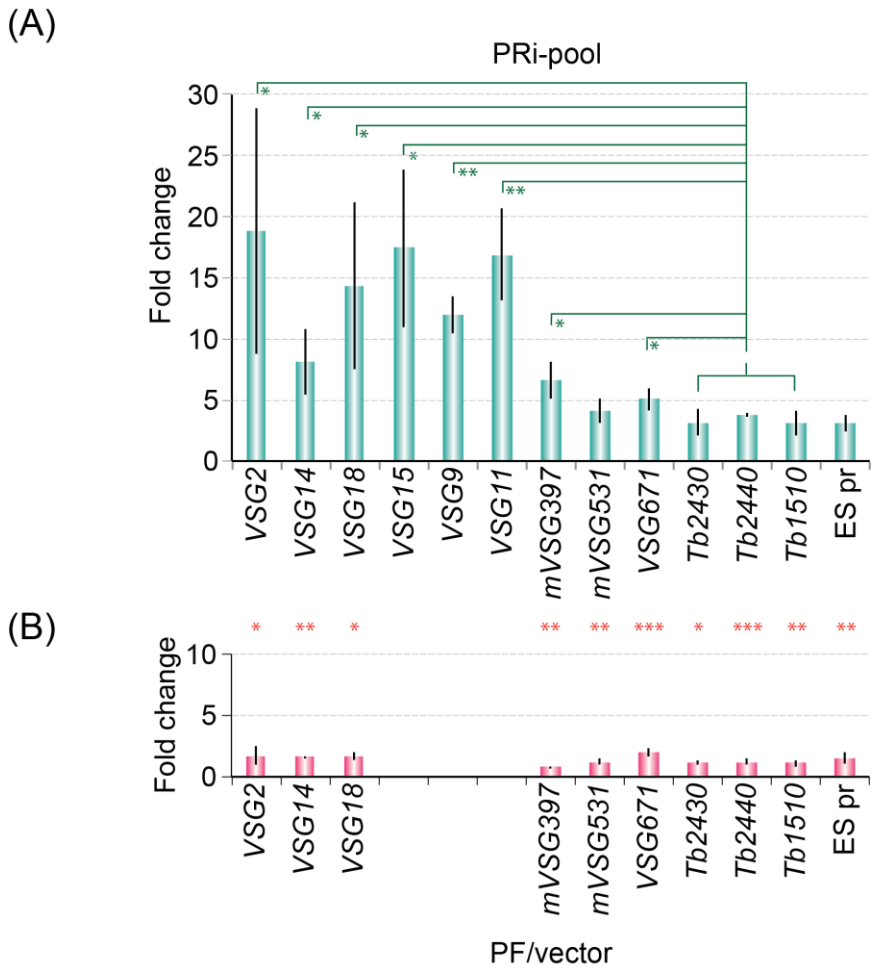

Figure 3-11: Depletion of *Tb*RAP1 led to a more loosened chromatin structure in the PF cells. FAIRE was performed before (day 0) and after (day 2.5) depletion of *Tb*RAP1 in (A) PRi-pool cells and (B) control cells. Quantitative PCR was done using primers specific to the indicated gene loci. Fold change was calculated from at least three independent experiments. Error bars represent standard deviation. In PRi-pool cells, P-values were calculated by comparing ES-linked *VSG* changes with the change of chromosome internal genes. Significant differences (P<0.05) are indicated with asterisks. P-values were also calculated for each gene between PRi-pool cells and the control cells shown by asterisks between corresponding columns from two histograms. Control genes are

indicated with the last four digits of their ID. *Tb927.2.2430*, *Tb927.2.2440, Tb09.211.1510.* *, $0.01<P\leq 0.05$; **, $0.001<P\leq 0.01$, ***, $P\leq 0.001$

FAIRE was performed in *Tb*RAP1 depleted PRi-pool cells. Upon depletion of *Tb*RAP1 8- to 19-fold increase in the enrichment of ES-linked *VSGs* was observed compared to that in the control cells. An increase in the enrichment of *mVSG* DNA of 4- to 7-fold was also observed. These differences were significantly higher compared to that in control cells. In order to determine that this effect of *Tb*RAP1 depletion is telomere specific, we also tested enrichment of DNA at several random chromosome-internal genes. A 3- to 4-fold increase in FAIRE-extracted DNA was observed at these loci, which are modest yet significantly higher than that in control cells. However, the enrichment at ES-linked loci (8- to 9-fold) was significantly higher compared to the chromosomal internal loci (3- to 4-fold), suggesting that *Tb*RAP1 has a more prominent effect on chromatin structure at subtelomeric loci. The BES promoter lies 40-60 kb upstream of the telomeres. *Tb*RAP1 depletion led to ~3-fold enrichment in FAIRE extracted DNA, which is similar to that of the chromosome internal loci.

It is possible that this change in chromatin structure could be due to an elevated transcription, rather than directly due to the loss of *Tb*RAP1. In order to test this possibility, the chromatin structure change of *VSG671* locus was examined before and after depletion of *Tb*RAP1. *VSG671* is located on a minichromosome and lacks an upstream promoter. Hence, it is not derepressed upon *Tb*RAP1 knockdown. An approximately 5-fold increase in FAIRE-extracted DNA was observed for *VSG671,* which is significantly higher compared to that in

control cells as well as chromosome internal loci, suggesting that the change in chromatin compaction upon *Tb*RAP1 depletion is not due to elevated transcription.

Subsequently, FAIRE analysis was also performed in BF cells to test whether *Tb*RAP1 has a similar effect on chromatin structure as that observed in the PF cells.

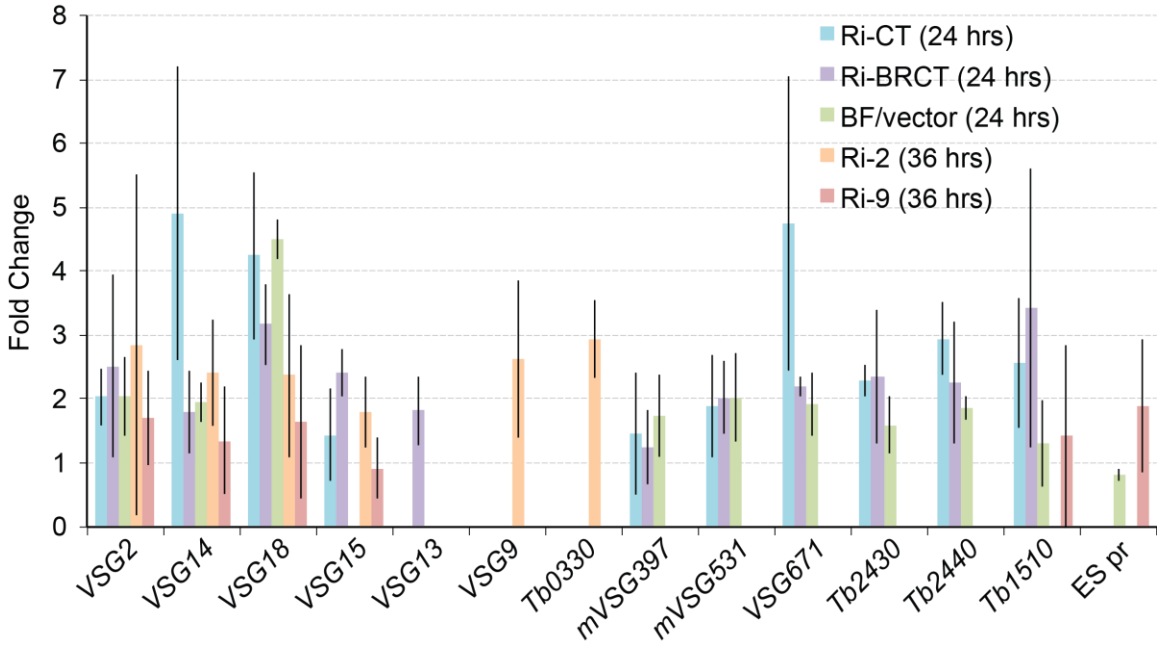

Figure 3-12: FAIRE analysis in BF cells. FAIRE was performed before (0 hr) and after (24 hr in Ri-CT, Ri-BRCT and control cells; 36 hr in Ri-2 and Ri-9 cells) depletion of *Tb*RAP1. Quantitative PCR was done using primers specific to indicated gene loci. Fold change was calculated from at least three independent experiments. Error bars represent standard deviation. Control genes used are *Tb11.0330*, *Tb927.2.2430*, *Tb927.2.2440, and Tb09.211.1510.*

FAIRE was performed in four independent *Tb*RAP1 RNAi cell lines (Ri-CT, Ri-BRCT, Ri-2 and Ri-9) as well as empty vector control cells. Fold change in FAIRE-extracted DNA was calculated for ES-linked *VSGs*, *mVSGS*, a minichromosome *VSG* (VSG*671*), ES promoter region and control genes. A moderate increase of 2- to 3-fold was observed for ES-linked *VSGs*, *mVSGs,* and a minichromosome *VSG,* which was not significantly different from that observed in the control cells. Also, a very small change of 1- to 3-fold was observed for the ES promoter and chromosome internal loci, which was similar to that observed in the control cells. P-values were calculated to compare ES-linked *VSGs* with chromosome internal loci within *Tb*RAP1 RNAi cells and to compare all loci between *Tb*RAP1 RNAi and control cells. All calculated P-values were >0.05, indicating that the changes in chromatin structure observed in BF cells are not significant. Thus, unlike PF cells, *Tb*RAP1 depletion in BF cells does not lead to significant changes in chromatin structure.

This difference in observed phenotype was not due to different degrees of *Tb*RAP1 depletion. This observation was confirmed by performing western blot analysis. At the time points when FAIRE was performed, protein levels of *Tb*RAP1 were around 4% for Ri-2 (figure 3-10 A), 10% for Ri-9 (figure 3-10 B), 6% for Ri-CT, 26% for Ri-BRCT, and 16% for the PRi-pool cells of wild-type level (figure 3-10 C). This finding indicates that *Tb*RAP1 was depleted in PF and BF cells at similar levels.

In order to confirm that *Tb*RAP1 depletion has different effects on chromatin structure in PF and BF cells, we performed a Micrococcal nuclease (MNase)

digestion assay. Ranjodh Sandhu, another graduate student from our lab, did this part of work. MNase digestion was performed to test accessibility of chromatin before and after depletion of *Tb*RAP1. *Tb*RAP1 RNAi cells in the PF and BF cells, as well as the control cells were treated with a fixed amount of Mnase for increasing length of time before and after depletion of *Tb*RAP1. Genomic DNA was then isolated and separated on an agarose gel. We subsequently performed Southern blot analysis by blotting DNA samples on nylon membranes followed by hybridization with probes specific to different loci.

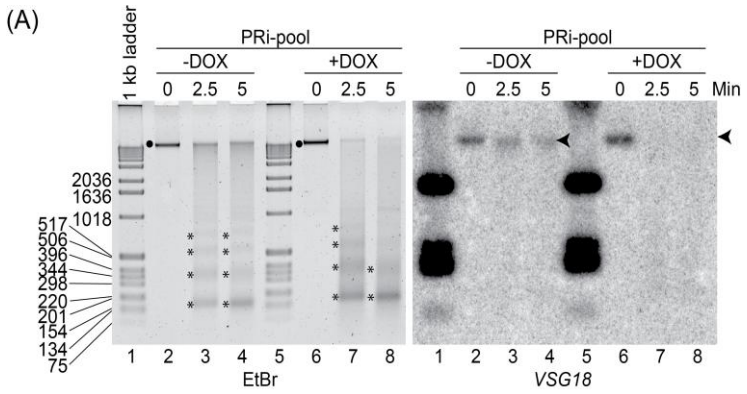
(A)
1 kb ladder
PRi-pool
-DOX
+DOX
0 2.5 5 0 2.5 5
PRi-pool
-DOX
+DOX
0 2.5 5 0 2.5 5 Min
2036
1636
1018
517
506
396
344
298
220
201
154
134
75
1 2 3 4 5 6 7 8
EtBr
1 2 3 4 5 6 7 8
VSG18

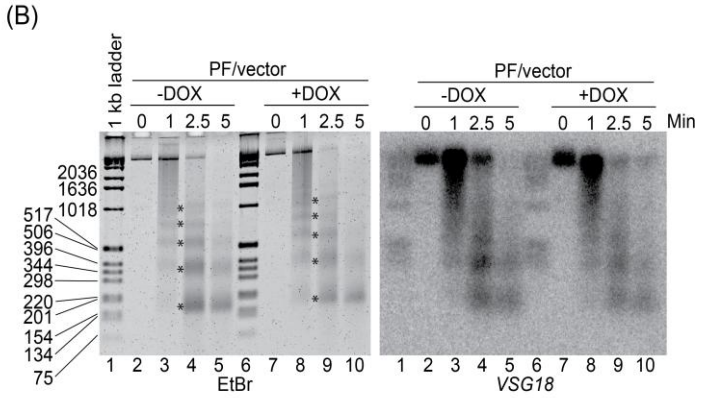
(B)
1 kb ladder
PF/vector
-DOX
+DOX
0 1 2.5 5 0 1 2.5 5
PF/vector
-DOX
+DOX
0 1 2.5 5 0 1 2.5 5 Min
2036
1636
1018
517
506
396
344
298
220
201
154
134
75
1 2 3 4 5 6 7 8 9 10
EtBr
1 2 3 4 5 6 7 8 9 10
VSG18

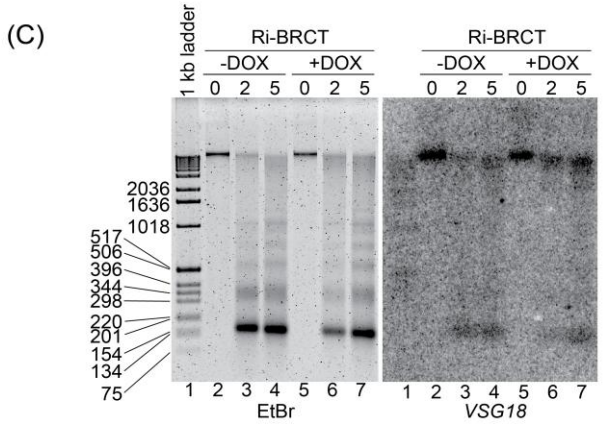
(C)
1 kb ladder
Ri-BRCT
-DOX
+DOX
0 2 5 0 2 5
Ri-BRCT
-DOX
+DOX
0 2 5 0 2 5
2036
1636
1018
517
506
396
344
298
220
201
154
134
75
1 2 3 4 5 6 7
EtBr
1 2 3 4 5 6 7
VSG18

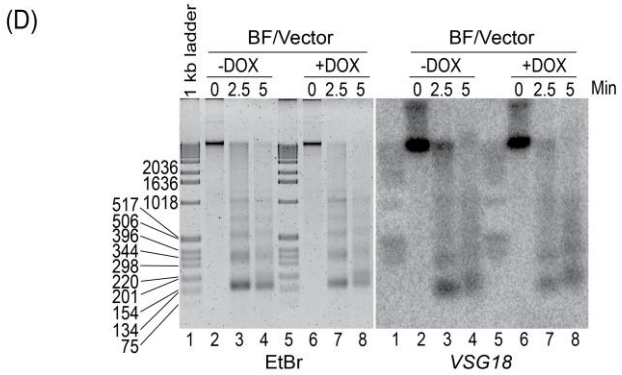
(D)
1 kb ladder
BF/Vector
-DOX
+DOX
0 2.5 5 0 2.5 5
BF/Vector
-DOX
+DOX
0 2.5 5 0 2.5 5 Min
2036
1636
1018
517
506
396
344
298
220
201
154
134
75
1 2 3 4 5 6 7 8
EtBr
1 2 3 4 5 6 7 8
VSG18

Figure 3-13: A micrococcal nuclease digestion to determine the chromatin structure changes. MNase assay was performed before and after depletion of *Tb*RAP1 in (A) PRi-pool cells (day 0 and day 2.5) (B) PF/Vector cells (day 0 and day 2.5) (C) Ri-BRCT (0 hr and 24 hr) (D) BF/Vector cells (0 hr and 24 hr). In each panel, the left panel shows an Ethidium Bromide-stained gel while the right panel shows the hybridization result with *VSG18* specific probe. Solid black dots and arrowheads represent the limiting mobility of genomic DNA in the agarose gel and Southern results, respectively. Asterisks indicate mono-, di-, tri-, and tetra-nucleosomes.

PRi-pool cells were treated with a fixed amount of MNase for increasing length of time. After 2.5-5 min, a portion of chromatin was digested into mono-, di-, tri- and tetra-nucleosomes. However, when *Tb*RAP1 was depleted, this digestion was much more rapid and by 5 minutes most of the chromatin was found in the mono-nucleosomal fraction (figure 3-13 A, compare lane 4 with lane 8 on the left). Control cells did not show any change in chromatin digestion upon adding doxycycline (figure 3-13 B, compare lane 5 with lane 10 on the left). This suggests that after depletion of *Tb*RAP1, the chromatin is more opened up and accessible to MNase digestion. Changes observed in chromatin digestion in the Ethidium Bromide- (EtBr)-stained gel suggested that *Tb*RAP1 depletion had a mild global effect. In order to test effects of *Tb*RAP1 knockdown on a specific locus, the MNase digested DNA was blotted from the agarose gel onto a nylon membrane and hybridized with the *VSG18* specific probe. In PRi-pool cells after *Tb*RAP1 depletion, the entire *VSG18* signal was lost by 2.5 minutes of digestion compared to before depletion (figure 3-13 A, compare lane 3 with lane 7 in right panel). The *VSG18*-specific signal remained unaffected upon adding doxycycline in control cells (figure 3-13 B, compare lane 5 with lane 10 in right panel). Thus it was proven that *Tb*RAP1 regulates *VSG* silencing in PF cells via chromatin

remodeling. We further performed a MNase assay for other ES-linked *VSGs*, *mVSGs,* and telomere DNA (Pandya et al. 2013). All of them gave similar results. *Tb*RAP1 depletion had a very mild effect on chromatin change at the ES promoter region. This was similar to the result of FAIRE analysis. The change in chromatin structure was also confirmed in PRi-C2 (independent PF/*Tb*RAP1 RNAi clone).

Interestingly, *Tb*RAP1 depletion had no affect on chromatin structure in BF when analyzed by MNase digestion. No change in the chromatin digestion was observed in EtBr-stained gels, before or after depletion of *Tb*RAP1 in Ri-BRCT cells (figure 3-13 C, compare lane 4 with lane 7 in the left panel). The digestion pattern was almost the same as that observed in control cells (figure 3-13 D, compare lane 4 with lane 8 in the left panel). We also tested the effect of *Tb*RAP1 depletion at the *VSG18* locus. No visible difference in the digestion pattern was seen between uninduced and induced cells (figure 3-13 C, compare lane 4 with lane 7 in the right panel, figure 3-13 D, compare lane 4 with lane 8 in the right panel). This phenotype was further confirmed for other ES-linked *VSGs*, *mVSGs,* and telomere repeats. No significant change in chromatin structure was detected, suggesting that *Tb*RAP1 does not affect chromatin structure significantly in BF cells.

TbRAP1 preferentially localizes to silent ES-marked telomeres (preliminary studies)

We wanted to test whether *Tb*RAP1 carries out silencing of *VSGs* in a cis-acting manner. Our previous observations indicated that the *Tb*RAP1-mediated

silencing effect is position-dependent, i.e. it is stronger at telomere-proximal loci than at telomere-distal loci (Yang et al. 2009). We wanted to test whether *Tb*RAP1-mediated silencing depends on the amount of *Tb*RAP1 protein associated with the local chromatin. If this is true, we expect that more *Tb*RAP1 protein is associated with the silent ES than the active ES-marked telomere in wild-type BF cells.

To test this hypothesis, we performed a *Tb*RAP1 chromatin immunoprecipitation (ChIP) experiment. The amount of the active ES-linked *VSG* DNA and a silent ES-linked *VSG* DNA co-immunoprecipitated with *Tb*RAP1 was estimated by quantitative PCR. The experiment was performed in two different ways. First, the same *VSG* was examined in different BF cell lines, where the *VSG* is either fully active or silent. Second, the active *VSG* and silent *VSGs* within the same cell line were examined to determine whether different amount *Tb*RAP1 binds to them. Immunoprecipitation was performed using an antibody against the endogenous *Tb*RAP1.

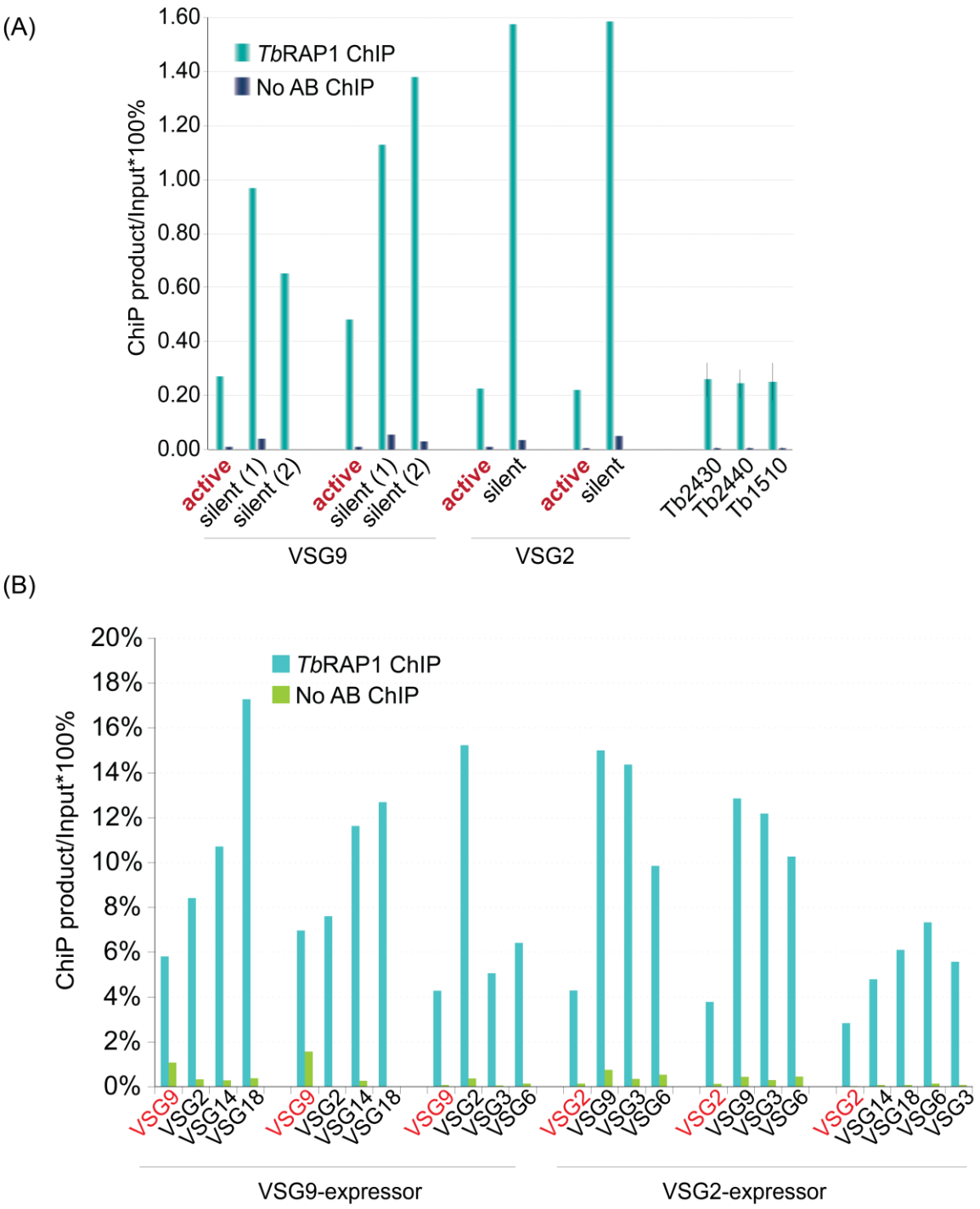

Figure 3-14: *Tb*RAP1 preferentially binds to the silent ES-marked telomere. (A) ChIP was performed in different BF cells lines where either *VSG9* is active (PVS3-2/OD1-1) or silent (SM and SM-derived cell line). Similar analysis was also done in BF cell lines where a different *VSG*, *VSG2,* is either active (SM) or silent (PVS3-2/OD1-1). After ChIP, quantitative PCR was performed using primers specific to *VSG9* and *VSG2* and the enrichment of the ES-linked *VSG* DNA was calculated as percent of input. Protein G beads with pre-immune serum

were used as a negative control. Three *VSG9* and two *VSG2* independent experiments are shown. As a control, enrichment of *Tb*RAP1 at three chromosome internally located gene was also estimaed in the same way. For control genes, average values were calculated from four independent experiments, and error bars represent standard deviation. Control genes are listed using the last 4 digits of their gene ID. Tb2430: Tb927.2.2430; Tb2440: Tb927.2.2440; Tb1510: Tb09.211.1510. (B) *Tb*RAP1 ChIP was performed in VSG9-expressors or VSG2-expressors and enrichment of various ES-linked *VSG*s (active and silent) was calculated as percentage of input. Protein G beads without any antibody was used as the negative control.

A *Tb*RAP1 ChIP was performed to follow the same *VSG* gene across multiple BF cell lines in which this *VSG* is either fully active or silent. We discovered that enrichment of the *VSG* DNA in the ChIP product is always lower in cells where it is fully active than in cells where it is silent. For example, enrichment of *VSG9* DNA in VSG9-expressors is always lower than that in two independent cell lines where *VSG9* is silent (figure 3-14 A). Similarly, enrichment of *VSG2* is always lower in VSG2-expressors compared to that in cells where *VSG2* is silent (figure 3-14 A). A ChIP experiment was also done to test binding of *Tb*RAP1 to active and silent ES-marked telomeres within the same cell line. Similar results were obtained with this approach. We found that enrichment of *VSG9* (active) was less compared to *VSG 2, 14, 18,* and *6* (silent) in VSG9-expressors (figure 3-14 B). Also, enrichment of *VSG2* (active) was less compared to *VSG 9, 3, 6, 14,* and *18* (silent) in VSG2-expressors.

As a control, we randomly selected three chromosome internally located genes, Tb927.2.2430, Tb927.2.2440, and Tb09.211.1510, and estimated the amount of their DNA co-immunoprecipitated with *Tb*RAP1 in the ChIP experiment. As shown in figure 3-14 A, a very low amount of these DNAs were detected in the *Tb*RAP1 ChIP product. The amount of precipitated control gene

DNA is similar to that of the active *VSGs*, suggesting that *Tb*RAP1 does not interact with the active *VSGs* at a significant extent.

It is not yet clear whether *Tb*RAP1 possesses any direct DNA binding ability. The current prevailing hypothesis is that, like hRAP1, *Tb*RAP1 depends on its interacting partner *Tb*TRF to be recruited to telomeres. *Tb*RAP1 was found to preferentially bind to silent ES-marked telomeres. We wanted to test whether *Tb*TRF mediates this preferential binding of *Tb*RAP1. If this is true, then *Tb*TRF will also binds preferentially more to silent ES-marked telomeres. In order to test this possibility *Tb*TRF ChIP was performed using an antibody against *Tb*TRF. The amount of the active ES-linked *VSG* DNA and a silent ES-linked *VSG* DNA co-immunoprecipitated with *Tb*TRF was estimated by quantitative PCR. ChIP was performed in VSG2-expressors (*VSG2* active). Enrichment of *VSG2* DNA as well as of *VSG 13, 14,* and *16* (silent *VSGs*) was estimated. Pull-down was also calculated for two control genes (Tb927.2.2430 and Tb927.2.2440) that are present at the chromosome internal regions.

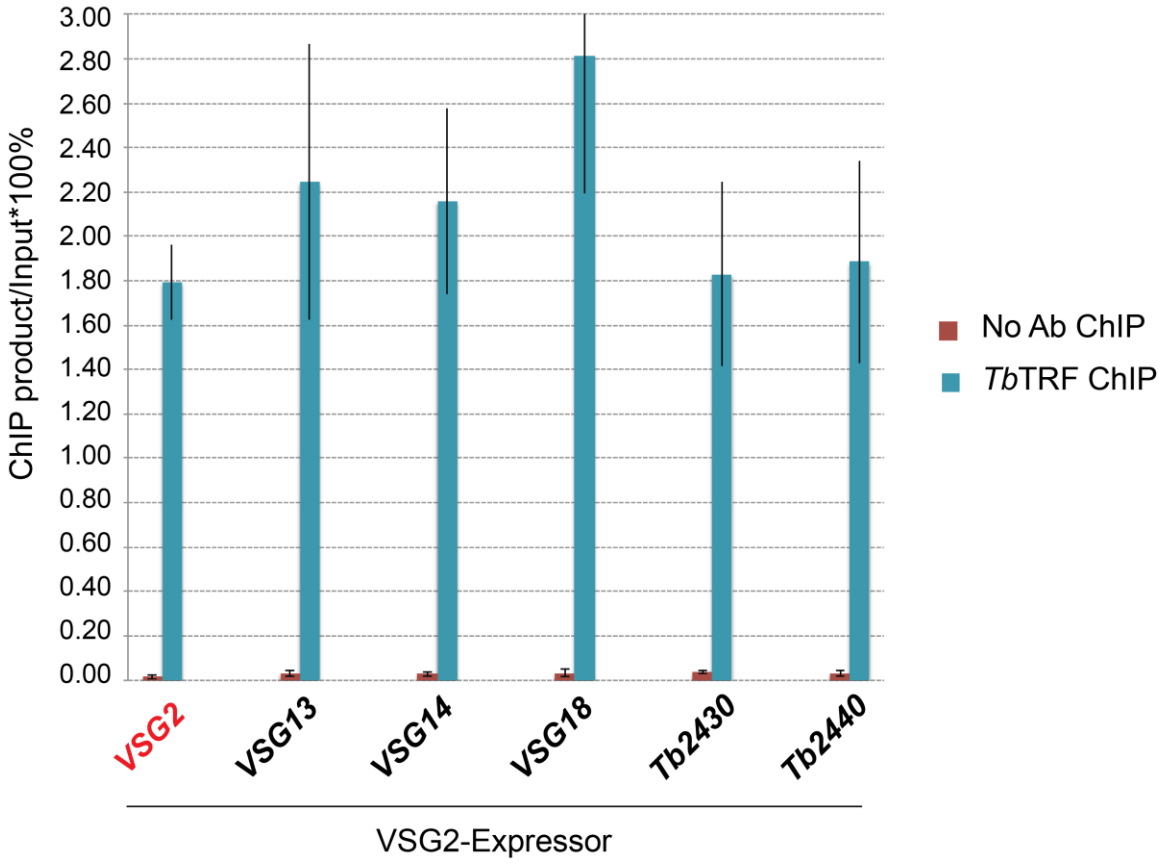

Figure 3-15: *Tb*TRF binding to subtelomeric *VSGs*. *Tb*TRF ChIP was performed in VSG2-expressors and enrichment of various ES-linked *VSG*s (active and silent) was calculated as percentage of input. Protein G beads without any antibody was used as a negative control. Average values were calculated from three independent experiments, and error bars represent standard deviation. Control genes are listed using the last 4 digits of their gene ID. Tb2430: Tb927.2.2430; Tb2440: Tb927.2.2440.

*Tb*TRF ChIP was performed in VSG2-expressors (*VSG2* active). As seen in figure 3-14, no significant difference in pull-down of active (*VSG2*) and silent *VSGs* (*VSG 13, 14,* and *18*) was observed, suggesting that *Tb*TRF does not differentially bind to silent ES-marked telomeres. Also, binding at all *VSGs* was almost equal to that seen for control genes (Tb2430 and Tb2440), suggesting that *Tb*TRF does not bind to *VSGs* in significant way and the binding observed is sequence non-specific. This result suggests that unlike *Tb*RAP1, probably *Tb*TRF does not spread towards the subtelomeric region. From our previously published IF data we know that all *Tb*TRF foci co-localizes with telomeres. However, not all *Tb*RAP1 foci co-localizes with *Tb*TRF, suggesting that *T*bRAP1 might be associated with non-telomeric chromatin (Li et al. 2005 and Yang et al. 2009).

*Tb*RAP1 ChIP will have to be repeated to determine whether *Tb*RAP1, preferentially associates with silent ES due to several reasons: i) There is a lot of variation in pull-down for the same *VSG* within different experiments, ii) In a few cases there is not a significant difference between pull-down of the active *VSG* and a silent *VSG* (figure 3-15 B, *VSG9* and *VSG2* in VSG9-exprssors). Owing to such differences it is hard to obtain a statistically significant value, although a clear trend does exist. More experiments may provide a clearer result.

DISCUSSION

In this study, we discovered that *Tb*RAP1 is required for maintaining ES-linked *VSG* silencing in PF cells as well as in BF cells. Depletion of *Tb*RAP1 led to an increase in steady-state levels of *VSG* mRNA from several ten- to several

hundred-fold. *Tb*RAP1 is also required for silencing *mVSGs* in both PF and BF cells. The strength of *Tb*RAP1-mediated ES-linked *VSG* silencing is stronger in PF compared to that in BF. Interestingly, steady-state mRNA levels of ES-linked *VSGs* are lower in PF cells than in BF cells (silent VSGs), possibly due to differential regulation of *VSG* mRNA stability by *VSG* 3' UTR in PF and BF cells (Berberof et al. 1995). However, regardless of the steady-state levels of *VSGs*, the changes detected in mRNA levels upon depletion of *Tb*RAP1 are solely due to the silencing effect of *Tb*RAP1. Upon depleting *Tb*RAP1, *VSG* derepression observed in PF cells was increased compared to that in the BF cells (Yang et al. 2009), indicating a stronger silencing by *Tb*RAP1 in PF cells. This comparative analysis was performed for only three *VSGs* due to limited strain availability. However, a comparison between previously published data and current data suggests that derepression for most of the ES-linked *VSGs* were higher in PF cells. Nevertheless, during derepression, every ES-linked *VSG* behaved differently and hence it is possible that for some *VSG* the derepression level might be similar in PF and BF cells.

The telomeric and subtelomeric chromatin structure was affected significantly upon depletion of *Tb*RAP1 in PF cells but not in BF cells, indicating that *Tb*RAP1-mediated *VSG* silencing in PF occurs through chromatin remodeling. Many previous studies have implied the role of chromatin modulation in regulation of ES-expression in BF forms. It is known that the active ES is highly devoid of nucleosomes compared to the silent ES in BF cells (Figueiredo and Cross 2010, Stanne and Rudenko 2010). Also, several chromatin-remodeling factors, such as

ISWI (Hughes et al. 2007, Stanne et al. 2011), DAC3 (Wang et al. 2010), Spt16 (Denninger et al. 2010), and Dot1b (Figueiredo et al. 2008) have been proven to be important for regulating activity of the ES promoter. We now find that *Tb*RAP1 also plays an important role in regulation of ES-linked *VSGs*, *mVSGs,* and minichromosomes *VSGs* via chromatin remodeling in PF cells.

Depletion of *Tb*RAP1 led to a change in chromatin structure at all tested subtelomeric *VSG* loci. The chromatin structure change was also observed for *VSG671*, which is located on a minichromosome. No change in the mRNA levels was observed for *VSG671* upon depletion of *Tb*RAP1, possibly due to lack of an upstream promoter. Therefore, opening up of chromatin structure at the *VSG671* locus after knocking down *Tb*RAP1 suggests that the change was not due to elevated transcription but was rather primarily due to *Tb*RAP1 depletion. ES-linked *VSGs* and *mVSGs* on the other hand possess upstream promoters and hence it is possible that the changes in chromatin structure may be one of the reasons for their derepression. FAIRE values obtained for ES-linked *VSGs* were higher compared to that obtained for the *VSG671* locus ($P<0.05$) (figure 3-11 A). Since all ES-linked *VSGs* were highly derepressed it is possible that the elevated transcription may result in an even more opened chromatin structure.

FAIRE and MNase data proved that *Tb*RAP1 had a mild global effect on chromatin structure as small changes were seen at chromosome internal loci as well as at the ES promoter regions upon *Tb*RAP1 depletion. In budding yeast, RAP1 is known to bind at non-telomeric sites and function as transcription regulator of multiple genes (Shore D 1994, Yarragudi et al. 2007, Teo et al. 2010,

Martinez et al. 2010, Yang et al. 2011). In yeast depletion of Abf1 and RAP1 led to altered nucleosome occupancy at more than a thousand loci, resulting in a genome-wide effect (Ganapathi et al. 2011). Thus, it is possible that similar to its yeast and human homologs, *Tb*RAP1 determines the chromatin structure at a global level. However, its effect on subtelomeric loci is much more significant and robust.

"To our surprise, we did not detect significant chromatin structure changes in BF cells on *Tb*RAP1 depletion. Our observations suggest that the significantly more severe chromatin structure change and the significantly stronger gene de-repression at ESs in PF cells than those in BF cells are linked. Currently, we favor several possible explanations (not necessarily mutually exclusive) for the different phenotypes observed in BF and PF cells. First, the BES chromatin may have different structures in BF and PF cells, and *Tb*RAP1 may be the responsible factor for this difference. An earlier work (Navarro et al. 1999) found that T7 polymerase-mediated transcription from a chromosomally integrated T7 promoter is repressed along the entire length of the BES in PF cells, but not in BF cells. Therefore, the chromatin structure at the silent BES appears to be more tightly packed in PF cells. It is possible that *Tb*RAP1 is the factor that maintains a more closed BES structure in PF cells. Second, as BF cells undergo antigenic variation and silent BESs need to be ready to switch to the active state, their silent state is likely metastable, similar to what is often observed for telomeric silencing in yeast (Gottschling et al 1990). Therefore, the BES may switch between the open and closed states more frequently in BF cells than in PF cells. In this case, *Tb*RAP1 may still be involved in determination of chromatin structures in BF cells, but our techniques are not sensitive enough to detect a significant change owing to the fast switching status of the BES. Another possibility is that more factors are involved in modulating BES chromatin structure and BES silencing independent of *Tb*RAP1 at the BF stage. Therefore, depletion of *Tb*RAP1 in BF cells may still affect the chromatin structure, but a lesser degree of change or no quantifiable differences can be detected. Glover and Horn showed that an rRNA promoter- driven reporter gene targeted 5 kb from the telomere in a silent BES was expressed in PF cells, but not in BF cells (Glover et al. 2006), suggesting that additional factors are involved in silencing BESs in BF cells. A recent study suggested that depletion of histone H1 led to a chromatin opening at multiple genomic loci only in BF cells, but not in PF cells (Povelones et al. 2012), which is also consistent with this hypothesis." (Pandya et al. 2013)

A unique DNA base modification, β-D-glucosyl-hydroxymethyluracil (base J) has been identified in *T. brucei* (Gommers-Ampt et al. 1993). Base J is present in

BF but absent in PF (Van Leeuwen et al. 1998a) and is highly enriched at telomeres (Van Leeuwen et al. 1998b). In *T. cruzi,* loss of base J led to elevated transcription of Pol II transcribed gene, with decrease in nucleosome abundance and increased histone acetylation (Ekanayake and Sabatini 2011). This suggests that base J can regulate chromatin structure. It is possible that lack of chromatin structure change observed in BF cells upon depletion of *Tb*RAP1 could be due to base J. In the future, depletion of base J in *Tb*RAP1 knockdown background can be performed to test whether there is any change in chromatin structure and any additional elevation of *VSG* derepression.

*Tb*RAP1 was found to preferentially locate with the silent ES-marked telomere. This suggests that *Tb*RAP1 functions in a cis-acting manner and it physically binds to silent *VSGs* to maintain their regulation. The amount of *Tb*RAP1 associated with the active *VSG* was not significantly different from that at the chromosome internal genes. This finding is in co-ordinance with the fact that the active *VSG* is highly transcribed in *T. brucei. Tb*RAP1-mediated *VSG* silencing was found to be stronger in PF cells compared to that in the BF cells. In the future, it would be interesting to perform ChIP and compare the relative binding of *Tb*RAP1 at *VSGs* in BF and PF cells. We hypothesize that; the amount of *Tb*RAP1 bound to ES-telomeres in PF cells would be more compared to that in the BF cells.

CHAPTER IV

ROLE OF *Tb*RAP1 IN TELOMERE BIOLOGY

INTRODUCTION

Chromosome ends need to be protected from being detected as double strand breaks from DNA damage repair machineries such as non-homologous end joining (NHEJ) and homology-directed repair (HDR). Telomeric proteins play a key role in the protection of the telomeres from being detected as DNA breaks and thereby preventing deleterious consequences. Another key role of telomere proteins is maintaining telomere length via regulating the access of telomerase to the telomeres.

*Sc*RAP1 is known to regulate the telomere length (Conrad et al. 1990, Lustig et al. 1990, Kyrion et al. 1992, Liu et al. 1994, Marcand et al 1997). The temperature sensitive alleles of *Sc*RAP1 with a C-terminal truncation had several phenotypes including dramatically elongated telomeres that are prone to rapid deletions (Kyrion et al. 1992). The C-terminal domain of *Sc*RAP1 is known to interact with Rif1 and Rif2. Rif1 and Rif2, along with *Sc*RAP1, contribute to

telomere length homeostasis (Hardy et al. 1992, Wotton and Shore, 1997). The overexpression of *Sc*RAP1 also led to reduced chromosome stability (Conrad et al. 1990). A “protein counting” model has been proposed in budding yeast, where a threshold number of RAP1 molecules bound to the telomere, prevents its further elongation by inhibiting the telomerase (Marcand et al. 1997). Mutation of *Sp*RAP1 in fission yeast leads to telomere elongation (Kanoh and Ishikawa 2001). It also regulates telomeric clustering since upon its mutation very few telomeres cluster towards the spindle pole body at the horsetail stage (Kanoh and Ishikawa 2001). Overexpressing hRAP1 or its domain-deletion mutation in telomerase positive cell lines leads to telomere elongation, suggesting that like its yeast homologs, hRAP1, also regulates telomere length (Li and De Lange 2000, Li and De Lange 2003). Thus, it is evident that in budding yeast, fission yeast, and humans, RAP1 has an important function in telomere length regulation.

The depletion of RAP1 also leads to the activation of various DNA damage repair pathways in yeast and human. The conditional knock-out of *Sc*RAP1 resulted in telomere fusions which were mediated by the NHEJ pathway (Pardo and Marcand 2005). The C-terminal truncation of *Sc*RAP1 culminated in rapid chromosome loss and elevated rates of chromosome nondisjunction (Kyrion et al. 1992). In budding yeast, non-dividing cells depend on yKu and RAP1 for telomere capping. G0 cells lacking RAP1 had telomere degradations, suggesting that RAP1 prevents nuclease activities at telomeres in resting cells (Momchil et al. 2010). Surprisingly, compared to the shorter telomeres, little or no DNA damage response was elicited at long telomeres having multiple RAP1-binding

sites upon induction of double strand breaks, suggesting that yeast RAP1 plays a role in telomere end concealment (Negrini et al. 2007). In *Kluyveromyces lactis* disruption of RAP1 binding by altering telomeric sequences results in elevated telomere recombination leading to the formation of t-circles (free circular telomeric DNA molecules) (Cesare et al. 2008). hRAP1 was also implicated in preventing NHEJ, as RAP1 artificially tethered to telomeres was able to inhibit telomere end fusions (Bae et al. 2007, Sarthy et al. 2009). Additional evidence came from *in vitro* analysis using telomeric oligos; the results showed that TRF2/RAP1 prevented ligase IV dependent end joining (Bombarde et al. 2010). In contrast, mouse RAP1 was implicated in preventing homology directed repair and was not required for preventing telomere fusions (Sfeir et al. 2010, Martinez et al. 2010). These results were confirmed using two independent approaches, where either the RAP1 gene was deleted or by using a TRF2 mutant allele that fails to recruit RAP1 to telomeres (Sfeir et al. 2010, Martinez et al. 2010). Regardless of the observed differences, it is evident that RAP1 is required for preventing activation of the DNA damage repair pathways at the telomere.

*Tb*RAP1 was identified as a *Tb*TRF interacting factor and was confirmed to be an intrinsic telomeric factor (Yang et al. 2009). A role of *Tb*RAP1 in the transcriptional gene silencing was identified. However, not much is known about the function of *Tb*RAP1 in telomere end protection. The lack of recognizable homologues of DNA ligase IV in *T. brucei* suggested that NHEJ is either absent or diverged (Burton et al. 2007). However, repair through homologous

recombination have been identified and studied in *T. brucei* (Alsford and Horn 2007, Barnes and McCulloch 2007, Glover et al. 2008, Glover et al 2010).

Recent work from our lab found that *Tb*RAP1 depletion in BF cells leads to an elevated rate of *VSG* switching through gene conversion mechanism (recombination based mechanism) (Nanavaty and Li, unpublished data). This finding suggests that *Tb*RAP1 has a role in preventing telomere recombination. Unlike its yeast homologs, the depletion of *Tb*RAP1 did not affect telomere length dramatically in BF cells within two days (Li, unpublished data). However, a decrease in the telomere G-overhang (single-stranded 3' overhang at the end of telomeres) signal was obtained after the knockdown of *Tb*RAP1 in BF cells, suggesting that it is required for protecting the G-overhang structure. The characterization of the role of *Tb*RAP1 in the telomere terminal structure at the PF stage is lacking. Also, it is not clear whether *Tb*RAP1 carries out all of these functions via direct DNA binding. Hence, we wanted to test whether *Tb*RAP1 has any DNA binding activity and whether it plays any role in telomere end protection in PF *T. brucei* cells.

RESULTS

The DNA-binding activity of TbRAP1

It is not known whether *Tb*RAP1 can directly bind to the telomeric DNA in *T. brucei,* similar to *Sc*RAP1. In order to test this possibility, electrophoretic mobility shift assay (EMSA) was performed. The *Tb*RAP1 gene with a Kozak sequence was cloned into the pBlueScript vector driven by a T3 promoter. The *Tb*RAP1 protein was obtained by performing *in vitro* transcription (mMESSAGE

mMACHINE® T3 transcription kit, Thermo Fisher Scientific Inc.) and translation (TNT® T7/T3 Coupled Reticulocyte Lysate System, Promega). GST-*Tb*TRF purified from *E. coli* was used as a positive control (Li et al. 2005).

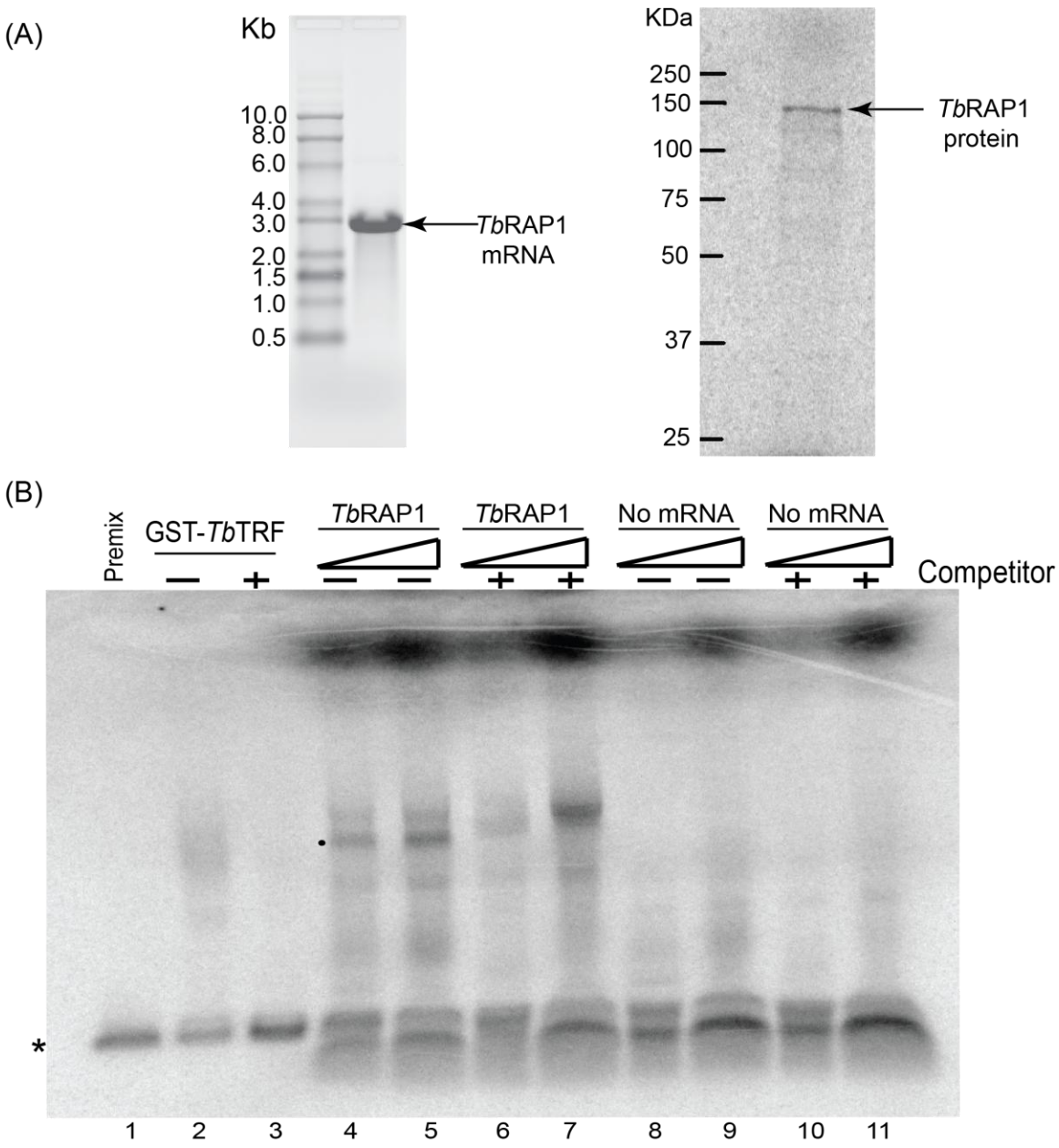

Figure 4-1: EMSA to test DNA-binding activity of *Tb*RAP1. (A) *Tb*RAP1 was obtained by performing *in vitro* transcription and translation. The left panel shows EtBr-stained RNA gel. A band of precise 2.6 kb for the *Tb*RAP1 transcript was obtained. The right panel shows a polyacrylamide gel with S^{35} labeled *Tb*RAP1 protein obtained by *in vitro* translation. (B) An EMSA assay was performed using GST-*Tb*TRF, *Tb*RAP1 (lysate containing translated protein) and no mRNA (lysate without *Tb*RAP1). P^{32} labeled $(TTAGGG)_{12}$ probe was used. The competitor used was nonradioactive $(TTAGGG)_5$ probe. 100 ng of GST-*Tb*TRF was used. 2 µl and 5 µl of lysate with (labeled as *Tb*RAP1) or without *Tb*RAP1 (labeled as no mRNA) protein were used. 3.45 µg of competitor was used. Asterisks indicate the free probe.

In vitro transcription was performed to obtain *Tb*RAP1 mRNA, as seen in figure 4-1 A. After confirming the correct size, mRNA was purified and further used for *in vitro* translation. Translation was performed in the presence of radioactive S^{35} to confirm successful translation of *Tb*RAP1. The translated product was seperated on a polyacrylamide gel, which was dried and exposed to a phosphorimager screen. A faint band of ~150 kDa corresponding to *Tb*RAP1 was obtained, indicating that *Tb*RAP1 was not translated at a very abundant level. We further used the translation product for EMSA. No mRNA sample was used as a control. S^{35} was also added to no mRNA sample for better comparison. A recombinant partially purified GST-*Tb*TRF is known to directly bind TTAGGG repeats *in vitro* and was used as a positive control (Li et al. 2005). As previously published, GST-*Tb*TRF binds the duplex TTAGGG repeat (figure 4-1 B lane 2), and the GST-*Tb*TRF/telomere DNA complex can be competed by adding non-radioactive TTAGGG duplex DNA probe, indicating that the binding is specific (figure 4-1 B lane 3). Mixing *in vitro* translated *Tb*RAP1 with the duplex telomere DNA probe resulted in several bands on the polyacrylamide gel (figure 4-1 B lane 4 and 5 depicted by solid black dot). However, these bands did not disappear upon adding cold competitors (figure 4-1 B lane 6 and 7), suggesting that the observed bands my not be complexes formed specifically between *Tb*RAP1 and the double stranded TTAGGG repeats. Since *in vitro* translated *Tb*RAP1 is radiolabeled, it is possible that one observed band in the polyacrylamide gel was free *Tb*RAP1 protein. Hence, we decided to perform another binding assay by using unlabeled *Tb*RAP1 protein.

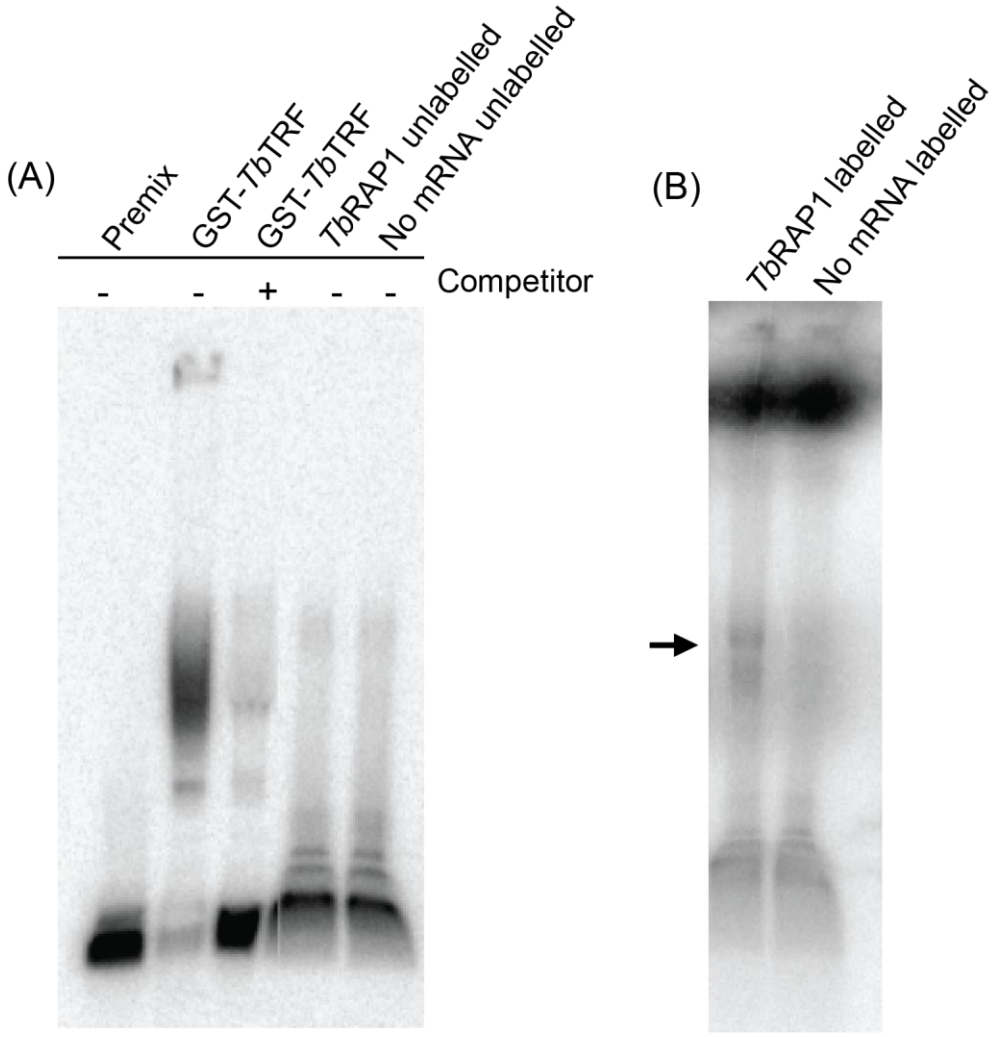

Figure 4-2: EMSA by using unlabeled *Tb*RAP1 protein. (A) EMSA was performed by using GST-*Tb*TRF, unlabeled *Tb*RAP1 and unlabeled empty mRNA. P^{32} labeled $(TTAGGG)_{12}$ probe was used to test the binding. The competitor used was nonradioactive $(TTAGGG)_5$ probe. 100 ng GST-*Tb*TRF was used. 5 µl of lysate with (labeled as *Tb*RAP1) or without *Tb*RAP1 (labeled as no mRNA) protein was used. 3.45 µg of competitor was used. (B) EMSA was performed using S^{35} labeled *Tb*RAP1 or no mRNA sample. The bold arrow represents free radiolabeled *Tb*RAP1 protein.

Using unlabeled or labeled *Tb*RAP1 containing lysate, EMSA was performed. As seen in figure 4-2 A, a shift was observed for GST-*Tb*TRF that was competed out using competitor, thus suggesting specific binding of *Tb*TRF to TTAGGG repeats. Interestingly, we did not observe the shifted bands on gel upon using unlabeled *Tb*RAP1 protein, which we previously observed. However, a smear was seen on the gel probably due to interference from the lysate (which is known to contain huge amount of globin proteins). Interestingly, the bands reappeared on the gel when EMSA was performed using radiolabeled *Tb*RAP1 (figure 4-2 B, bold arrow). This suggests that, the bands observed on the gel were due to free radiolabeled *Tb*RAP1 protein. Thus it seems that *Tb*RAP1 does not possess DNA binding activity. However, due to interference of lysate with free probe migration and due to very low levels of *Tb*RAP1 translation, it is difficult to reach any clear conclusions at this point.

TbRAP1 and telomere length regulation

In BF cells, it is known that the telomere length is not affected upon *Tb*RAP1 depletion within two days. Southern blot analysis was performed to determine if *Tb*RAP1 plays any role in telomere length regulation in PF cells. Genomic DNA was collected before and after depletion of *Tb*RAP1 and digested with the frequent DNA cutters, AluI and MboI. After digestion, chromosome internal genomic DNA was digested into small fragments leaving only the telomeric tracts intact. The digested genomic DNA was then separated on an agarose gel where most chromosome internal DNA fragments were run off the gel. The larger sized

telomeric DNA fragments were subsequently blotted onto a nylon membrane followed by hybridization with a telomere specific probe.

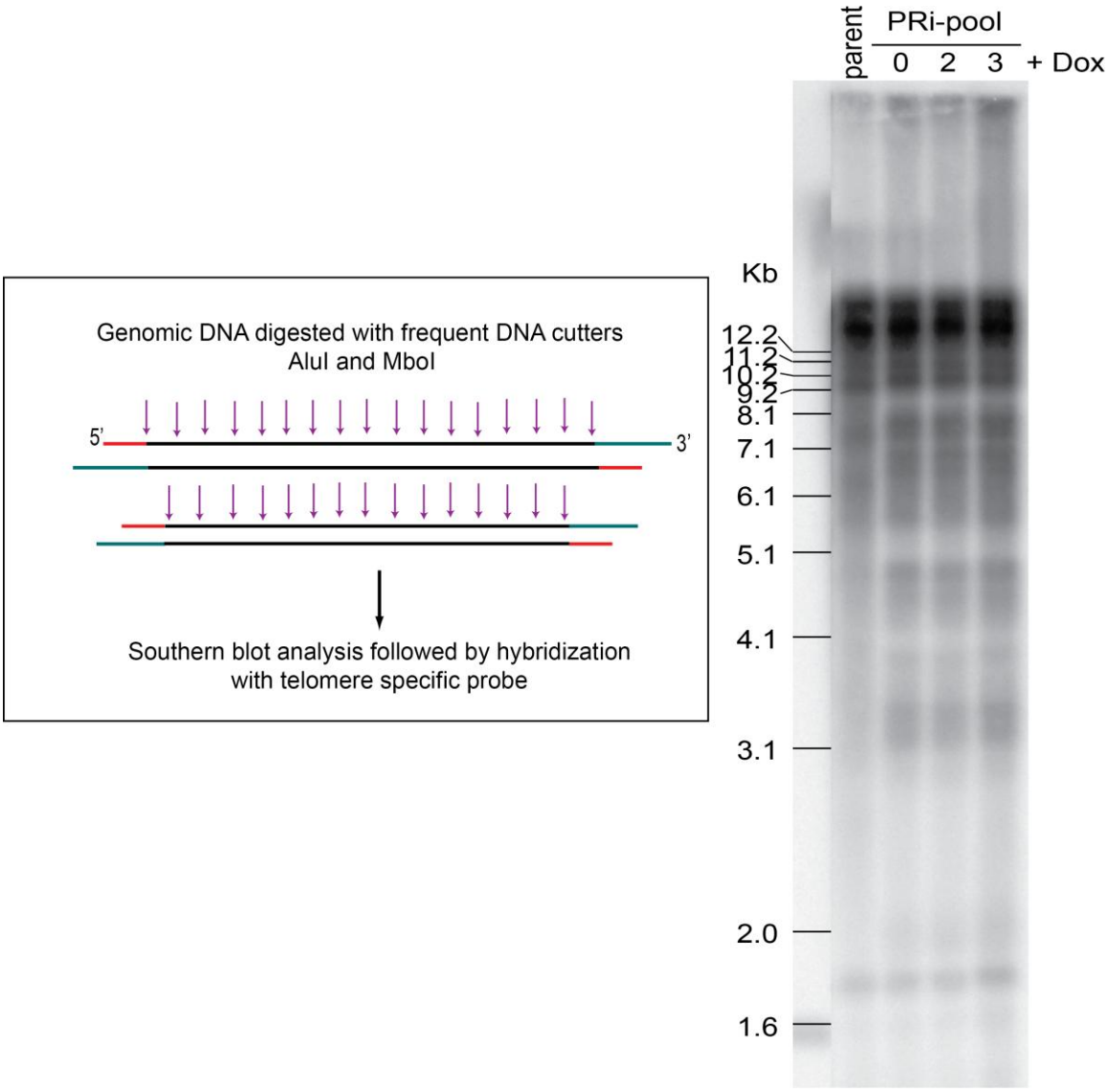

Figure 4-3: Telomere Southern blot in PRi-pool cells. Protocol for performing the telomere Southern blot is described on the left. On the right the result of hybridization with a telomere specific probe is shown. Genomic DNA was collected before (day 0) and after (day 2 and 3) depletion of *Tb*RAP1 in PRi-pool cells (PF cells). The parent cell line not carrying the RNAi vector was used as a control.

As seen from figure 4-3, no change in the telomere length was observed upon depleting *Tb*RAP1 in PF cells within 3 days. The telomere length in *T. brucei* ranges from 2-12 kb. Telomere fragments of 3 kb to more than 12kb were observed for PRi-pool cells when the bulk telomeres were detected by a TTAGGG repeat probe. No apparent change in size of the telomere fragments was observed, indicating that *Tb*RAP1 depletion does not affect telomere length in PF cells. However, if *Tb*RAP1's effect on telomere length is subtle then it will be hard to capture in the bulk telomere Southern blot. Hence, we decided to follow a single telomere and analyze its length before and after depletion of *Tb*RAP1, by performing terminal restriction fragment (TRF) analysis. *T. brucei* telomeres are marked with unique *VSG* genes at subtelomeric loci, which allows us to measure length change at individual telomeres. Genomic DNA was digested with restriction enzymes that cut specifically upstream of a particular *VSG* gene, releasing a terminal restriction fragment containing the *VSG* gene and its downstream telomere. This TRF can be visualized on a Southern blot by hybridization with the *VSG* specific probe.

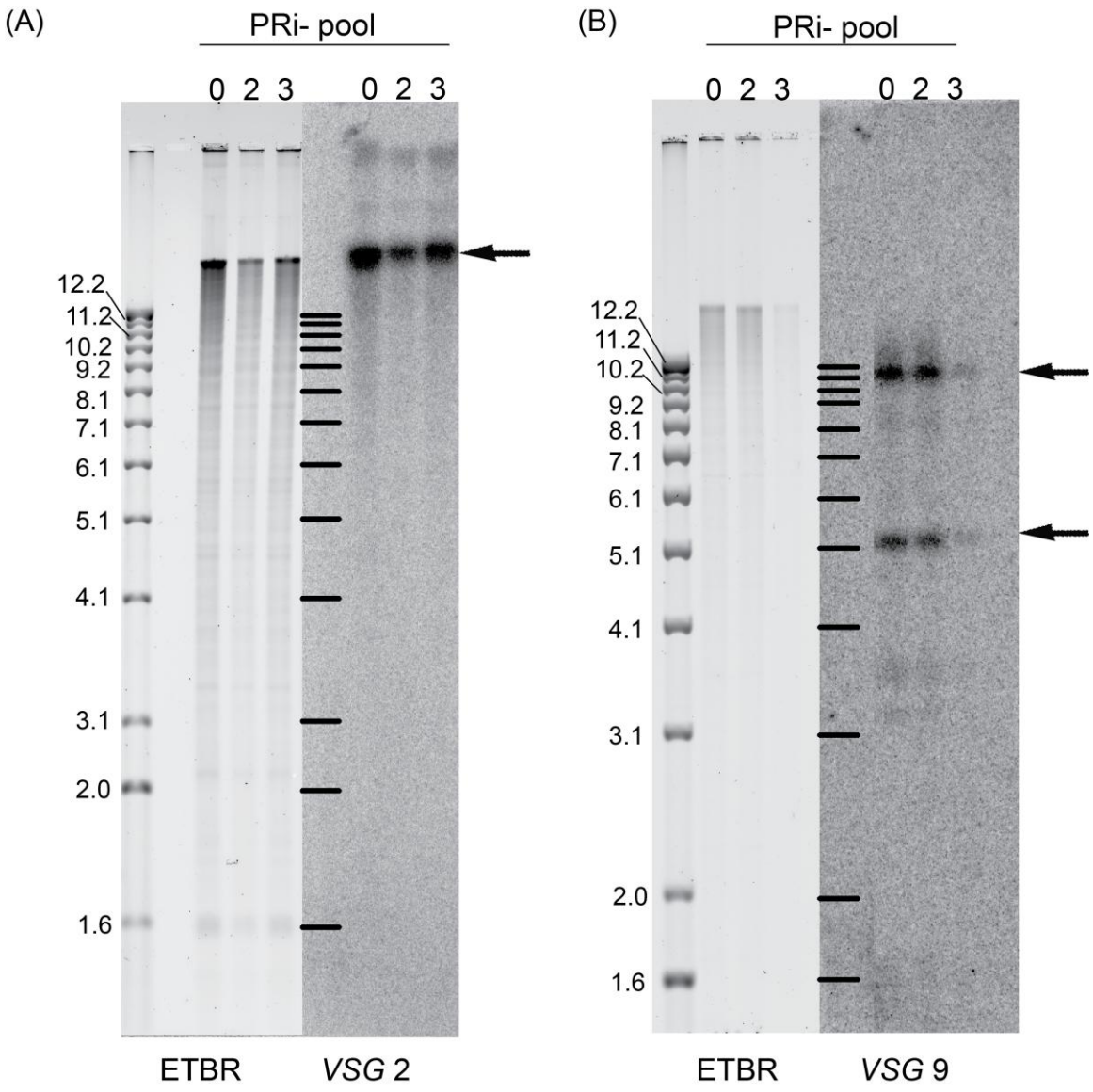

Figure 4-4: Terminal restriction fragment analysis to measure telomere length in PRi-pool cells. Genomic DNA was collected before (day 0) and after (day 2 and 3) depletion of *Tb*RAP1 and digested with EcoRI. Southern blot analysis was performed and blots were hybridized with (A) *VSG2* and (B) *VSG*9 specific probes. Left panel shows EtBr-stained gel, while right panel shows the hybridized Southern blot. Arrowheads indicate telomeric fragments containing *VSG*2 and *VSG*9.

Two *VSG*-marked telomeres were tested. As seen in figure 4-4 A, the size of the *VSG2* TRF remained unchanged, suggesting that the telomere length is not affected upon depletion of *Tb*RAP1 within a short frame of time. Similar analysis was done for telomere associated with *VSG9*. Unlike *VSG2,* which is a single copy gene, *VSG9* have two copies in the genome and two DNA bands were observed on the gel. Although the loading of genomic DNA was unequal between different samples (figure 4-4 B left panel), no change in the size of the *VSG9*-containing fragments was observed (arrowheads in figure 4-4 B right panel). We also tested the *VSG11*-marked telomere and similar results were obtained (data not shown). Thus from the bulk telomere southern blot (figure 4-3) and terminal restriction fragment analysis (figure 4-4) it was evident that *Tb*RAP1 does not affect telomere size in PF cells within three days.

G-overhang structure analysis

Since telomere length was not affected upon depletion of *Tb*RAP1, we wanted to test whether the telomere G-overhang structure is affected. *T. brucei* telomeres end in a 3' overhang (containing TG repeats). The telomere complex protects the G- overhang in mammals (de Lange 2005).

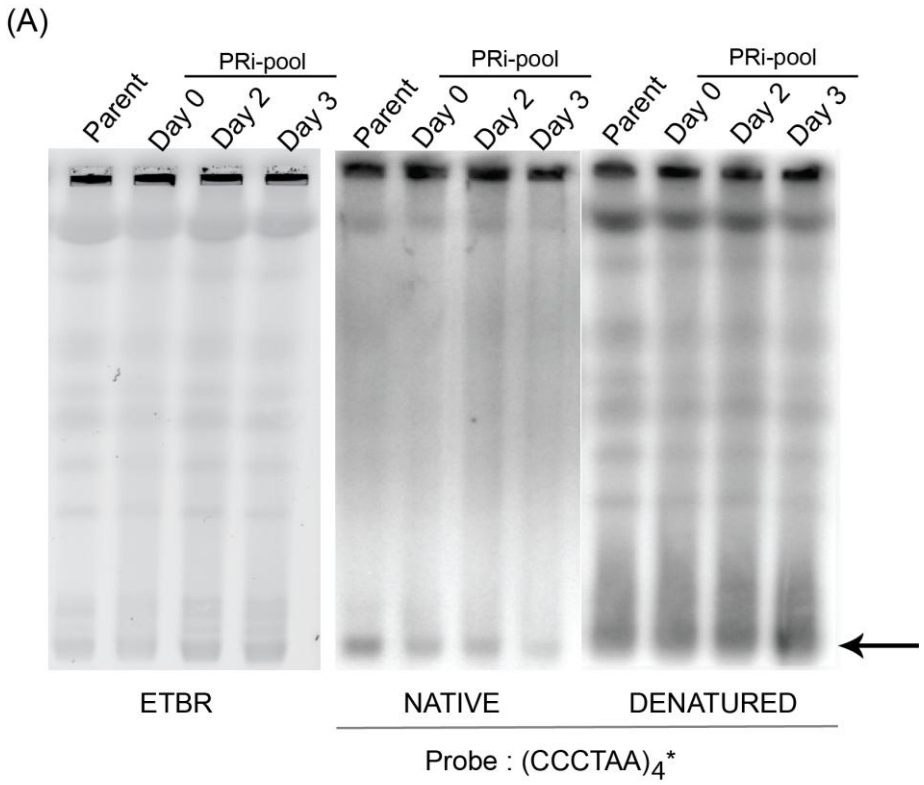

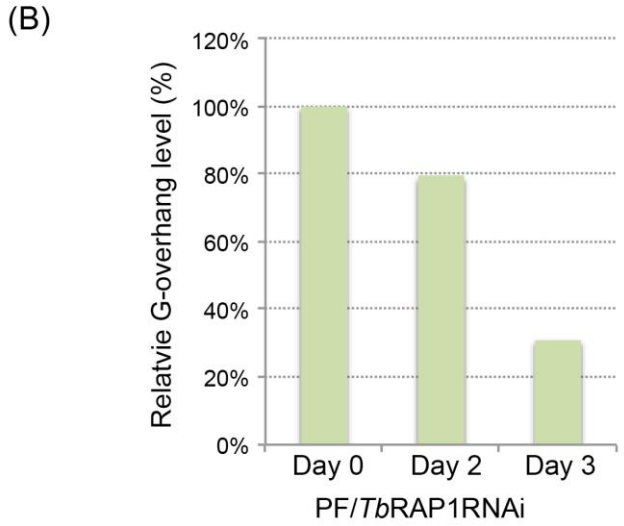

Figure 4-5: In-gel hybridization analysis of the telomere G-overhang in PRi-pool cells. (A) DNA plugs were prepared before (day 0) and after (day 2 and 3) depletion of *Tb*RAP1. Plugs were also prepared from the parent cell line without any RNAi construct. Intact chromosomes were separated by pulsed filed gel electrophoresis as seen in EtBr-stained gel (left panel). The gel was dried and hybridized with an end-labeled $(CCCTAA)_4$ oligo probe either before (middle panel) or after (right panel) denaturation of the gel. Arrowheads indicate the signal from the minichromosomes. (B) An average of quantification of the G-

overhang signal calculated from two independent experiments. The relative G-overhang signal was calculated for either day 2 or day 3 by dividing their signals to that of the day 0 signal.

DNA plugs were prepared from induced and uninduced PRi-pool cells. A parent cell line devoid of any RNAi construct was used as a control. Intact chromosomes were separated using Pulse Field Gel Electrophoresis (PFGE). The *T. brucei* genome consists of ~100 minichromosomes. Under our electrophoresis conditions, they all migrate at the same position. The telomere G-overhang signal is therefore most prominent at minichromosomes and is used for calculation (arrowheads in figure 4-5 A). To detect the G-overhang signal, the native gel was first hybridized with the $(CCCTAA)_4$ probe and the signal was quantified (figure 4-5 A middle panel). The same gel was subsequently denatured and hybridized with the same probe and the signal quantified again (figure 4-5 A right panel). The G-overhang signal is therefore calculated by dividing the amount of the native hybridization signal by that of the hybridization signal after denaturation. After obtaining the G-overhang signal for each sample, relative G-overhang levels were calculated by dividing values of day 2 and day 3 with the value of day 0. As seen in figure 4-5 B, a 20% reduction in G-overhang signal was seen by day 2 upon inducing RNAi against *T*bRAP1. By day 3, only ~30% of the G-overhang signal was left. Thus, we concluded that *Tb*RAP1 is required for protecting the telomere G-overhang structure in PF cells.

DISCUSSION

EMSA analysis suggested that *Tb*RAP1 does not bind to the telomeric DNA directly. However, the experiment encountered certain technical difficulties. The

Rabbit Reticulocyte Lysate system used for translation contains a huge amount of globin protein. These proteins present in the binding reaction interfered with the migration of the probe, making it difficult to interpret the results. Also, the *in vitro* translated *Tb*RAP1 was in a very low amount. In the future, translation can be done using a baculovirus expression system to obtain higher amounts of translated protein. The full length GST-*Tb*RAP1 is not soluble when expressed in *E. coli.* Instead of full-length recombinant protein, only the C-terminal half of *Tb*RAP1 can be expressed in *E. coli* with reasonable solubility. We are currently working on solving the NMR structures of *Tb*RAP1 myb and myb-like domains in collaboration with Dr. Yanxiang Zhao at Hong Kong Polytechnic University. This will help reveal whether *Tb*RAP1 has any sequence-specific DNA binding activities.

Telomere length seems to be unaffected upon depleting *Tb*RAP1 in PF cells, at least within a short frame of time. *Tb*RAP1 knockdown leads to growth arrest within 72 hours in the PF cells and within 24 hours in the BF cells. The decrease in telomere size due to the absence of telomerase activity is 3-6 bp/population doubling (Dreesen et al. 2005). It is possible that we do not observe telomere length change due to a limited time window before the cells arrest upon *Tb*RAP1 depletion. In the future, viable point mutants of *Tb*RAP1 can be used to further analyze its role in telomere length maintenance. Overexpression of hRAP1 led to telomere elongation (Li and De Lange 2000, Li and De Lange 2003). *Tb*RAP1 can presumably be overexpressed in order to study its role in telomere maintenance, although attempted overexpression of *Tb*RAP1 led to massive

degradation of the ectopic *Tb*RAP1 allele (data not shown). If *Tb*RAP1 does not have any telomere DNA binding activity, it will depend on *Tb*TRF to be recruited to the telomere. Establishing *Tb*TRF mutants with weakened interaction with *Tb*RAP1 (described in chapter V) can also be helpful in elucidating *Tb*RAP1's function in telomere length regulation.

*Tb*RAP1 depletion affects G-overhang structure in PF cells. A 70% loss of G-overhang signal was observed by day 3 of *Tb*RAP1 RNAi induction, suggesting that *Tb*RAP1 is required for the chromosomal end protection. Deprotection of telomeres in mammalian cells leads to DNA damage responses and results in activation of ATM/p53 dependent apoptosis or senescence-like cell cycle arrest (Van steensel et al. 1998, Karlseder et al. 1999, Takai et al. 2003). Since we observed growth arrest upon *Tb*RAP1 depletion, it is possible that this deprotection at telomeres (loss of G-overhang) might elicit a DNA damage response.

CHAPTER V

FUNCTIONAL ANALYSIS OF *Tb*TRF

INTRODUCTION

TbTRF functions in telomere end protection

*Tb*TRF (Tb10.389.0680) was identified as a component of the telomere complex, and it directly binds to the telomeric DNA in *T. brucei* (Li et al. 2005). *Tb*TRF is an essential protein, and cells stop proliferating after *Tb*TRF depletion within 24 (in BF cells) or 48 hours (in PF cells). *Tb*TRF depletion in *T. brucei* did not affect ES-linked *VSG* silencing (Yang et al. 2009, Pandya et al. 2013). However, *Tb*TRF is required for the protection of the telomere G-overhang structure (Li et al. 2005). Due to this acute growth arrest upon knockdown of *Tb*TRF, it is difficult to define all of the functions of *Tb*TRF at the telomere. Hence, identification of viable mutants of *Tb*TRF would be very useful for characterization of all its roles at telomeres.

*Tb*TRF contains a C-terminal myb domain that is required for DNA binding and a TRF homology (TRFH) domain towards the N-terminus that is essential for homodimerization (Li et al. 2005). .

The *Tb*TRFH domain also interacts with *Tb*RAP1 (Yang et al. 2009) and *Tb*TIF2 (Jehi et al. 2014), suggesting its role in recruitment of other telomeric proteins. Hence, the *Tb*TRFH domain is critical for several functions at the telomeres.

Similarly, in mammalian cells, TRF1 forms a homodimer via its TRFH domain and binds to telomere DNA through its C-terminal myb domain (Bianchi et al. 1997). The TRFH domain of TRF1 is required for recruiting another telomere protein, TIN2, to the telomeres (Kim et al. 1999, Houghtalin et al. 2004). It was discovered that the TRFH domain of TRF1 is not only required for protein-protein interaction and for recruitment of telomere proteins, but it is also required for stabilizing the telomere structure. Disruption of this domain led to an abnormal telomere structure, such as broken or lost telomeres (Okamoto and Shinkai 2009). We are, therefore, interested in obtaining viable mutants of *Tb*TRFH domain that would allow us to dissect its role in protein-protein interaction as well as its function in maintaining telomere structure integrity.

Dr. Bibo Li predicted the secondary structure of *Tb*TRFH domain by using PHD (service to predict the secondary structure of protein based on the sequence information) and 3D-PSSM (software to predict the 3D structure of a protein by matching it with existing database of available 3D structures of other proteins). It was predicted that *Tb*TRFH contains seven α-helices. This is very similar to the secondary structure of mammalian TRFH domain of TRF1 and TRF2, which consists of 9 α-helices (Fairall et al. 2001).

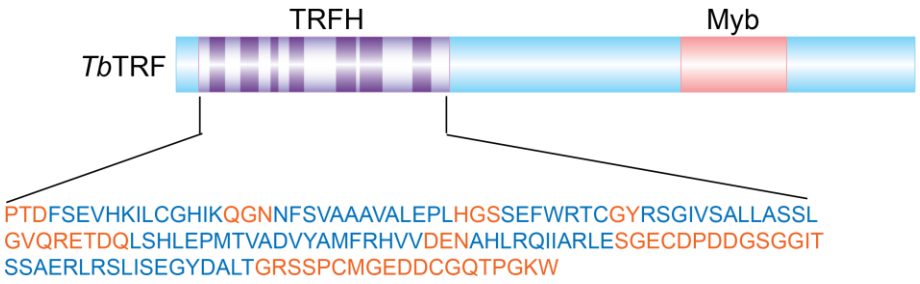

Figure 5-1: The domain structure of *Tb*TRF. *Tb*TRF contains two domains: (i) a *Tb*TRFH (homodimerization) domain and (ii) a myb domain (DNA binding domain). Software prediction suggested that the *Tb*TRFH domain consists of seven helices. The amino acid sequence of the TRFH domain is marked in orange. The seven predicted helices are marked in blue.

Deleting large fragments of the *Tb*TRFH domain can lead to abrogation of its homodimerization function, which is essential for the *Tb*TRF's telomere DNA binding activity; normally, at least two myb repeats are required for DNA recognition. Hence, we decided to perform subtle mutations by disrupting individual helices to study the effects of mutants on *Tb*TRF homodimerization and protein-protein interaction. Our goal was to identify mutants that cannot interact with the wild type *Tb*TRF or other telomere proteins but can form homodimers. Such mutants, when expressed *in vivo*, will be able to bind telomeric DNA but will probably be defective in other protein-protein interactions. This will give us information regarding functions of *Tb*TRF in telomere protein complex formation.

Roles of TRF in chromatin modulation

Apart from its role in telomere end protection, there has been evidence that TRF also plays an important role in chromatin compaction and remodeling. The overexpression of TRF2 in mice led to decreased heterochromatin marks at telomeres and subtelomeres, a decrease in abundance of core nucleosomes, and an increase in nucleosomal spacing at the telomeres (Benetti et al. 2008, Galati et al. 2012). In another instance, an *in vitro* biophysical analysis of TRF2 and telomeric nucleosome fibers determined that TRF2 could promote folding of these fibers and also increase their compaction, thus suggesting its role in chromatin remodeling (Baker et al. 2009, Baker et al. 2011, Poulet et al. 2012). Interestingly, *in vitro* analysis suggested that TRF1 can form a ternary complex with the telomeric DNA bound nucleosomes and can alter its structure,

suggesting that TRF1 can modulate chromatin structure at telomeres (Galati et al. 2006). Also, it is known that TRF2 interacts with TERRA (telomeric transcript), which further facilitates ORC recruitment and heterochromatin formation at telomeres (Deng et al. 2009). Thus, it is evident that along with RAP1, TRF also plays a role in chromatin modulation at telomeres.

Knockdown of *Tb*TRF does not lead to ES-linked *VSG* derepression (Li et al. 2005). However, it is possible that *Tb*TRF may play a secondary role in *VSG* silencing by inducing chromatin compaction. Our goal was to test whether *Tb*TRF possess any chromatin remodeling activity at *T. brucei* telomeres.

RESULTS

Establishing TbTRFH domain mutants

We wanted to identify interaction-deficient mutants by performing yeast 2-hybrid analysis. The *Tb*TRF gene containing a single helix (in *Tb*TRFH domain) deleted at a time was amplified and cloned in the lexA vector.

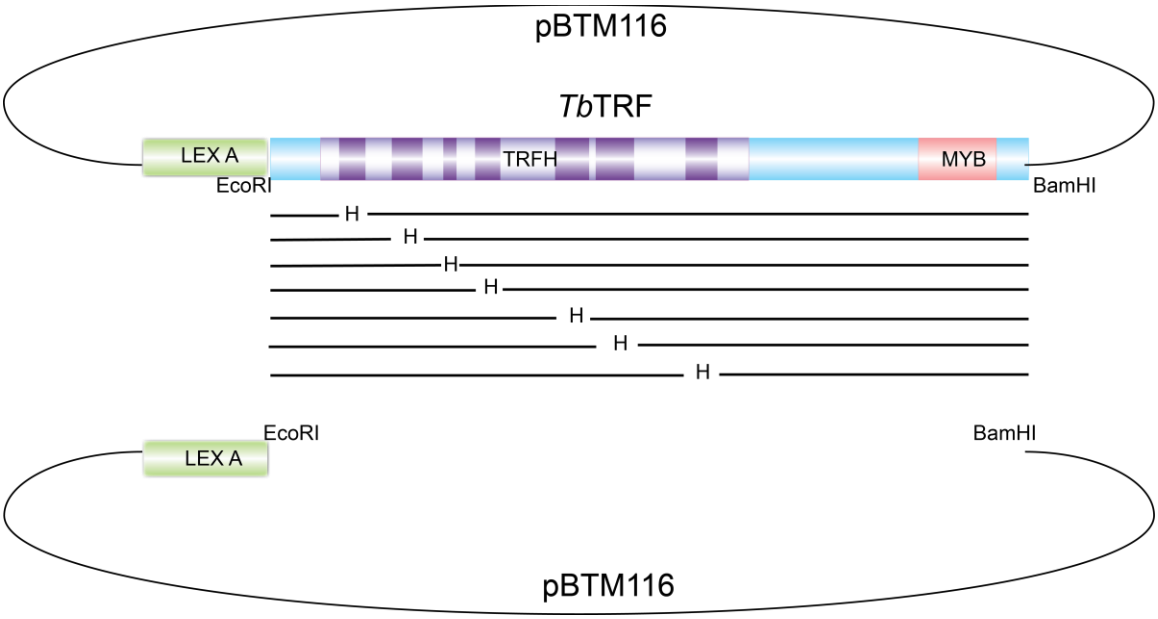

Figure 5-2: Strategy of making *Tb*TRFH deletion mutants. pBTM116 (LexA) vector containing wild type *Tb*TRF was used for PCR amplification (top). Mutants with individual helices deleted were cloned in pBTM116 vector (bottom). H represents HindIII sites. Black bar represents PCR products generated for each helix.

As shown in figure 5-2, fragments upstream and downstream of the helix to be deleted were generated using PCR amplification. Both fragments were then simultaneously ligated into vector to obtain LexA-fused mutant *Tb*TRF. Thus the *Tb*TRF gene was obtained containing a single helix deleted in the *Tb*TRFH domain. This protocol was repeated for each helix.

Analyzing TbTRFH mutant interactions

All the mutants were further transformed in the yeast L40 reporter strain along with the wild-type GAD-fused *Tb*TRF protein. After transformation, a liquid ONPG assay was performed to test interactions between mutants with wild-type *Tb*TRF protein. β-galactosidase activity were measured in order to estimate the *lacZ* reporter gene expression level. Interaction of wild type LexA-fused *Tb*TRF with GAD-fused *Tb*TRF was used as a positive control while the interaction between two empty vectors was used as a negative control.

LEX ABD –MUTANT *Tb*TRF	GAD-*Tb*TRF FL	GAD
*Tb*TRFH1Δ	83.23 +/- 21.7	0.6 +/- 0.06
*Tb*TRFH2Δ	38.74 +/- 8.47	0.57 +/- 0.14
*Tb*TRFH3Δ	38.72 +/- 14.09	0.49 +/- 0.09
*Tb*TRFH4Δ	0.063 +/- 0.02	0.08 +/- 0.01
*Tb*TRFH5Δ	17.84 +/- 10.25	0.91 +/- 0.13
*Tb*TRFH6Δ	7.42 +/- 2.09	0.63 +/- 0.04
*Tb*TRFH7Δ	40.25 +/- 11.68	0.41 +/- 0.05
*Tb*TRF Fullength	42.96 +/- 7.93	
LEX ABD		0.18 +/- 0.02

Table 2: Interaction of *Tb*TRFH mutants with the wild-type *Tb*TRF protein. β-galactosidase activities were measured by performing liquid assay containing ONPG as the substrate. Values were calculated for interactions between each mutant and the wild type full-length *Tb*TRF protein, as well as with the empty vector. Each value is calculated from nine independent experiments +/- standard deviations. LEX ABD, Lex A binding domain; GAD, Gal4 activation domain.

As seen in Table 2, deletion of helix 1, 2, 3, and 7 did not affect their interaction swith the wild type *Tb*TRF protein, suggesting that these helices are not required for homodimerization of *Tb*TRF. Deletion of helix 4, 5, and 6 affected interaction with the wild type *Tb*TRF to different degrees. Helix 5 deletion seems to have weakened interaction with *Tb*TRF compared to full-length protein. Expression of helix 4 deletion mutant was decreased compared to other mutants and hence that could possibly lead to a dramatically decreased interaction with the wild type *Tb*TRF (data not shown).

GAD–MUTANT *Tb*TRF	LEX ABD –MUTANT *Tb*TRF	LEX ABD
*Tb*TRFH1Δ	31.61 +/- 20.63	0.17 +/- 0.12
*Tb*TRFH2Δ	55.05 +/- 16.2	0.19 +/- 0.13
*Tb*TRFH3Δ	22.74 +/- 17.2	0.59 +/- 0.57
*Tb*TRFH4Δ	0.05 +/- 0.02	0.24 +/- 0.07
*Tb*TRFH5Δ	3.55 +/- 6.8	1.50 +/- 1.10
*Tb*TRFH6Δ	6.69 +/- 3.81	1.97 +/- 1.28
*Tb*TRFH7Δ	11.47 +/- 2.89	0.29 +/- 0.06
*Tb*TRF Fullength	51.14 +/- 9.6	
GAD		0.36 +/- 0.37

Table 3: *Tb*TRFH mutant-mutant self-interaction. β-galactosidase activity units were measured by performing liquid assay containing ONPG as the substrate. Values were calculated for interaction of each mutant with itself as well as with the empty vector. Each value is calculated from nine independent experiments +/- standard deviations. LEX ABD, Lex A binding domain; GAD, Gal4 activation domain.

Next, we wanted to test mutant-mutant self-interaction. Each *Tb*TRF mutant was amplified from the pBTM116 vector using primers having BamHI and XhoI restriction sites and cloned into the pACT2 (GAD-fused) vector. Hence, we obtained each mutant fused with LexA and GAD. These mutants were co-transformed in the L40 yeast strain. Liquid ONPG assay was performed to test their interaction. Interaction of LexA-fused wild type *Tb*TRF with GAD-fused wild type *Tb*TRF was used as a positive control, while interaction between two empty vectors was used as a negative control. As seen in table 2, helix 4, 5, 6, and 7 mutants had a significantly decreased self-interaction activity while helix 1, 2, and 3 mutants were dispensable for self-interaction. Again, the loss of interaction observed for helix 4 could be due to its low expression level in yeast. From both yeast 2-hybrid experiments it is evident that helix 4, 5, 6, and 7 are required for homodimerization of *Tb*TRF.

Function of TbTRF in chromatin remodeling

Initially, it was established that depletion of *Tb*TRF does not affect ES-linked *VSG* silencing in PF (unpublished data) and BF cells (Yang et al. 2009). From our studies, it is evident that *Tb*RAP1 is a major regulator of *VSG* silencing and that it regulates this silencing via chromatin remodeling in PF forms. It is possible that *Tb*TRF may also play an important role in *VSG* silencing. However, due to acute growth arrest upon its depletion the phenotype might not be evident. Mammalian TRF1 and TRF2 possess the ability to compact telomeric chromatin and form higher order chromatin structure. Hence, it was logical to test *Tb*TRF's function in chromatin modulation. In order to investigate this, FAIRE analysis was

performed in *Tb*TRF RNAi cells in PF and BF cells. By performing quantitative PCR using specific primers, changes in chromatin structure of ES-linked *VSGs* were determined.

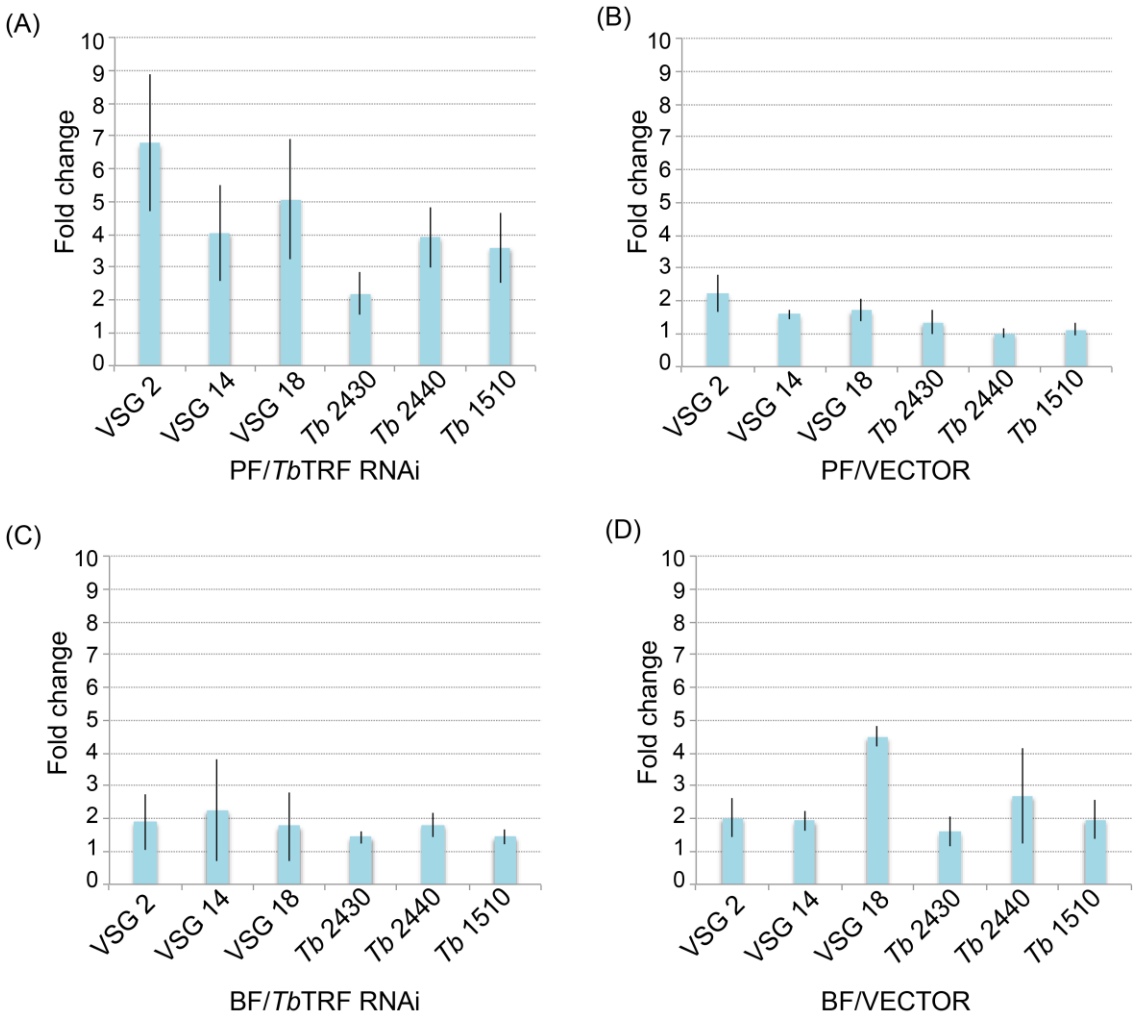

Figure 5-3: FAIRE analysis in *Tb*TRF RNAi cells. FAIRE was performed in (A) PF/*Tb*TRF RNAi cells, (B) PF/Vector control cells, (C) BF/*Tb*TRF RNAi cells and (D) BF/Vector control cells. Samples were collected before (0 hr in PF and BF cells) and after (48 hr in PF and 24 hr in BF cells) depletion of *Tb*TRF. Quantitative PCR was done using primers specific to indicated gene loci. Fold change was calculated from four independent experiments and standard deviation was calculated. Control genes are indicated with the last four digits of their ID. *Tb927.2.2430*, *Tb927.2.2440, Tb09.211.1510.*

Upon depletion of *Tb*TRF in PF cell, a 5-7 fold of increased enrichment of ES-linked *VSGs (VSG 2, 14* and *18*) was observed (figure 5-3 A). This difference was significantly different than observed in the vector control cells ($P<0.05$, figure 5-3 B). Enrichment of three chromosomal internal genes was also tested as a control. Increase in enrichment of *VSG2* and *VSG18* was significantly different from that of *Tb927.2.2440* ($P<0.05$), suggesting that *Tb*TRF has a mild but significant effect on the chromatin structure of the ES-linked *VSGs*. Also, changes observed at chromosome internal genes after depletion of *Tb*TRF were significantly different compared to that in the vector control cells, indicating that *Tb*TRF depletion might have a mild effect on global chromatin structure (figure 5-3 A and B).

Strikingly, depletion of *Tb*TRF had no effect on chromatin structure of ES-linked *VSGs* in BF cells. The increase in enrichment after depletion of *Tb*TRF in BF cells was not significantly different than that in the vector control cells (figure 5-3 C and D). Thus, *Tb*TRF only affects chromatin structure of ES-linked *VSGs* in PF cells but not in the BF cells.

We subsequently wanted to test whether *Tb*TRF depletion had any effect on regulation of *mVSGs*. Derepression of *mVSGs* upon depletion of *Tb*TRF in PF cells was tested before analyzing changes in chromatin structure.

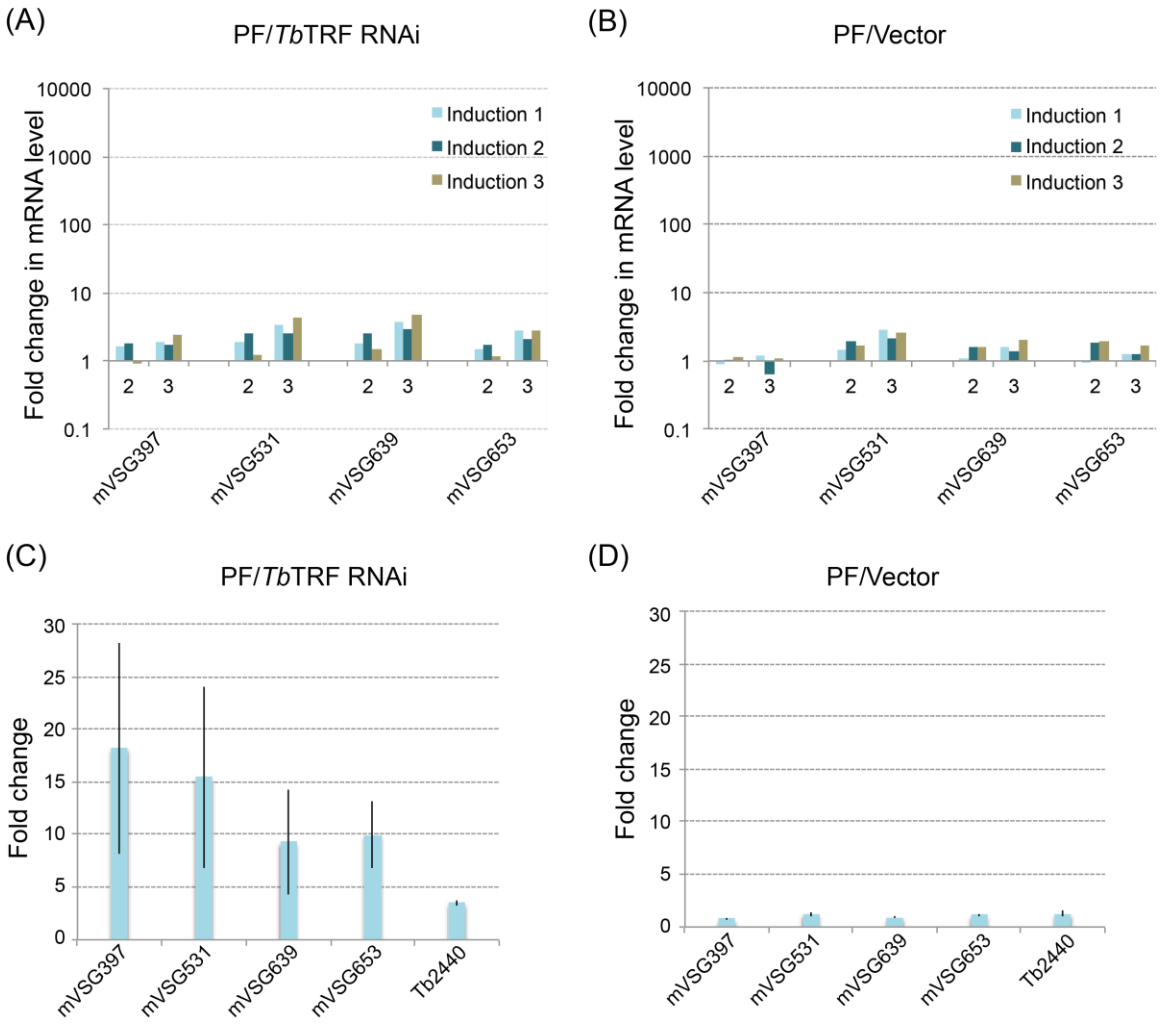

Figure 5-4: Quantitative RT-PCR and FAIRE analysis of *mVSGs* in PF *Tb*TRF RNAi cells. Fold change in steady state mRNA levels of *mVSGs* upon induction were tested in (A) PF/*Tb*TRF RNAi cells and (B) PF/Vector cells. Samples were collected before (day 0) and after (day 2 and 3) adding doxycycline. Fold change in steady state mRNA levels for day 2 and 3 were calculated by normalizing against day 0 value (not shown). Values for three independent experiments are depicted. FAIRE analysis was performed to determine change in the chromatin structure of *mVSGs* in (C) PF/*Tb*TRF RNAi cells and (D) PF/Vector cells. Samples were collected before (day 0) and after (day 2 for *Tb*TRF RNAi, day 3 for vector control) induction. Quantitative PCR was performed using specific primers for indicated loci in order to calculate the fold change. Fold change was calculated by dividing values obtained post depletion with that of the values obtained pre-depletion. Values were calculated from four independent experiments. Bar represents standard deviation.

After depletion of *Tb*TRF in PF cells, steady state levels of *mVSGs* mRNA were measured. No derepression of mVSGs was observed in PF/*Tb*TRF RNAi cells compared to the vector control cells (figure 5-4 A and B). Hence it is established from current studies and previously published data that *Tb*TRF does not play a role in ES-linked *VSG* or *mVSG* silencing. However, derepression analysis of *mVSGs* upon depletion of *Tb*TRF in BF form still remains to be tested. FAIRE analysis was performed to determine whether there are any changes in chromatin structure of *mVSGs* upon depletion of *Tb*TRF in PF cells. Quantitative PCR was performed to measure relative enrichment of *mVSG* specific DNA after depletion of *Tb*TRF. A 10-16 fold enrichment of *mVSGs* DNA was observed after knockdown of *Tb*TRF in PF cells (figure 5-4 C). This enrichment was significantly different from the chromosome internal gene used as a control (*Tb927.2.2440*) as well as from the vector control cells (figure 5-4 D). Thus, *Tb*TRF influences telomere/subtelomere chromatin structure and its depletion lead to opening up of the chromatin structure at ES-linked *VSGs* and *mVSGs* in PF cells.

DISCUSSION

Due to acute growth arrest upon depletion of *Tb*TRF, it was difficult to reveal all the functions of *Tb*TRF, especially in telomere structure maintenance and protection. Therefore, establishing viable mutants of *Tb*TRF was pivotal. *Tb*TRFH domain is deemed to be important for its role in *Tb*TRF self-dimerization as well as in interaction with other telomeric proteins, such as *Tb*RAP1 and *Tb*TIF2. Our goal was to establish several helix deletion mutants of *Tb*TRFH domain that

would affect *Tb*TRF homodimerization or its interaction with other telomere proteins. Seven deletion mutants were generated and their interaction with wild-type *Tb*TRF as well as self-interaction was tested *in vitro* by yeast 2-hybrid analysis. It was established that Helix 4, 5, 6, and 7 are important for homodimerization of *Tb*TRF while helix 1, 2 and 3 are dispensable. These results were very exciting since it suggested that not all helices are required for TbTRF homodimerization and few may be utilized for interaction with other proteins. Yeast 2-hybrid analysis can be further performed to test interaction of *Tb*TRFH mutants with *Tb*RAP1 and *Tb*TIF2 to determine which helices are involved in these interactions. It is possible that a similar set of helices might also interact with other telomeric proteins. If that is the case, then how does *Tb*TRF regulate the formation of telomere complex? Do they compete with each other for binding at telomeres? These will be a few interesting questions to answer. If distinct helices are used for different interactions then separation of function mutants can be obtained. These mutants will be very valuable in elucidating role of *Tb*TRF as well as other telomeric proteins in telomere end regulation. So far the mode of recruitment of *Tb*RAP1 and *Tb*TIF2 to the telomeres is unknown. Mutants defective in binding to *Tb*RAP1 and *Tb*TIF2 can be utilized to test their binding to telomeres.

Mutants that are able to self-dimerize can be knocked-in to replace the unique wild-type *Tb*TRF allele in a *Tb*TRF single-allele knockout background. As long as the mutants are capable of performing essential functions of *Tb*TRF, the cells should be viable. These mutants can be further used to study the role of *Tb*TRF

in recruiting other telomeric proteins and also its role in telomere structure maintenance.

Helix 4 deletion had a dramatic effect on expression of *Tb*TRF protein in yeast. It is possible that its deletion could affect proper folding of *Tb*TRF protein. Hence, point mutations can be made in this helix to study the role of helix 4 in homodimerization. Since helix 1, 2, and 3 are dispensable for the homodimerization of *Tb*TRF, simultaneous deletions of more than one helix can also be made to further analyze critical functions of *Tb*TRF.

Telomeric proteins are known to be involved in telomere heterochromatic structure formation/maintenance. Our aim was to determine whether *Tb*TRF had any role in *VSG* silencing by chromatin compaction. *Tb*TRF depletion does not lead to ES-linked *VSG* derepression in PF and BF cells (Yang et al. 2009). Our studies further established that *Tb*TRF is not required for *mVSG* silencing in PF cells. Interestingly, depletion of *Tb*TRF does affect chromatin structure of ES-linked *VSGs* and *mVSGs* in PF cells. In contrast, similar to *Tb*RAP1, no effect on chromatin structure was observed in BF cells after depletion of *Tb*TRF. Monoallelic *VSG* expression is of crucial importance in BF cells. Hence, it is possible that additional mechanisms other than telomeric proteins may play important roles in *VSG* silencing. Elucidating these mechanisms can further shed light on chromatin structure differences in PF and BF cells.

*Tb*TRF is a DNA binding protein. It seems that *Tb*TRF holds the telomeric complex together and maintains its integrity. This observation explains the acute growth arrest observed upon its depletion compared to *Tb*RAP1 (Yang et al.

2009, Pandya et al. 2013) and *Tb*TIF2 (Jehi et al., 2014). For *VSG* derepression to occur, a certain level of functional transcriptional machinery is required. It is possible that the whole telomere complex may fall apart upon *Tb*TRF depletion, stalling all the machineries in cell. In the future, domain mutants of *Tb*TRF can be used to study its function in *VSG* regulation.

CHAPTER VI

CHARACTERIZATION OF *TRYPANOSOMA BRUCEI* TELOMERIC TRANSCRIPT: TERRA

INTRODUCTION

Telomeres were long considered transcriptionally silent due to their repressive chromatin structure This dogma was overcome with the discovery of telomeric transcription called TERRA: telomeric repeat containing RNA. Telomere transcription was first identified in birds, trypanosomes, and diptera (Morcillo et al. 1988, Rudenko & Ploeg 1989, Solovei et al. 1994). Till this date TERRA has been identified in humans, rodents, budding yeast, fission yeast, and zebra fish (Azzalin et al. 2007, Luke et al. 2008, Schoeftner and Blasco 2008, Greenwood and Cooper 2011).

In mammals, TERRA is transcribed from the C-rich strand, giving rise to UUAGGG repeats with sizes ranging from 100 bp-9 kb (Azzalin et al. 2007). In trypanosomes TERRA is also transcribed from the C-rich strand ranging from

0.5-4 kb (Rudenko and ploeg 1989). In budding yeast its size is usually <500 bp. Along with TERRA, budding yeast also expresses molecules called ARRET that are antisense to the subtelomere and do not contain any detectable telomeric repeats (Luke et al. 2008). On the other hand, the transcriptome of fission yeast is much more complicated and contains multiple transcripts namely TERRA, ARRET, ARIA, and αARRET (Bah et al. 2012).

TERRA is transcribed by RNA polymerase II in humans, mouse, and budding yeast (Schoeftner and Blasco, 2008, Luke et al. 2008). In trypanosomes, however, it is established that TERRA transcription is not sensitive to α-amanitin, suggesting that it is transcribed by RNA polymerase I (Rudenko and Ploeg 1989). A portion of TERRA is poly-adenylated in human, yeast, and trypanosomes (Rudenko and Ploeg 1989, Azzalin and Lingner 2008, Luke et al. 2008). In humans, a CpG island consisting of “61-29-37” repeats located in the subtelomeric region is the promoter for TERRA transcription, and TERRA is found mostly in the nucleus co-localizing with telomeres (Azzalin et al. 2007, Schoeftner and Blasco 2008, Nergadze et al. 2009).

Not only does TERRA co-localizes physically with telomeres, but also it interacts with telomeric proteins, such as TRF1, TRF2, and ORC subunits *in vivo* in mammalian cells. TERRA interaction with several heterochromatin associated factors including heterochromatin protein 1 (HP1) and H3K9 methyltransferases has also been established (Deng et al. 2009). Telomeric proteins are known to play a role in regulation of TERRA levels. In budding yeast, Rap1/Sir and Rap1/Rif complexes regulate TERRA transcription, and TERRA levels are

upregulated upon introducing Rap1 mutant that fails to recruit Sir proteins (Iglesias et al. 2011). In fission yeast, deletions of Taz1 or Rap1 lead to upregulation of TERRA transcription (Greenwood and Cooper 2011). Thus, it is clear that telomeric proteins are important in regulation of TERRA expression.

Functions of TERRA are not well characterized. Depletion of TERRA RNA using siRNA led to loss of cell viability and formation of telomere dysfunction induced foci (TIFs) in mammalian cells (Deng et al. 2009). Interestingly, depletion of TERRA also affected telomere heterochromatin with reduced recruitment of ORC and decreased amount of H3K9 trimethylation (Deng et al. 2009). This observation suggests that TERRA might have a role in regulating telomere heterochromatin. However, further studies are needed in order to rule out possible secondary effects from siRNA.

T. brucei telomeres are unique in terms of the presence of *VSG* genes at subtelomeres. From our studies with *Tb*RAP1, we determined that de-repression of silent *VSGs* is linked to chromatin compaction. Thus, it is possible that TERRA may be involved in *VSG* silencing regulation via chromatin remodeling. This hypothesis makes TERRA an excellent candidate to study regulation of antigenic variation in *T. brucei*. Mammalian telomeres are gene-less, making them unsuitable for studying telomere position effect, while many *T. brucei* telomeres are marked with natural subtelomeric *VSG* genes. Hence, *T. brucei* is an excellent model system to study functions of TERRA in telomere position effect.

RESULTS

Characterization of TERRA in wild-type PF and BF cells

TERRA has been previously detected in *T. brucei* BF and PF cells (Rudenko and Ploeg 1989). However data were shown only for PF cells. It was established that the C-rich telomeric strand is transcribed, giving rise to the UUAGGG repeat transcript and that this transcription is unidirectional, running 5' to 3' from chromosome internal region towards the telomere. However, *T. brucei* subtelomeric regions are quite plastic due to antigenic variation. The same strain used in the previous study has been cultured *in vitro* for a long period of time. It's therefore possible that some detailed subtelomeric sequences have changed, which might lead to variations from previously reported data on TERRA. Hence, we decided to determine TERRA in wild-type BF (SM) and PF (WT427) cells. Northern blot analysis was performed to detect TERRA size distribution as well as the directionality of its transcription (Figure: 5-1 A). The northern blot was hybridized with either the radioactively labeled $(*CCCTAA)_{133}$ or $(*TTAGGG)_{133}$ probe.

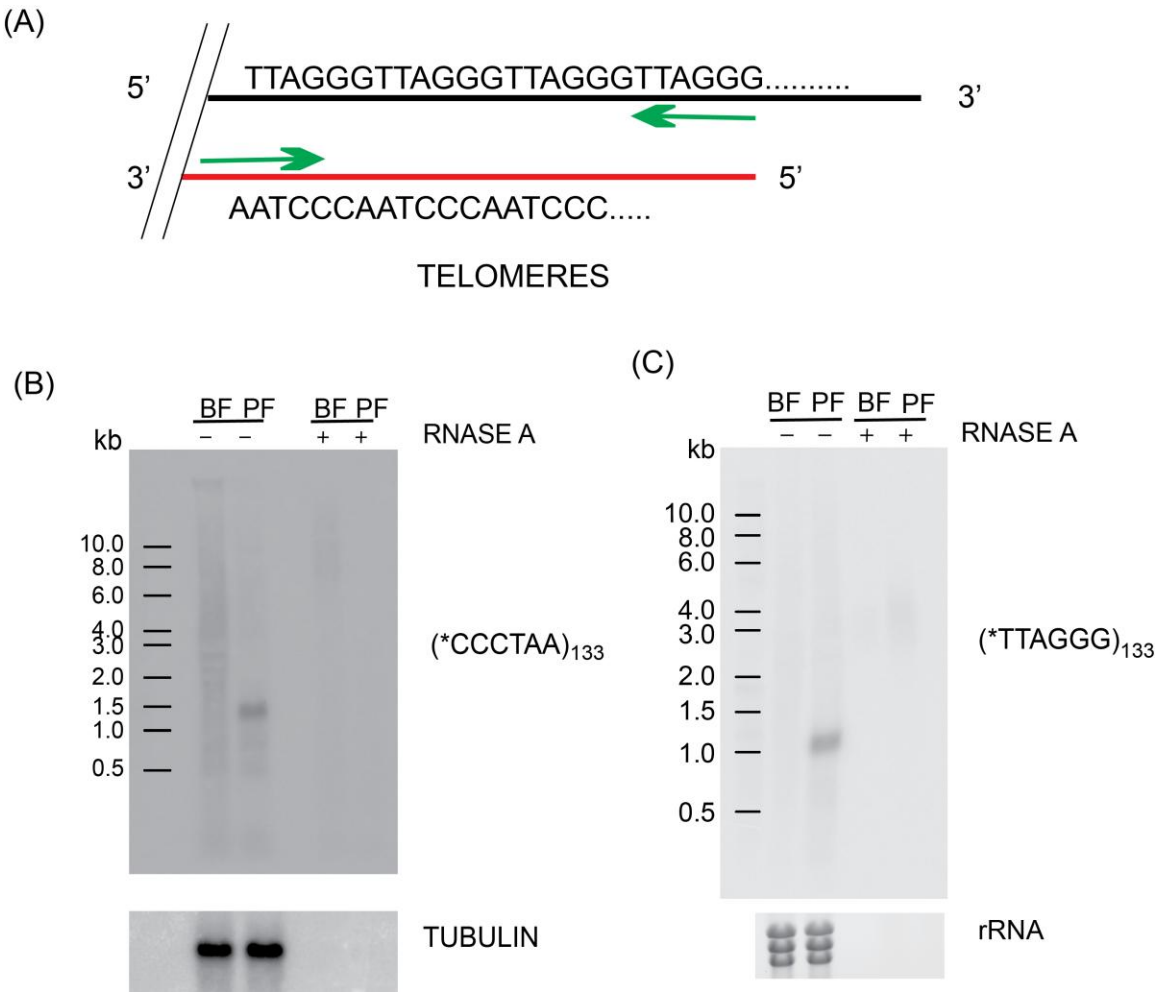

FIGURE 6-1: TERRA in wild-type *T. brucei* cells. (A) Directionality of TERRA transcription. The C-rich strand is transcribed when transcription proceeds from chromosome internal region towards the telomere, giving rise to UUAGGG transcript. However, if the transcription proceeds from telomere towards chromosome internal region, then the G-rich strand will be transcribed, giving rise to CCCUAA transcript. (B) Northern blot analysis to detect transcription from C-rich strand in BF and PF cells. The northern blot was hybridized with radioactively labeled (*CCCTAA)$_{133}$ probe. Samples were treated with or without RNase A. Tubulin was used as internal loading control. (C) Northern blot analysis to detect transcription from G-rich strand in BF and PF cells. Northern blot was hybridized with radioactively labeled (*TTAGGG)$_{133}$ probe. Samples were treated with or without RNase A. A rRNA was used as an internal loading control.* indicates radiolabeled nucleotide.

Northern blot analysis detected TERRA molecules ranging from the 0.5-10 kb in BF cells. However, in procyclic form, the size of TERRA molecules is between 0.5-1.5 kb with a major band of ~1.5 kb long. Upon RNase A treatment, signals were lost in both BF and PF samples, indicating that the TERRA signal was contributed specifically from the RNA and was not due to DNA contamination. The majority of transcription in BF cells was detected when the blot was hybridized with the $(*CCCTAA)_{133}$ probe, suggesting that TERRA transcription proceeds towards telomere ends giving rise to the UUAGGG transcript. Transcription detected from G-strand was almost negligible in BF cells. However, in PF TERRA was detected from both strands, suggesting that the nature of TERRA molecules might be different in BF and PF cells. More experiments will be required to analyze the nature of TERRA molecules in PF cells.

Interaction of TERRA with telomeric proteins

Our lab has characterized the telomeric complex of *T. brucei*. So far, three telomeric proteins have been identified. *Tb*TRF is a duplex TTAGGG repeat binding factor, while *Tb*RAP1 and *Tb*TIF2 were identified as *Tb*TRF interacting factors. Since TERRA is transcribed from telomeres, we are curious whether TERRA interacts with any of the known telomeric proteins in *T. brucei* (Figure 6-2). In addition, *Tb*KU80 has been shown to play an important role in maintaining telomere length (Janzen et al. 2004), although its mechanism is unknown. It is possible that *Tb*KU80 may interact with TERRA in order to regulate the telomere length. In order to test this we performed RNA-Immunoprecipitation (RNA-IP) assay. Various cell lines containing telomeric proteins tagged with either GFP or

F2H (Flag-HA-HA tag) tags were used for this purpose. Pull-down of telomeric proteins was performed using antibodies against either the GFP or HA epitope. Co-Immunoprecipitated RNA was detected by dot blot analysis by hybridization with telomere specific probes.

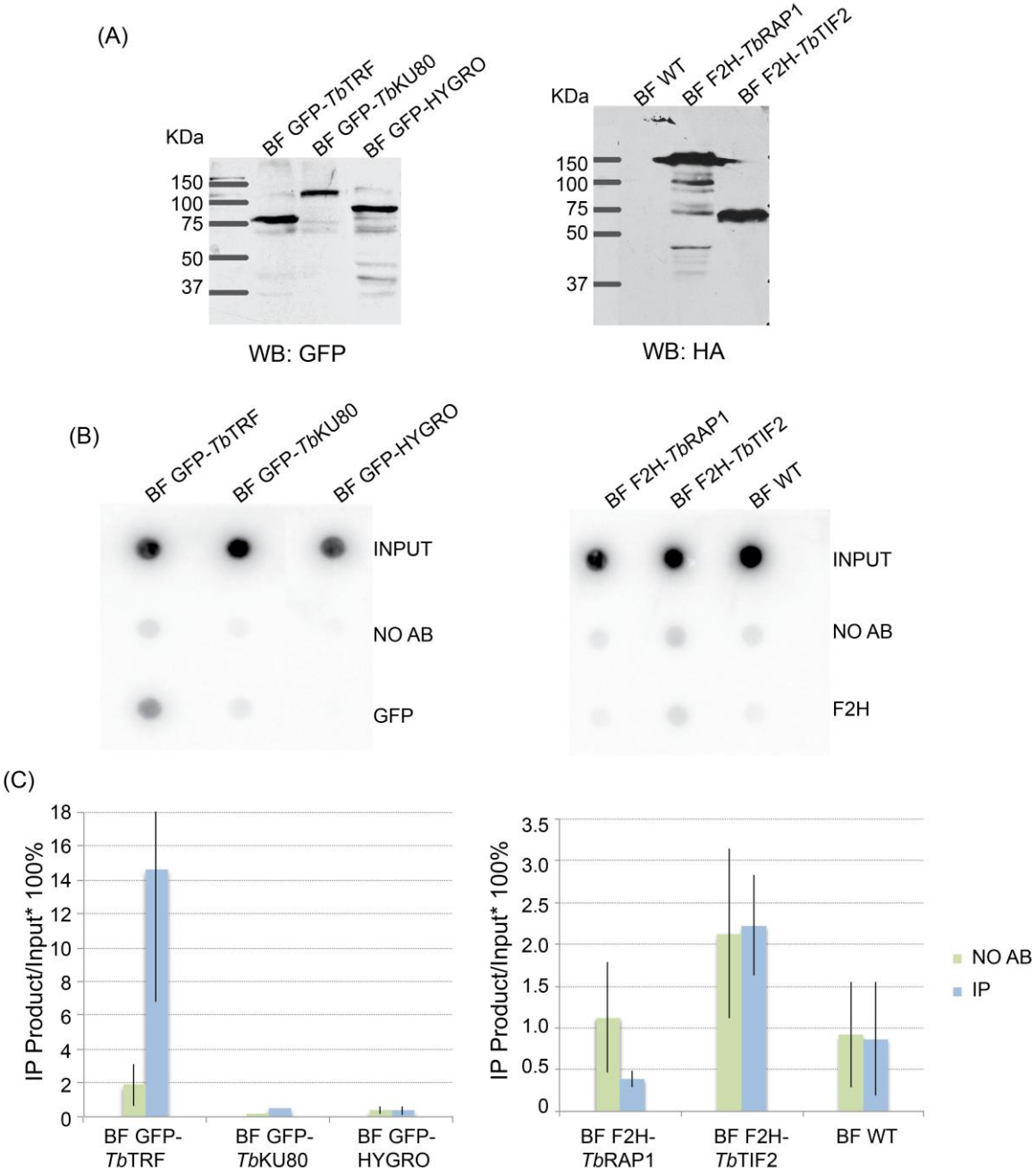

FIGURE 6-2: Interaction of TERRA with telomeric proteins. (A) Western analysis showing expression of various tagged telomeric proteins in BF cells. Levels of GFP-*Tb*TRF and GFP-*Tb*KU80 were detected using rabbit anti-GFP antibody (Life Technologies). A cell line expressing GFP alone was used as a negative control. F2H-*Tb*RAP1 and F2H-*Tb*TIF2 were detected using an antibody against the HA tag (F-7, Santa Cruz Biotechnology Inc.). The wild-type cell line, not expressing any F2H tag was utilized as negative control (BF WT). (B) RNA slot blot analysis to detect TERRA molecules co-immunoprecipitated with various telomeric proteins. Dynabeads IgG without any antibody was used as negative control. The blot was hybridized with radioactive labeled (*CCCTAA)$_{133}$ probe. (C)

Quantification of RNA slot blot experiments. The average of enrichment of pull-down sample over input (%) was calculated from three independent experiments. Error bars represent standard deviation.

GFP-*Tb*TRF showed an ~14 fold enrichment of TERRA RNA compared to control (Fig. 6-2C), suggesting that *Tb*TRF interacts with TERRA. Our preliminary data showed that *Tb*KU80 might interact with TERRA (Fig. 6-2C). The fold enrichment observed is much less compared to that obtained for *Tb*TRF, however, it is ~5 fold more compared to no antibody control. More experiments are needed to confirm whether this result is reproducible. F2H-*Tb*RAP1 does not interact with TERRA, as the fold enrichment is almost similar to negative control (when IP using the HA antibody was done in wild-type cells carrying no F2H tag) (Fig. 6-2C). F2H-*Tb*TIF2 IP showed elevated levels of TERRA enrichment that was not significantly different from the negative control due to large variations, suggesting that *Tb*TIF2 does not interact with TERRA (Figure 6-2C). All the IP samples were treated with DNase I, suggesting that the signal obtained on slot blot is due to RNA. However, additional controls such as RNase A treatment before IP needs to be done. Based on our current preliminary observations, we conclude that *Tb*TRF and *Tb*KU80 interact with TERRA while *Tb*RAP1 and *Tb*TIF2 do not interact with TERRA RNA.

Regulation of TERRA levels by telomeric proteins

TERRA expression is influenced by telomeric protein in yeast (Greenwood and Cooper 2011). We therefore wanted to test whether any of the known telomeric proteins in *T. brucei* plays any role in regulation of TERRA levels. We depleted individual telomeric proteins by RNAi in different inducible telomeric

protein RNAi strains. Upon induction of RNAi using doxycycline, knockdown of *Tb*TRF, *Tb*RAP1, and *Tb*TIF2 was confirmed by western blotting. Imaan Benmerzouga performed *Tb*TRF western blot analysis and Sanaa Jehi did *Tb*TIF2 western blot analysis. Total RNA was isolated before and after depletion of individual telomeric protein. Northern blot analysis was performed using the $(*CCCTAA)_{133}$ probe in order to detect changes in TERRA levels and sizes. Since TERRA molecules have a large size distribution and it is hard to estimate the total amount of TERRA from the northern blot, we also performed slot blot analysis to quantify changes in the TERRA levels.

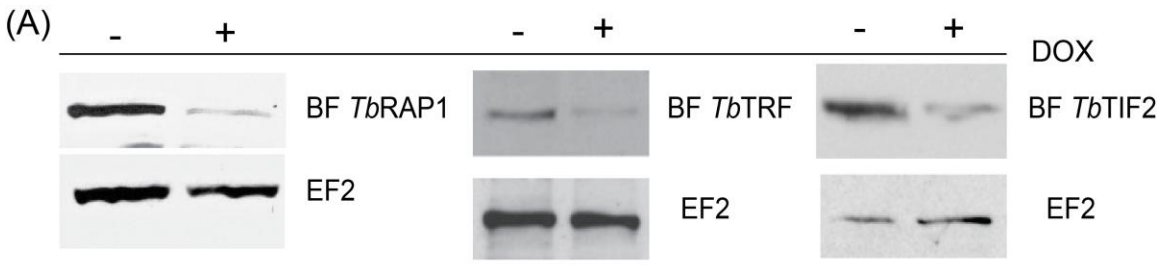
(A)
-
+
-
+
-
+
DOX
BF TbRAP1
EF2
BF TbTRF
EF2
BF TbTIF2
EF2

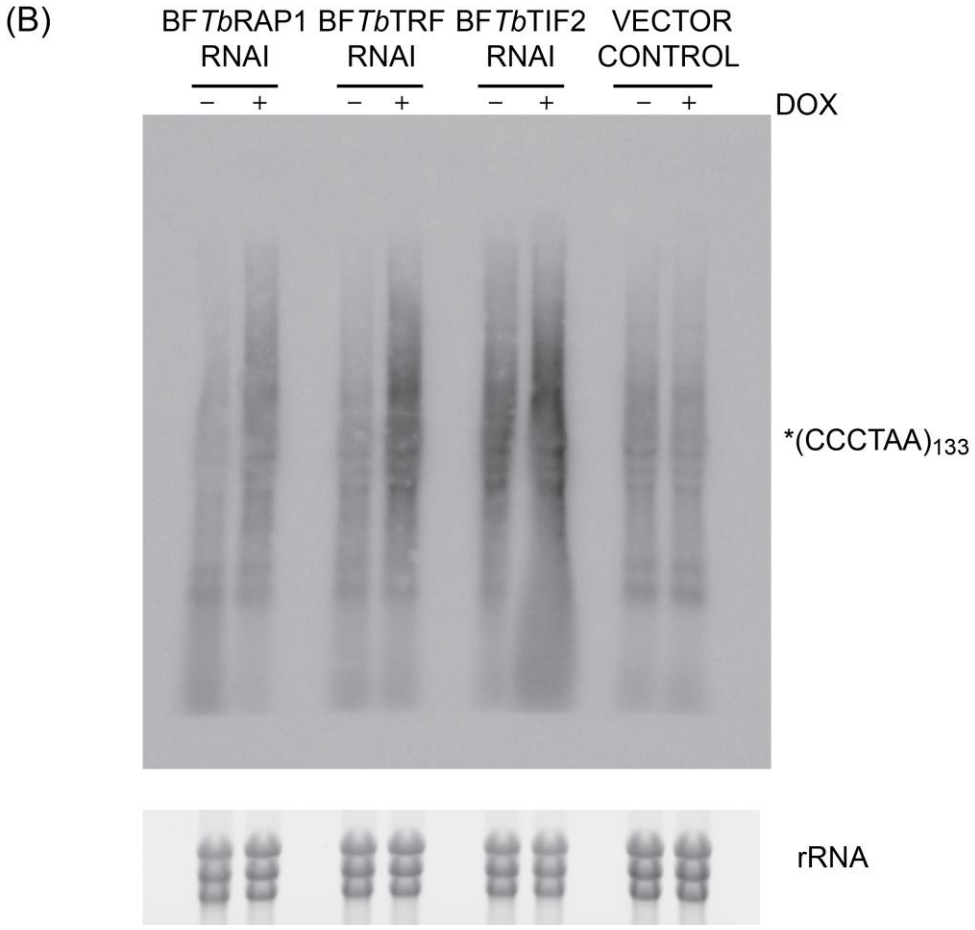
(B)
BF TbRAP1 RNAI
BF TbTRF RNAI
BF TbTIF2 RNAI
VECTOR CONTROL
– + – + – + – +
DOX
*(CCCTAA)133
rRNA

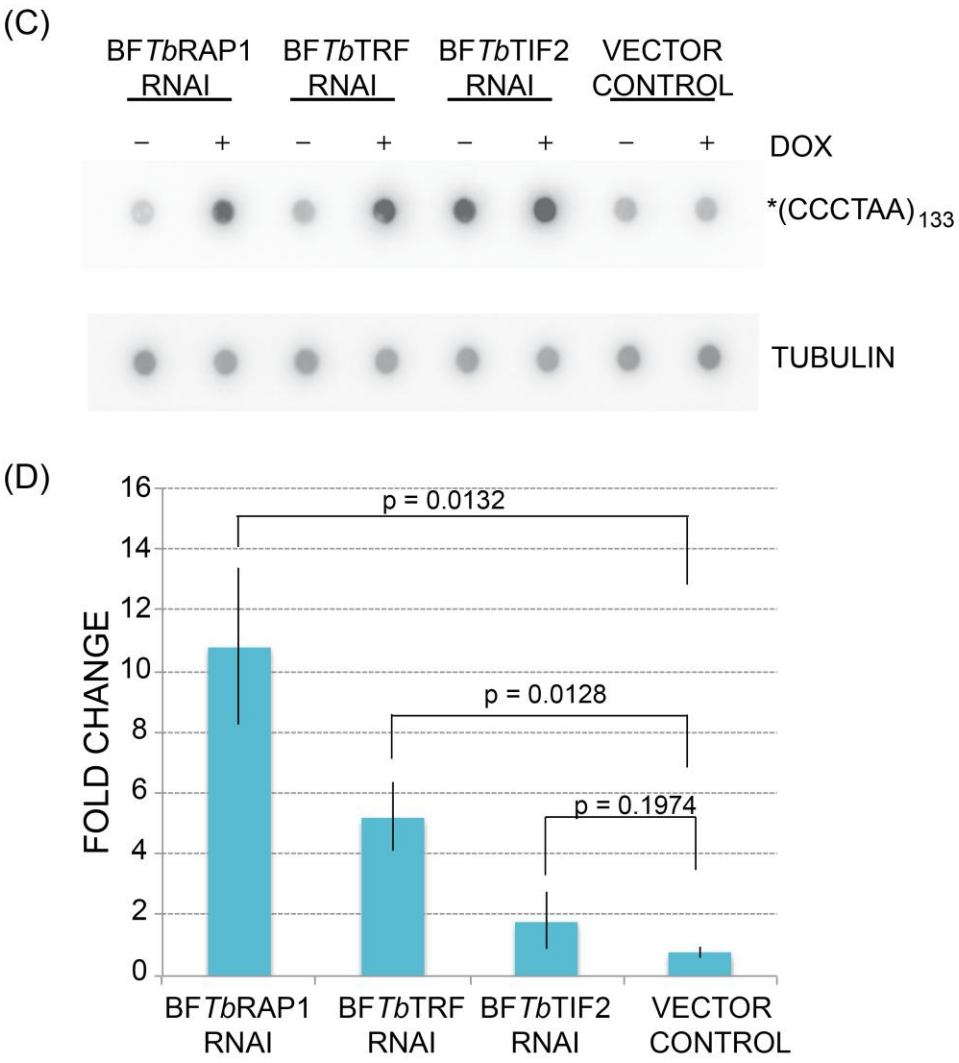

FIGURE 6-3: Regulation of TERRA RNA level by telomeric proteins. (A) Western blot analysis to determine knockdown of *Tb*RAP1, *Tb*TRF, and *Tb*TIF2 in BF cells. Whole cell lysate was collected before (0 hour) and after (24 hours for *Tb*RAP1 and *Tb*TRF, 30 hours for *Tb*TIF2) (B) Northern blot analysis to detect levels and distribution of TERRA before and after depletion of *Tb*RAP1, *Tb*TRF and *Tb*TIF2. Cells transfected with an empty RNAi vector was used as a negative control. RNA was collected before (-) and after (+) doxycycline induction (24 hours for *Tb*RAP1 and *Tb*TRF, 30 hours for *Tb*TIF2. The blot was hybridzed with the $(*CCCTAA)_{133}$ probe. rRNA precursors are shown as a loading control. (C) Slot blot analysis to quantify changes in TERRA level. The blot was hybridzed with the $(*CCCTAA)_{133}$ probe. Hybridization to the tubulin probe was used as an internal loading control. (D) Quantification of slot blot analyses. Fold changes in TERRA amount was calculated by dividing post-induction TERRA signal intensity by pre-induction signal intensity. Standard deviations are shown as error bars. P values of unpaired t-tests were calculated compared to control cells from four independent experiments.

Northern analysis was performed to compare the TERRA levels and distribution before and after depletion of *Tb*RAP1, *Tb*TRF, and *Tb*TIF2. We observed that the steady state level of TERRA RNA increased upon depletion of all telomeric proteins compared to the control cells transfected with an empty RNAi vector (Fig. 6-3B). However, for *Tb*TIF2, the effect was the same as in the control cells (Fig. 6-3B). No major changes in the size distribution of TERRA molecules were detected (Fig. 6-3B). In the slot blot analysis, RNA collected before and after depletion of telomeric proteins was blotted on the membrane followed by hybridization with the $(*CCCTAA)_{133}$ probe. Figure 6-3C shows increases in TERRA amount upon depletion of *Tb*RAP1 and *Tb*TRF, suggesting that both proteins play important roles in TERRA expression regulation. A mild increase in TERRA level was also seen upon depletion of *Tb*TIF2 (Fig. 6-3C). However, quantification of signals obtained from slot blot analyses (Figure 6-3D) showed that *Tb*TIF2's effect on the steady state level of TERRA was not significantly different from the vector control cells (P= 0.1974). In contrast, depletion of *Tb*RAP1 and *Tb*TRF showed significant increase in the steady state level of TERRA. *Tb*RAP1 appeared to have more profound effect on TERRA levels (~10 fold) compared to *Tb*TRF (~5 fold). This suggests that different telomeric proteins may contribute differently to TERRA expression regulation.

Telomeres contributing to TERRA transcription

As previously described (Rudenko and ploeg 1989), transcription of TERRA RNA in *T. brucei* is not sensitive to α-amanitin treatment, indicating that unlike mammalian systems, TERRA in *T. brucei* is not transcribed by RNA polymerase

II but likely by RNA polymerase I. In *T. brucei,* the active *VSG* is transcribed exclusively from one of ~15 BESs located at subtelomeres by RNA polymerase I (Gunzl et al. 2003, Hertz-Fowler et al. 2008). Hence, it is possible that the majority of TERRA RNA might be transcribed as a result of read-through from the telomere transcribing the active *VSG*. *T. brucei* has 11 pairs of megabase chromosomes carrying all essential genes, ~5 intermediate chromosomes, and ~100 of minichromosomes carrying mostly repetitive sequences (Weiden et al. 1991, Zomerdijk et al. 1992, Alsford et al. 2001, Wickstead et al. 2004). There are ~250 telomeres in a *T. brucei* nucleus (Figure 6-4).

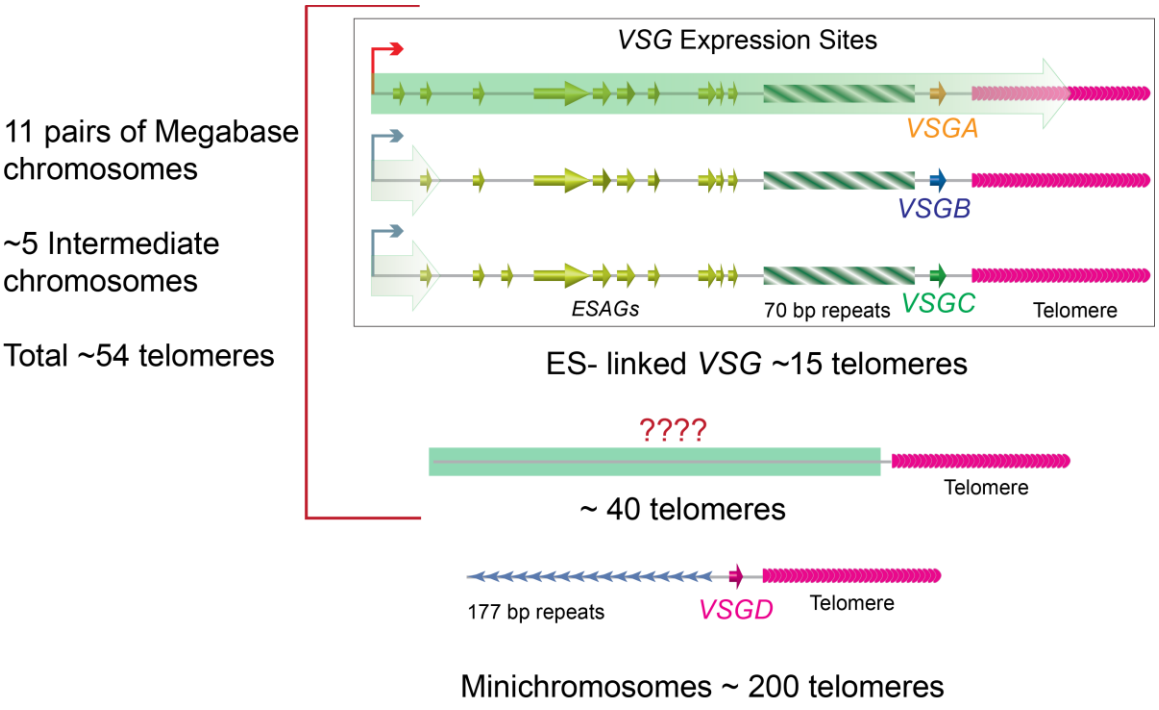

Figure 6-4: Total telomeres in a *T. brucei* nucleus. *T. brucei* consists of 11 pairs of megabase chromosomes and ~5 intermediate chromosomes. Among these ~54 telomeres, 15-20 are known to carry the well-characterized BESs. However, for the rest of 35-40 telomeres no sequence information is available for the subtelomeric region. The rest of ~200 telomeres are on minichromosomes. Many of these telomeres carry a *VSG* gene at the subtelomeric region.

Although minichromosomes carry a *VSG* gene at their subtelomeric region, it is known that no active transcription occurs on minichromosomes due to the lack of an upstream promoter. Hence, out of these ~250 telomeres only ~54 telomeres have a possibility of active transcription at the subtelomeric region. 15-20 telomeres on megabase and intermediate chromosomes carry a BES at their subtelomeric regions. Sequences of these BESs are well known, allowing their easy characterization. We can also easily differentiate telomeres marked with the active *VSG* from those with silent *VSGs*. However, for the rest of the 35-40 telomeres on the megabase and intermediate chromosomes, no sequence information is available for the subtelomeric region. Due to lack of sequence information it is difficult to test whether any transcription occurs at these telomeres. We hypothesized that TERRA is transcribed from the telomere carrying the active *VSG.* In order to test this possibility, we collected total RNA from cells exclusively transcribing *VSG2* and cells exclusively transcribing *VSG6*. RNA was reverse transcribed using a telomeric backward primer (5' CCCTAACCCTAA 3'). This would lead to reverse transcription of all the TERRA containing transcripts since TERRA contains UUAGGG repeat sequences. After reverse transcription, PCR was performed using primers specific to the active and silent *VSGs* and cDNA as the template (Figure 6-5 A &B). Although we do not know the structure of mature TERRA transcripts, we are aware that TERRA is transcribed from chromosome internal region towards the telomere. In addition, *T. brucei* genes are transcribed in a polycistronic fashion, so is the transcription of BESs. Hence we predict that we will be able to detect precursor and/or mature

TERRA molecules using primers specific to *VSGs* located immediately upstream of telomeres if TERRA is polycistronically transcribed with other genes in the BES by RNA polymerase I. In addition, we predict that only primers specific to the active *VSG* can amplify the RT product but not primers specific to silent *VSGs*, if only the active BES transcription contributes significantly to TERRA expression.

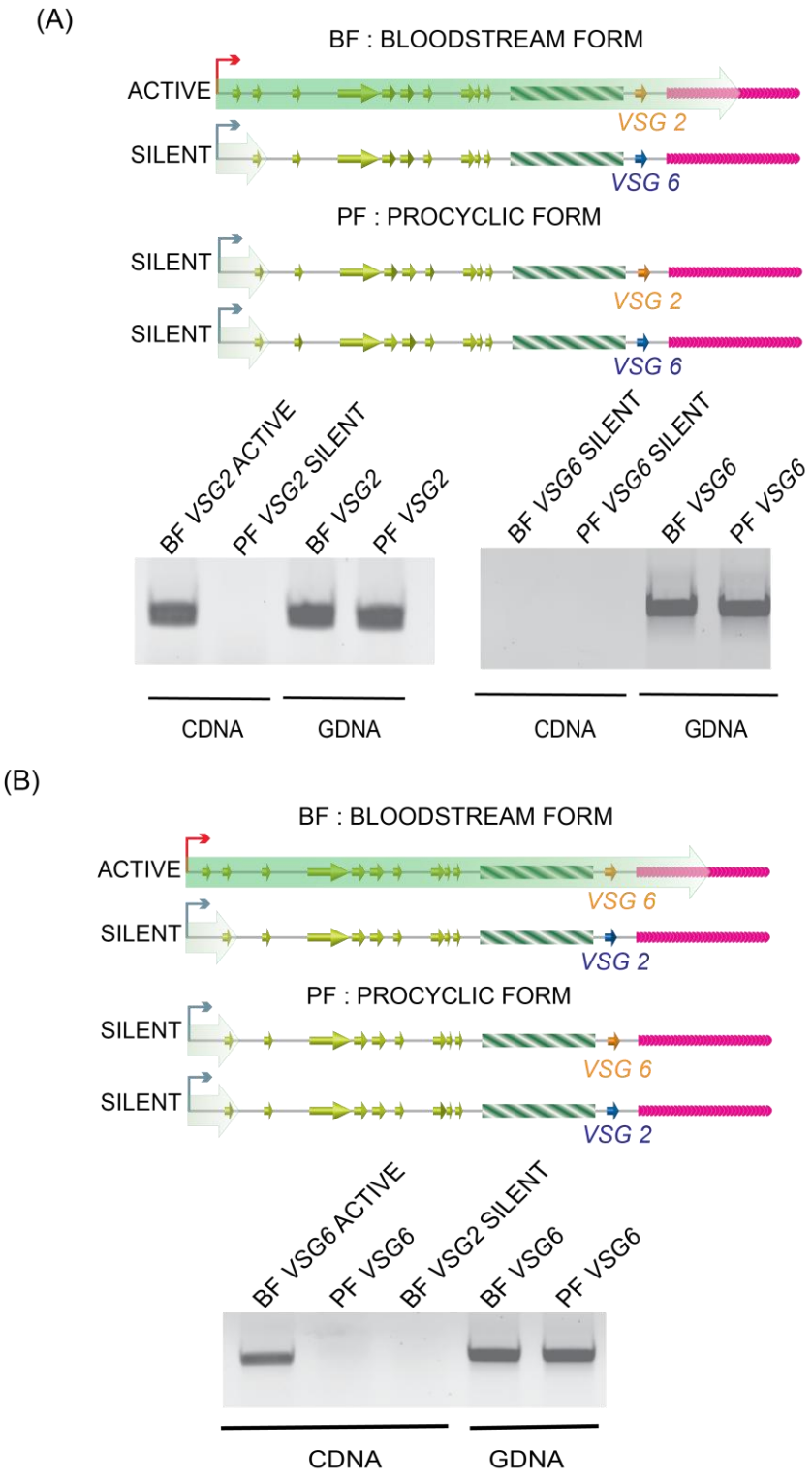

Figure 6-5: TERRA transcription from an active ES. (A) cDNA and gDNA (genomic DNA) was obtained from BF cells exclusively expressing *VSG2* and from PF cells where no *VSG* is expressed. PCR was performed using primers specific for *VSG2* and *VSG6*. (B) cDNA and gDNA (genomic DNA) was obtained

from BF cells expressing exclusively *VSG6* and from PF cells. PCR was performed using primers specific for *VSG2* and *VSG6*.

As seen from figure 6-5A, a PCR product was obtained using *VSG2* primers when cDNA obtained from BF cells expressing *VSG2* was used as the template. *VSGV6* is silent in these cells. No product was obtained using *VSG6* primers when the same cDNA was used as the template. PF cells do not express any *VSGs*. No PCR product was obtained using either *VSG2* or *VSG6* primers when cDNA prepared from PF cells was used as the template. Genomic DNA from either BF or PF cells gave amplification products when both *VSG* primers were used, indicating that lack of PCR product in the reactions using cDNA as the template was not due to loss of either *VSG* gene. Similarly, in figure 6-5B, a PCR product was obtained using *VSG6* primers when cDNA obtained from BF cells expressing *VSG6* was used as the template. No product was obtained using primers specific to the silent *VSG2*. CDNA obtained from PF cells did not give any amplification using either *VSG6* or *VSG2* primers. However, products were obtained when genomic DNA was used as a template, indicating that both *VSG* genes were present in these BF and PF cells. These results suggest that a significant amount of TERRA RNA is transcribed from the telomere with the active *VSG* in BF cells. On the other hand, in PF cells TERRA RNA appears not transcribed from any of the BES marked telomeres. It is possible that in PF cells TERRA might be transcribed from other telomeres whose sequence information is not available. In the future, sequencing of TERRA RNA from PF cells can be carried out to help a better understanding of its transcription.

TERRA RNA in BF cells is transcribed form the telomere carrying the active VSG

We found that transcription of the active BES contributes significantly to TERRA expression in BF cells (Fig. 6-5). To confirm this discovery, we used an alternative independent approach. It is known that the active *VSG* marked telomere undergoes frequent truncations, possibly due to its highly transcribed status (Bernards et al. 1983). In addition, in the absence of telomerase, the active *VSG* marked telomere is not elongated after each truncation, resulting in this telomere being shortened within a short period time (Dressen and Cross 2006). We decided to take advantage of this notion and obtained a telomerase null clone where most telomeres still have similar sizes as those in WT cells but the active *VSG* marked telomere is less than 1 kb long (Fig. 6-6). We hypothesized that TERRA RNA size distribution will be affected when the active telomere is much shorter than other telomeres if the majority of TERRA is transcribed from the active telomere. We also expected to detect a TERRA transcript of precise size (in contrast to a smear) in these cells if the mature TERRA molecules are processed at defined positions since the active telomere has a precise size in these clonal cells.

Ranjodh Sandhu in our lab did limiting dilution of BF *Tb*TRDKO cells (telomerase RNA null cells) and obtained a clone with extremely short active *VSG2*-marked telomere. Specifically, cells were plated at the density of 1 cell/well. After reaching an appropriate concentration, cells were harvested, and Southern blot analysis was performed to determine the size of the *VSG2*-marked

telomere (Fig. 6-6). The clone with the shortest active telomere was used for subsequent studies. It is important to note that this clone was obtained within a short range of time (~15 weeks), a time during which except for the active telomere, the majority of the bulk telomeres were still long and have similar sizes to wild-type telomeres. The parent BF *Tb*TRDKO cells were also cultured for ~2 weeks, a time during which all the telomeres are long and were used as a control to exclude any possible effect of *Tb*TR deletion on TERRA.

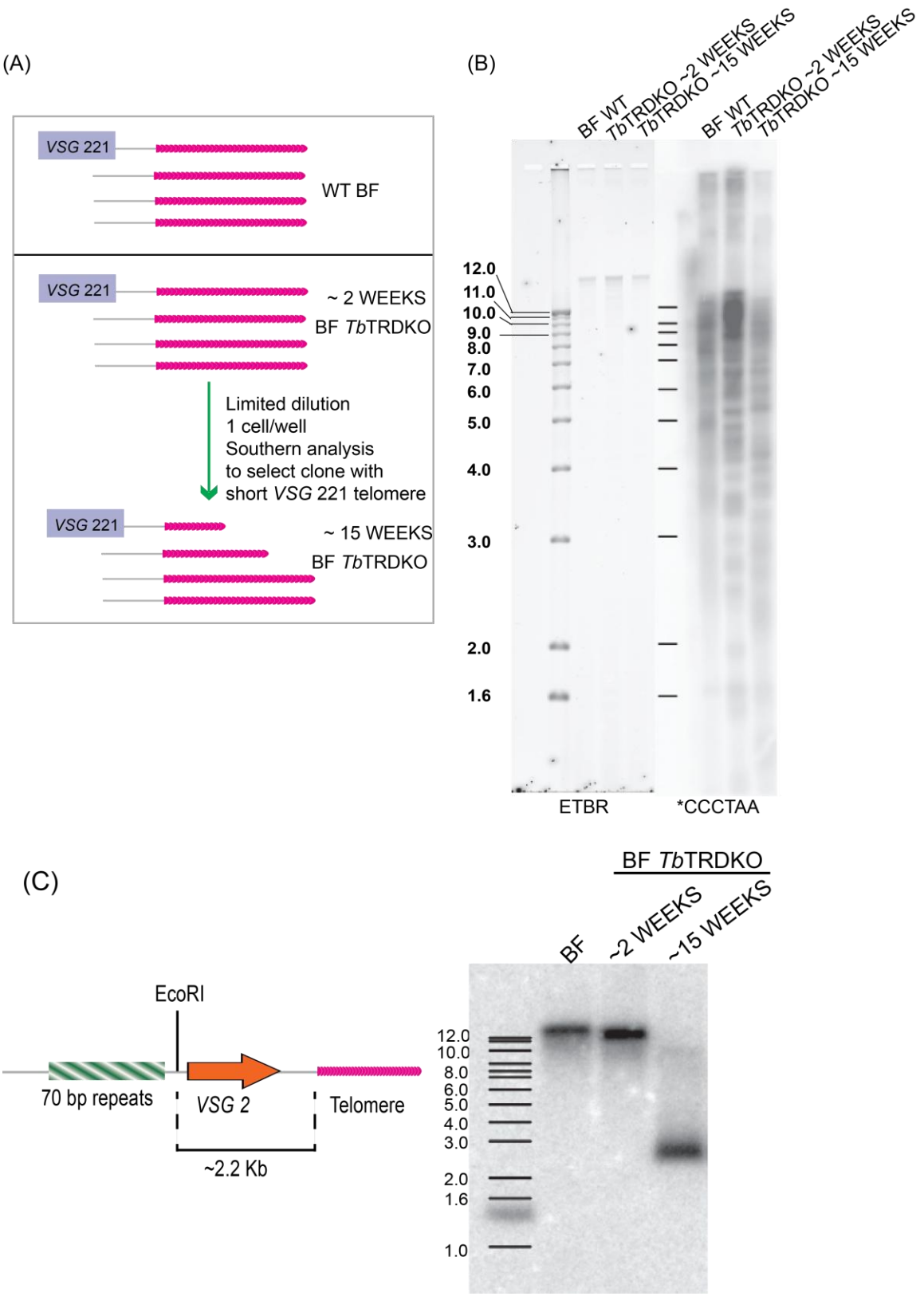

Figure 6-6: Establishing *Tb*TRDKO cells with short active ES-marked telomere. (A) Schematic representation of *Tb*TRDKO cell lines on the left. A freshly

obtained clone of *Tb*TRDKO (~2 weeks BF *Tb*TRDKO) had telomeres of same sizes as those in wild-type BF cells (WT BF). After limiting dilution, a clonal population was obtained that has a very short active *VSG*-marked telomere (within 15 weeks), with the rest of the bulk telomeres still long. (B) Southern blot analysis to determine bulk telomere length in all cell lines. Left panel shows the Ethidium Brimide (EtBr) staining of the agarose gel before hybridization. Right panel shows hybridization results with telomere specific probe. (C) Southern blot analysis to determine the size of the active *VSG2*-marked telomere all cell lines. *VSG2* BES has an EcoRI site upstream of the *VSG2* gene. Upon digestion with EcoRI, a terminal restriction fragment is obtained from which the telomere length can be calculated. The Southern blot was hybridized with a *VSG2* specific probe.

As seen from figure 6-6B, wild-type cells and *Tb*TRDKO (~2 weeks) cells have telomeres of comparable sizes. The short time cultured (~15 weeks) clone obtained after limiting dilution has only a mild telomere shortening phenotype with the sizes of bulk telomeres ranging from ~2 to 12 kb and still similar to those in wild-type cells. Southern blot analysis using the *VSG2* probe showed that wild-type and *Tb*TRDKO cells cultured for 2 weeks have terminal *VSG2* restriction fragments of ~12 kb (figure 6-6C). This indicates that in both of these cell lines the telomere adjacent to *VSG2* is long and more than 10 kb. While *Tb*TRDKO cells cultured for 15 weeks have a terminal *VSG2* restriction fragment of less than 3 kb, indicating that the size of *VSG2* marked telomere is only 600-800 bp long. Thus we successfully obtained an experimental system to determine the effect of a shortened active telomere on TERRA transcription without altering the lengths of bulk telomeres. This will further aid in confirming that transcription of the active BES-marked telomere contributes significantly to the total amount of TERRA.

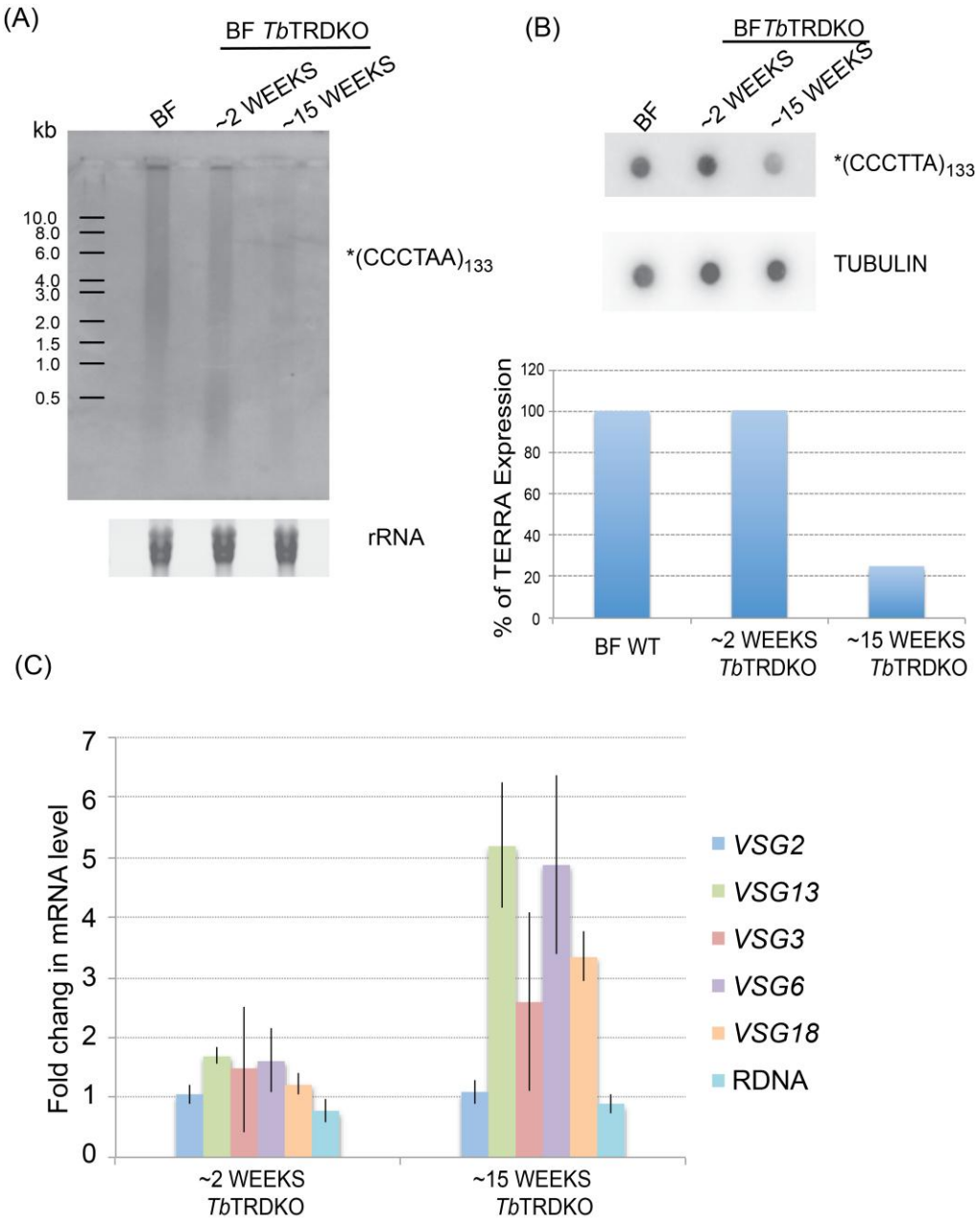

Figure 6-7: Amount of TERRA transcript in *Tb*TRDKO cells and VSG derepression analysis. (A) Northern blot analysis to determine the size distribution of TERRA RNA in wild-type cells and *Tb*TRDKO cells cultured for 2 weeks (carrying >10 kb long *VSG2*-marked telomere) or for 15 weeks (carrying <1 kb *VSG2*-marked telomere). The rRNA precursor is shown as a loading control. (B) Slot blot analysis to determine the amount of TERRA in wild type cells and *Tb*TRDKO cells. Tubulin is probed as an internal loading control. The quantification result is shown below the slot blot. TERRA expression level is calculated as percent of that in wild-type cells (BF WT). All samples are normalized against the tubulin hybridization signal. (C) Quantitative RT-PCR was performed to measure steady state mRNA levels of various *VSGs* in *Tb*TRDKO

cells cultured for 2 or 15 weeks. *VSG* mRNA levels in wild type cells are used as the normalization standard and are set to 1 (not shown in the figure). Fold difference in mRNA levels compared to wild type cells are calculated from three independent experiments. Tubulin mRNA amount was used as an internal loading control.

We collected RNA from all these cell lines and performed northern blot analysis to determine the size distribution of TERRA molecules. RNA samples were separated by agarose gel electrophoresis followed by in gel hybridization with radioactively labeled (*CCCTAA)$_{133}$ probe (figure 6-7A). TERRA sizes range from 1.0 to 10 kb in both wild type BF cells and *Tb*TRDKO cells cultured for only 2 weeks, indicating that TERRA is not affected by the telomerase null background *per se*. However, in *Tb*TRDKO cells cultured for 15 weeks that carry the short (<1 kb) active *VSG2*-marked telomere, TERRA size distribution was 2-8 kb. The larger sized (~ 10 kb long) molecules were not observed in these cells, suggesting that shortening of the active *VSG2*-marked telomere affected TERRA size distribution. We did not observe a sharp band of TERRA molecules, suggesting that the mature TERRA may not be processed at precise locations. Importantly, even though equal amount of RNA was loaded for all three lanes (figure 6-7A), the signal for TERRA was the weakest for the *Tb*TRDKO cells cultured for 15 weeks, indicating that the total amount of TERRA transcripts is decreased. We subsequently performed slot blot analysis to better quantify the amount of TERRA transcripts. As seen in figure 6-7B, we observed a more than 70% decrease in the amount of TERRA transcripts when the active telomere is < 1 kb long. This result supports our hypothesis that a significant amount of TERRA is transcribed from the active telomere. However, our probe only

recognizes the telomeric sequence, hence the decrease in northern blot hybridization signal might be just due to the lack of telomeric repetitive sequences in TERRA transcripts rather than indicating a lower level of TERRA expression. Northern analysis using a subtelomeric probe should be able to distinguish between these two scenarios in the future. In either case, our hypothesis that a significant amount of TERRA is contributed by transcription of the active telomere holds true.

We hypothesize that TERRA might be involved in *VSG* silencing regulation. In order to test this possibility we have been trying to achieve knock down of TERRA using RNAi. Despite of using various versions of RNAi constructs we have not yet achieved knockdown of TERRA. Since we observed a decreased TERRA amount in *Tb*TRDKO cells cultured for 15 weeks, we decided to test whether *VSG* silencing was affected in these cells. Total RNA was collected from wild type and *Tb*TRDKO cells cultured for 2 or 15 weeks and subjected to reverse transcription. Quantitative RT-PCR was subsequently performed using *VSG* specific primers to detect steady state mRNA levels of several *VSGs*. Indeed, we observed 3-5 folds of de-repression of silent *VSGs* in *Tb*TRDKO cells cultured for 15 weeks. This result suggests that TERRA is important for *VSG* silencing.

DISCUSSION

Telomere transcription has been recently detected in a number of organisms. However, many facts about TERRA still remain to be discovered. Most importantly, the biological functions of TERRA are not well known. Telomere

transcription in *T. brucei* was discovered long ago. However, no further studies were carried out. Our lab is focused on understanding the regulation of *VSG* silencing in *T. brucei*. In mammalian system TERRA is known to be important for forming heterochromatic region around telomeres, and depletion of TERRA leads to telomere dysfunction (Deng et al. 2009). In *T. brucei VSGs* are expressed from subtelomerically located BESs and it is well established that telomeres play an important role in their regulation (Yang et al. 2009, Benmerzouga et al. 2013, Pandya et al. 2013). Hence, we are interested in determining whether TERRA plays any role in *VSG* silencing regulation.

TERRA RNA size ranges from 0.5 to 10 kb in wild-type BF cells and from 0.5 to 1.5 kb in PF cells. This striking difference between different stages of *T. brucei* life cycle is very interesting and suggests a possible different nature of TERRA transcripts in both forms. In addition, TERRA is mostly transcribed from the C-rich strand in BF cells, but in PF cells both strands appear to be transcribed. At this point it is unclear whether TERRA exists as dsRNA in PF cells. All *VSG*s are silent in PF and a different surface coat composed mainly of procycylins is expressed. This different nature of TERRA transcripts can be due to different roles played by TERRA at life cycle stages. Since the BF form of *T. brucei* is clinically more important, we decided to focus on this stage for further studies.

Telomeric proteins, such as TRF1 and TRF2 interact with TERRA in mammalian cells (Deng et al. 2009). Our preliminary RNA IP results in *T. brucei* showed that *Tb*TRF and *Tb*KU80 interact with TERRA, while *Tb*RAP1 and *Tb*TIF2 do not. Additional controls are needed, such as RNase A treatment

before IP to prove that the signals obtained is solely due to direct interaction between protein and RNA. Although all IP products were treated with DNase I, it will be important to perform DNase I treatment before IP to exclude any DNA-mediated interactions.

We found that depletion of *Tb*RAP1 and *Tb*TRF elevated TERRA levels. Depletion of *Tb*TIF2, on other hand, did not significantly affect TERRA levels. However, it seems that TERRA levels are high even before *Tb*TIF2 RNAi induction (figure 6-3 B lane 5), suggesting that there might be leaky expression of *Tb*TIF2 RNAi in this cell line. Different clones will be used in future analysis to determine whether *Tb*TIF2 plays any role in regulation of TERRA. Effects of *Tb*RAP1 and *Tb*TRF depletion on TERRA levels were different (~10 and ~5 fold increase, respectively) even though both proteins were knocked-down at similar levels. From IP results we know that *Tb*TRF interacts with TERRA while *Tb*RAP1 does not. *Tb*RAP1 depletion in BF cells leads to de-repression of silent subtelomeric *VSGs,* while *Tb*TRF does not affect BES-linked *VSG* silencing. Therefore, *Tb*RAP1 and *Tb*TRF probably regulate TERRA levels through different pathways. Our previous studies suggest that *Tb*RAP1 may affect transcription elongation along silent BESs and therefore affect *VSG* silencing. It is possible that *Tb*RAP1 regulates TERRA expression in a similar way. *Tb*TRF, on the other hand, may play a post-transcriptional role in maintaining stability of TERRA transcripts.

TERRA transcription in *T. brucei* is not sensitive to α-aminitin treatment (Rudenko & Ploeg 1989), suggesting that it is not transcribed by RNA

polymerase II or III. BESs are located at subtelomeres in *T. brucei* and are transcribed at very high level by RNA polymerase I. We hypothesize that TERRA might result from transcription read through of the active BES-marked telomere. Indeed, RT-PCR analysis suggests that a significant amount of TERRA is transcribed from the active BES-marked telomeres. It is possible that TERRA might be transcribed from other telomeres as well. Metacyclic *VSGs* in *T. brucei* are transcribed from monocistronic transcription units (MES) located at subtelomeres. We will perform RT-PCR analysis to test whether TERRA can be transcribed from these MES-marked telomeres. However, our current knowledge does not allow us to test transcription from telomeres unmarked by any *VSG* transcription unit.

We have taken an independent approach to prove that TERRA is mostly contributed by transcription of the active telomere. We obtained a *Tb*TR deletion cell line carrying only the shortened active telomere and long bulk telomeres. Northern analysis showed that TERRA size distribution was affected and longer transcripts were absent in the cells carrying a shortened active telomere. We did not observe a sharp band of TERRA RNA product even through the active telomere has precise size in the clonal population, suggesting that trans-splicing of TERRA may not occur at a precise location. Importantly, in the cells carrying a shortened active BES-marked telomere, the TERRA levels were significantly reduced and several silent *VSGs* were mildly de-repressed. It is possible that such derepression of silent BESs might lead to transcription of TERRA from these previously silent telomeres. Strikingly, the *VSG* de-repression phenotype

was very interesting, as it suggests that TERRA can influence *VSG* silencing and that its levels are regulated in wild type cells. Depletion of TERRA in the future would help to confirm this function of TERRA in *T. brucei*.

CHPATER VII

SUMMARY AND FUTURE PERSPECTIVES

Roles of TbRAP1 in VSG silencing

Telomeres play an important role in *VSG* silencing. *Tb*RAP1, a telomeric protein was previously identified to regulate ES-linked *VSG* silencing in BF cells (Yang et al. 2009). We further established that *Tb*RAP1 also regulates ES-linked *VSG* silencing in PF cells (where essentially all *VSGs* are silent). *Tb*RAP1 is an essential protein and its depletion affects cell growth in the PF stage. Metacyclic *VSGs* are kept silent at BF and PF stages. So far, not much is known about its regulation. We determined that *Tb*RAP1 is required for *mVSG* silencing at both BF and PF stage. The strength of the *Tb*RAP1 mediated *VSG* silencing is stronger in PF cells compared to that in the BF cells. This is likely due to the fact that BF cells need to switch their active *VSG* regularly and, hence, *VSGs* might be less tightly regulated. On the contrary, in PF cells expression of *VSGs* is detrimental for the parasite survival and hence a stronger regulation is required. Interestingly, *Tb*RAP1 regulates *VSG* silencing at the PF stage through chromatin remodeling. .

Depletion of *Tb*RAP1 in PF cells led to more opened chromatin structure at ES-linked *VSGs*, *mVSGs,* and minichromosome *VSGs*. However, no significant change in chromatin structure was detected in BF cells. This interesting contradiction in mechanisms gives rise to several interesting models (discussed in Chapter III). One possible reason is the presence of additional regulatory mechanisms in BF cells. In the future, simultaneous depletion of *Tb*RAP1 and histone H1 or base J can be preformed to determine whether there is any additional effects on *VSG* transcription and chromatin structure.

*Tb*RAP1 was found to associate preferentially with silent ES-marked telomeres compared to the active ES-linked telomere in BF cells. Although the data are preliminary, they provide some interesting insights into the mechanism of *Tb*RAP1 mediated *VSG* silencing. *Tb*RAP1 needs to be physically bound to the chromatin to carry out its nearby gene silencing. Several studies suggest that epigenetic regulation is involved in *VSG* silencing. Previously, it was established that depletion of *Tb*Sir2rp1 (yeast Sir2 homolog) affected subtelomeric silencing without affecting *VSG* transcription (Alsford et al. 2007). In contrast, depletion of histone deacetylase DAC3 affected ES promoter transcription (Wang et al. 2010). Finally, depletion of histone methyltransferase Dot1B affected *VSG* expression mildly (Figueiredo et al. 2008). Interestingly, unlike the mammalian and yeast homologues, *T. brucei* Dot1b lacks a chromatin-binding domain, suggesting an additional player is required for its recruitment to the chromatin (Frederiks et al. 2010). It is interesting to propose that *Tb*RAP1 may recruit these factors to regulate *VSG* silencing. In the future, Co-Immunoprecipitation can be

performed to determine whether *Tb*RAP1 interacts with these factors. Upon *Tb*RAP1 knockdown, the derepressed *VSGs* are expressed at a level that is still 100 – 1,000 fold lower than that of the active *VSG*. Simultaneous depletion of *Tb*RAP1 and these factors can be carried out to determine whether there is any additional effect on *VSG* expression.

It will be crucial to determine how *Tb*RAP1 is recruited to the telomere, knowing that *Tb*RAP1 regulates *VSG* silencing and that it is preferentially bound to the silent ES-linked telomeres. It is thought so far that *Tb*TRF recruits *Tb*RAP1 to the telomere. No direct telomere DNA binding activity of *Tb*RAP1 was observed by EMSA. However, further experiments are required to confirm this finding. Interestingly, unlike *Tb*RAP1, *Tb*TRF did not show preferential binding to the ES-linked telomeres, suggesting that *Tb*RAP1 might be recruited to telomeres through an additional factor. Another piece of evidence comes from a very preliminary work, where depletion of *Tb*TRF did not affect the binding of *Tb*RAP1 to the telomere (data not shown). Instead, in a few cases, increased binding for *Tb*RAP1 to the telomeres was observed upon *Tb*TRF depletion. This not only suggests that *Tb*RAP1 has a *Tb*TRF-independent mode of recruitment but also suggests that *Tb*TRF and *Tb*RAP1 likely compete with each other for telomere binding. Previous work in our lab by Dr. Yang found that *Tb*RAP1 can co-immunoprecipitate with histones. It is possible that *Tb*TRF might still be a primary means for *Tb*RAP1 recruitment to the telomere. However, *Tb*RAP1 might also interact with histones or additional factors to be targeted to silent ES-linked telomeres. The *Tb*TRFH domain in *Tb*TRF is known to interact with *Tb*RAP1. We

have established several *Tb*TRFH mutants (discussed in Chapter V). Analyzing loss of interaction mutants *in vivo* can further shed light on recruitment of *Tb*RAP1 to the telomere.

*Tb*RAP1 was found to be important for maintaining telomere G-overhang length. Depletion of *Tb*RAP1 led to a decrease in G-overhangs signal when analyzed by in-gel native hybridization. It is known that in mammalian cells, DNA damage at telomeres results in reduced histone biosynthesis (Sullivan et al. 2010). Additionally, in budding yeast it was found that during senescence (due to telomere shortening), *Sc*RAP1 binds to the promoters of core-histone encoding genes and repress their transcription (Platt et al. 2013). We wanted to test whether histone levels were affected upon *Tb*RAP1 depletion.

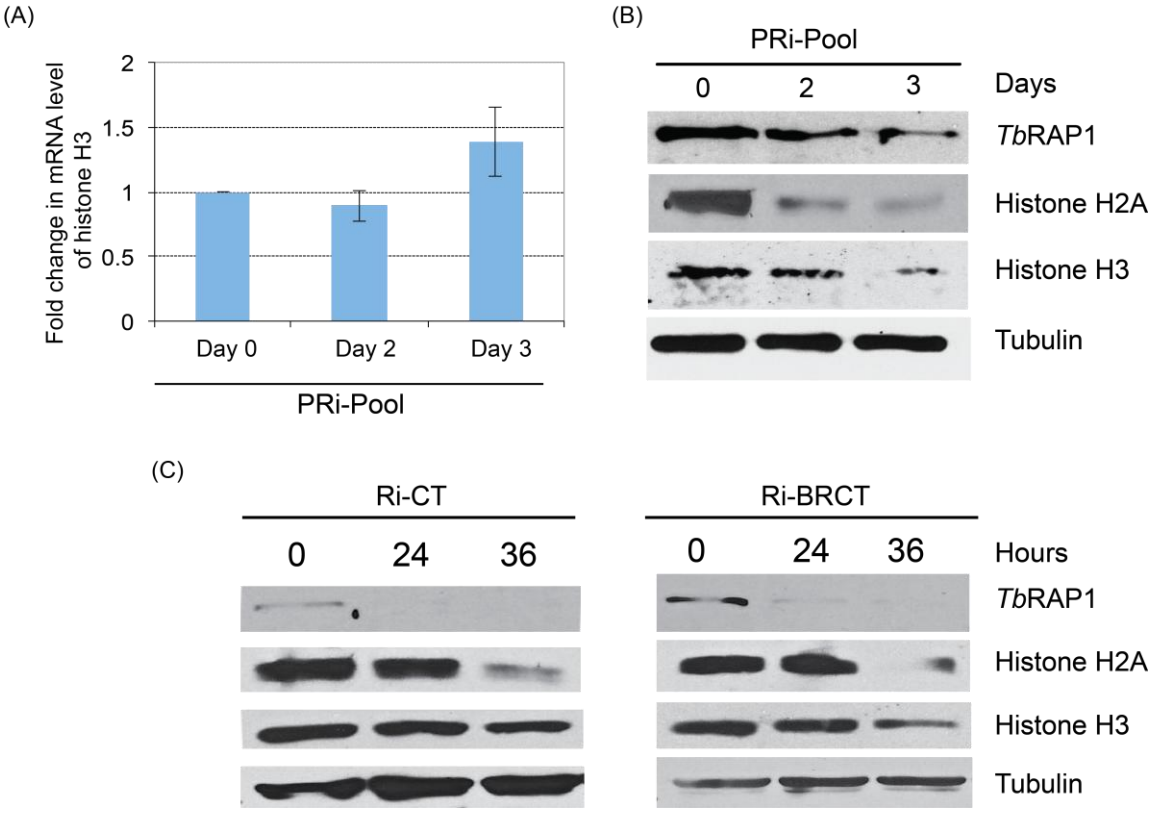

Figure 7-1: Histone levels upon *Tb*RAP1 depletion. (A) RT-PCR analysis was performed to measure steady state mRNA levels of histone H3 before (day 0) and after (day 2 and 3) depletion of *Tb*RAP1 in PRi-pool cells (PF). Fold change in mRNA level was calculated compared to day 0 whose value was arbitrarily set to 1.Total cell lysate was collected before and after depletion of *Tb*RAP1 in (B) PRi-pool (PF), (C) Ri-CT and Ri-BRCT (BF) cells. Levels of histone H2A and histone H3 was determined by western analysis using antibodies specific to histone H2A and H3.

We determined whether *Tb*RAP1 depletion affected levels of histones in PF and BF cells. No change in mRNA levels of histone H3 was observed upon depletion of *Tb*RAP1 in PF cells (figure 7-1 A). However, the protein levels of core histones H2A and H3 were decreased upon depletion of *Tb*RAP1 in both PF and BF cells (figure 7-1 B and C). The decrease in the levels of histone protein was similar to that of the *Tb*RAP1 protein in PF cells (figure 7-1 B, day 2) possibly explaining the loosening of chromatin structure observed upon *Tb*RAP1 depletion. However, in BF cells the depletion of histones was observed at much later stage after *Tb*RAP1 depletion (figure 7-1 C, 24 and 36 hours). We know that even at later stages the chromatin structure in BF cells remains unaffected even though the total histone protein level decreased. However, we only analyzed ES loci during FAIRE experiments and it is possible that its chromatin compaction may still remain unaffected. Another possible reason might be due to the presence of linker histone H1, which is known to form a higher order chromatin structure. Depletion of histone H1 affects chromatin structure only in BF cells, suggesting its role in maintaining higher order chromatin compaction at this stage (Povelones et al. 2012). Western blot analysis could not differentiate between the nucleosome bound versus the nucleosome free fraction of histone proteins. Hence it is not clear at this moment that the decline observed is in free fraction or nucleosome bound fraction or both. Also, *T. brucei* histones are very divergent hence; due to lack of specific antibodies it is not feasible at this time to test levels of all histone proteins or specifically modified histones. *Tb*RAP1 depletion leads to cell growth arrest in PF and BF cells. Is there a DNA damage response? Is the

depletion of levels in histone due to trigger of such pathways and is it related to growth arrest? If so can histones (being highly divergent) be used as a drug target? These are few interesting questions that to be answered need further research in the future.

TbTRF and its role at telomeres

*Tb*TRF directly binds to telomeric DNA (Li et al 2005). The homodimerization domain of *Tb*TRF is required for self-dimerization of *Tb*TRF as well as for interaction with other telomeric proteins, such as *Tb*RAP1 and *Tb*TIF2. We speculate that *Tb*TRF acts at the center of the telomeric complex and holds the entire complex together. Depletion of *Tb*TRF leads to very acute growth arrest (Li et al. 2005), making it impossible to elucidate all of its function in telomere end protection. We established seven *Tb*TRFH domain mutants and tested their interaction with wild-type *Tb*TRF and mutant *Tb*TRF *in vitro*. We determined the helices required for *Tb*TRF homodimerization function. In the future, these mutants can be utilized to determine critical helices required for interaction with other telomeric proteins. Loss of interaction mutants can then be introduced *in vivo* to study the role of *Tb*TRF in telomere complex maintenance and telomere protection.

Depletion of *Tb*TRF does not lead to ES-linked *VSG* derepression in BF and PF cells (Li et al. 2005). For *VSG* derepression to occur, a certain level of functional transcription machinery is required in the cell. *Tb*TRF depletion had a very acute growth arrest and it is possible that due to disruption of the whole telomeric complex and trigger of DNA damage response we do not observe *VSG*

derepression. However, *Tb*TRF being directly bound to telomeric DNA we wanted to determine whether it has any role in chromatin remodeling at telomeres. Depletion of *Tb*TRF led to more opened chromatin structure at ES-linked *VSGs* in PF but not BF cells. *Tb*TRF depletion did not affect transcription of *mVSGs,* however, loosening of chromatin structure was observed at *mVSGs* in PF cells. These results collectively suggest that *Tb*TRF possesses the ability to modulate chromatin at telomeres. In the future, mutants of *Tb*TRF can be utilized to study its role in regulating *VSG* silencing.

TERRA and its function in antigenic variation

Telomeres are transcribed into long non-coding RNA called TERRA. TERRA was reported in *T. brucei* in 1989 but no further characterization was performed (Rudenko and Ploeg 1989). With increasing knowledge of TERRA function in telomere regulation, we decided to characterize it and to determine whether it plays any role in antigenic variation. We characterized that TERRA is transcribed from the C-rich strand in BF cells and from both strands in PF cells. RNA-IP determined that TERRA interacts with *Tb*TRF and *Tb*KU80, but not with *Tb*RAP1 and *Tb*TIF2, suggesting that TERRA might be associated to telomeres through the telomeric complex. However, its association with telomeres *in vivo* needs to be determined.

Telomeric protein *Tb*RAP1 and *Tb*TRF regulates TERRA transcription and their depletion leads to elevated levels of TERRA, suggesting that telomeric complex regulates TERRA expression. Elevated or deregulated TERRA transcription is known to induce telomere shortening in yeast (Sandell et al. 1994,

Maicher et al. 2012). Hence, it is very important to regulate its level *in vivo* and it seems that in *T. brucei* telomeric complex is one of the key regulators of TERRA transcription. By performing PCR analysis we determined that within ES-linked telomeres, TERRA is transcribed from active ES. This result correlates with the high RNA Pol I mediated transcription of active ES. Most interestingly, shortening of the active ES-linked telomeres led to a significant decrease in the amount of TERRA molecules and mild derepression of silent ES-linked *VSGs*. Thus, we hypothesize that TERRA plays a role in antigenic variation and it regulates *VSG* silencing at least in BF cells. However, to confirm its role in *VSG* silencing and to study its function in PF cells, it is critical to achieve knockdown of TERRA. So far, all the efforts to knockdown TERRA by RNAi have been fruitless and all the strategies employed were unsuccessful. In the future alternative strategies need to be employed to achieve knock down of TERRA molecules.

The work performed in this thesis collectively determined that telomeres are a key regulator of antigenic variation in *T. brucei*. We have further contributed to the understanding of pathogenesis of *T. brucei.* This knowledge can be applied towards the eradication of this parasite in the future.

BIBLIOGRAPHY

Alarcon, C. M., Son, H. J., Hall, T., & Donelson, J. E. (1994). A monocistronic transcript for a trypanosome variant surface glycoprotein. *Mol Cell Biol, 14*(8), 5579-5591.

Alsford, S., & Horn, D. (2012). Cell-cycle-regulated control of VSG expression site silencing by histones and histone chaperones ASF1A and CAF-1b in Trypanosoma brucei. *Nucleic Acids Res, 40*(20), 10150-10160. doi: 10.1093/nar/gks813

Alsford, S., Kawahara, T., Isamah, C., & Horn, D. (2007). A sirtuin in the African trypanosome is involved in both DNA repair and telomeric gene silencing but is not required for antigenic variation. *Mol Microbiol, 63*(3), 724-736. doi: 10.1111/j.1365-2958.2006.05553.x

Alsford, S., Wickstead, B., Ersfeld, K., & Gull, K. (2001). Diversity and dynamics of the minichromosomal karyotype in Trypanosoma brucei. *Mol Biochem Parasitol, 113*(1), 79-88.

Atouguia, J.L.M. & Kennedy, P.G.E. (2000) Neurological aspects of human African trypanosomiasis. In Infectious diseases of the nervous system [L.E. Davis & P.G.E. Kennedy (eds.)]. Butterworth-Heinemann. Oxford, United Kingdom. 321– 372.

Azzalin, C. M., & Lingner, J. (2008). Telomeres: the silence is broken. *Cell Cycle, 7*(9), 1161-1165.

Azzalin, C. M., Reichenbach, P., Khoriauli, L., Giulotto, E., & Lingner, J. (2007). Telomeric repeat containing RNA and RNA surveillance factors at mammalian chromosome ends. *Science, 318*(5851), 798-801. doi: 10.1126/science.1147182

Bae, N. S., & Baumann, P. (2007). A RAP1/TRF2 complex inhibits nonhomologous end-joining at human telomeric DNA ends. *Mol Cell, 26*(3), 323-334. doi: 10.1016/j.molcel.2007.03.023

Bah, A., Wischnewski, H., Shchepachev, V., & Azzalin, C. M. (2012). The telomeric transcriptome of Schizosaccharomyces pombe. *Nucleic Acids Res, 40*(7), 2995-3005. doi: 10.1093/nar/gkr1153

Baker, A. M., Fu, Q., Hayward, W., Lindsay, S. M., & Fletcher, T. M. (2009). The Myb/SANT domain of the telomere-binding protein TRF2 alters chromatin structure *Nucleic Acids Res* (2009/06/18 ed., Vol. 37, pp. 5019-5031).

Baker, A. M., Fu, Q., Hayward, W., Victoria, S., Pedroso, I. M., Lindsay, S. M., & Fletcher, T. M. (2011). The telomere binding protein TRF2 induces chromatin compaction. *PLoS One, 6*(4), e19124. doi: 10.1371/journal.pone.0019124

Balk, B., Maicher, A., Dees, M., Klermund, J., Luke-Glaser, S., Bender, K., & Luke, B. (2013). Telomeric RNA-DNA hybrids affect telomere-length dynamics and senescence. *Nat Struct Mol Biol, 20*(10), 1199-1205. doi: 10.1038/nsmb.2662

Barnes, R. L., & McCulloch, R. (2007). Trypanosoma brucei homologous recombination is dependent on substrate length and homology, though displays a differential dependence on mismatch repair as substrate length decreases. *Nucleic Acids Res, 35*(10), 3478-3493. doi: 10.1093/nar/gkm249

Barry, J. D., Graham, S. V., Fotheringham, M., Graham, V. S., Kobryn, K., & Wymer, B. (1998). VSG gene control and infectivity strategy of metacyclic stage Trypanosoma brucei. *Mol Biochem Parasitol, 91*(1), 93-105.

Barry, J. D., Marcello, L., Morrison, L. J., Read, A. F., Lythgoe, K., Jones, N., . . . Berriman, M. (2005). What the genome sequence is revealing about trypanosome antigenic variation. *Biochem Soc Trans, 33*(Pt 5), 986-989. doi: 10.1042/BST20050986

Barry, J. D., & McCulloch, R. (2001). Antigenic variation in trypanosomes: enhanced phenotypic variation in a eukaryotic parasite. *Adv Parasitol, 49*, 1-70.

Baur, J. A., Zou, Y., Shay, J. W., & Wright, W. E. (2001). Telomere position effect in human cells. *Science, 292*(5524), 2075-2077. doi: 10.1126/science.1062329

Benetti, R., Garcia-Cao, M., & Blasco, M. A. (2007). Telomere length regulates the epigenetic status of mammalian telomeres and subtelomeres. *Nat Genet, 39*(2), 243-250. doi: 10.1038/ng1952

Benetti, R., Schoeftner, S., Munoz, P., & Blasco, M. A. (2008). Role of TRF2 in the assembly of telomeric chromatin. *Cell Cycle, 7*(21), 3461-3468.

Benmerzouga, I., Concepcion-Acevedo, J., Kim, H. S., Vandoros, A. V., Cross, G. A., Klingbeil, M. M., & Li, B. (2013). Trypanosoma brucei Orc1 is essential for nuclear DNA replication and affects both VSG silencing and VSG switching. *Mol Microbiol, 87*(1), 196-210. doi: 10.1111/mmi.12093

Bernards, A., Michels, P. A., Lincke, C. R., & Borst, P. (1983). Growth of chromosome ends in multiplying trypanosomes. *Nature, 303*(5918), 592-597.

Berriman, M., Ghedin, E., Hertz-Fowler, C., Blandin, G., Renauld, H., Bartholomeu, D. C., . . . El-Sayed, N. M. (2005). The genome of the African trypanosome Trypanosoma brucei. *Science, 309*(5733), 416-422. doi: 10.1126/science.1112642

Berriman, M., Hall, N., Sheader, K., Bringaud, F., Tiwari, B., Isobe, T., . . . Rudenko, G. (2002). The architecture of variant surface glycoprotein gene expression sites in Trypanosoma brucei. *Mol Biochem Parasitol, 122*(2), 131-140.

Bianchi, A., Smith, S., Chong, L., Elias, P., & de Lange, T. (1997). TRF1 is a dimer and bends telomeric DNA. *EMBO J, 16*(7), 1785-1794. doi: 10.1093/emboj/16.7.1785

Blackburn, E. H., & Challoner, P. B. (1984). Identification of a telomeric DNA sequence in Trypanosoma brucei. *Cell, 36*(2), 447-457.

Blum, J., Schmid, C., & Burri, C. (2006). Clinical aspects of 2541 patients with second stage human African trypanosomiasis. *Acta Trop, 97*(1), 55-64. doi: 10.1016/j.actatropica.2005.08.001

Bombarde, O., Boby, C., Gomez, D., Frit, P., Giraud-Panis, M. J., Gilson, E., . . . Calsou, P. (2010). TRF2/RAP1 and DNA-PK mediate a double protection against joining at telomeric ends. *EMBO J, 29*(9), 1573-1584. doi: 10.1038/emboj.2010.49

Bork, P., Hofmann, K., Bucher, P., Neuwald, A. F., Altschul, S. F., & Koonin, E. V. (1997). A superfamily of conserved domains in DNA damage-responsive cell cycle checkpoint proteins. *FASEB J, 11*(1), 68-76.

Borst, P. (1986). Discontinuous transcription and antigenic variation in trypanosomes. *Annu Rev Biochem, 55*, 701-732. doi: 10.1146/annurev.bi.55.070186.003413

Boulton, S. J., & Jackson, S. P. (1998). Components of the Ku-dependent non-homologous end-joining pathway are involved in telomeric length maintenance and telomeric silencing. *EMBO J, 17*(6), 1819-1828. doi: 10.1093/emboj/17.6.1819

Bourns, B. D., Alexander, M. K., Smith, A. M., & Zakian, V. A. (1998). Sir proteins, Rif proteins, and Cdc13p bind Saccharomyces telomeres in vivo. *Mol Cell Biol, 18*(9), 5600-5608.

Broccoli, D., Smogorzewska, A., Chong, L., & de Lange, T. (1997). Human telomeres contain two distinct Myb-related proteins, TRF1 and TRF2. *Nat Genet, 17*(2), 231-235. doi: 10.1038/ng1097-231

Brun, R., Blum, J., Chappuis, F., & Burri, C. (2010). Human African trypanosomiasis. *Lancet, 375*(9709), 148-159. doi: 10.1016/S0140-6736(09)60829-1

Buguet, A., Bisser, S., Josenando, T., Chapotot, F., & Cespuglio, R. (2005). Sleep structure: a new diagnostic tool for stage determination in sleeping sickness. *Acta Trop, 93*(1), 107-117. doi: 10.1016/j.actatropica.2004.10.001

Burri, C., & Brun, R. (2003). Eflornithine for the treatment of human African trypanosomiasis. *Parasitol Res, 90 Supp 1*, S49-52. doi: 10.1007/s00436-002-0766-5

Burton, P., McBride, D. J., Wilkes, J. M., Barry, J. D., & McCulloch, R. (2007). Ku heterodimer-independent end joining in Trypanosoma brucei cell extracts relies upon sequence microhomology. *Eukaryot Cell, 6*(10), 1773-1781. doi: 10.1128/EC.00212-07

Callejas, S., Leech, V., Reitter, C., & Melville, S. (2006). Hemizygous subtelomeres of an African trypanosome chromosome may account for over 75% of chromosome length. *Genome Res, 16*(9), 1109-1118. doi: 10.1101/gr.5147406

Cano, M. I., Dungan, J. M., Agabian, N., & Blackburn, E. H. (1999). Telomerase in kinetoplastid parasitic protozoa. *Proc Natl Acad Sci U S A, 96*(7), 3616-3621.

Capewell, P., Veitch, N. J., Turner, C. M., Raper, J., Berriman, M., Hajduk, S. L., & MacLeod, A. (2011). Differences between Trypanosoma brucei gambiense groups 1 and 2 in their resistance to killing by trypanolytic factor 1. *PLoS Negl Trop Dis, 5*(9), e1287. doi: 10.1371/journal.pntd.0001287

Cesare, A. J., Groff-Vindman, C., Compton, S. A., McEachern, M. J., & Griffith, J. D. (2008). Telomere loops and homologous recombination-dependent telomeric circles in a Kluyveromyces lactis telomere mutant strain. *Mol Cell Biol, 28*(1), 20-29. doi: 10.1128/MCB.01122-07

Cockell, M., Palladino, F., Laroche, T., Kyrion, G., Liu, C., Lustig, A. J., & Gasser, S. M. (1995). The carboxy termini of Sir4 and Rap1 affect Sir3 localization: evidence for a multicomponent complex required for yeast telomeric silencing. *J Cell Biol, 129*(4), 909-924.

Conrad, M. N., Wright, J. H., Wolf, A. J., & Zakian, V. A. (1990). RAP1 protein interacts with yeast telomeres in vivo: overproduction alters telomere structure and decreases chromosome stability. *Cell, 63*(4), 739-750.

. Control and surveillance of African trypanosomiasis. Report of a WHO Expert Committee. (1998) *World Health Organ Tech Rep Ser* (1999/03/10 ed., Vol. 881, pp. I-VI, 1-114).

Conway, C., McCulloch, R., Ginger, M. L., Robinson, N. P., Browitt, A., & Barry, J. D. (2002). Ku is important for telomere maintenance, but not for differential expression of telomeric VSG genes, in African trypanosomes. *J Biol Chem, 277*(24), 21269-21277. doi: 10.1074/jbc.M200550200

Cornelissen, A. W., Bakkeren, G. A., Barry, J. D., Michels, P. A., & Borst, P. (1985). Characteristics of trypanosome variant antigen genes active in the tsetse fly. *Nucleic Acids Res, 13*(13), 4661-4676.

Cross, G. A. (1975). Identification, purification and properties of clone-specific glycoprotein antigens constituting the surface coat of Trypanosoma brucei. *Parasitology, 71*(3), 393-417.

Cusanelli, E., Romero, C. A., & Chartrand, P. (2013). Telomeric noncoding RNA TERRA is induced by telomere shortening to nucleate telomerase molecules at short telomeres. *Mol Cell, 51*(6), 780-791. doi: 10.1016/j.molcel.2013.08.029

De Lange, T., & Borst, P. (1982). Genomic environment of the expression-linked extra copies of genes for surface antigens of Trypanosoma brucei resembles the end of a chromosome. *Nature, 299*(5882), 451-453.

de Lange, T., Shiue, L., Myers, R. M., Cox, D. R., Naylor, S. L., Killery, A. M., & Varmus, H. E. (1990). Structure and variability of human chromosome ends. *Mol Cell Biol, 10*(2), 518-527.

Denchi, E. L., & de Lange, T. (2007). Protection of telomeres through independent control of ATM and ATR by TRF2 and POT1. *Nature, 448*(7157), 1068-1071. doi: 10.1038/nature06065

Deng, X., & Meller, V. H. (2006). Non-coding RNA in fly dosage compensation. *Trends Biochem Sci, 31*(9), 526-532. doi: 10.1016/j.tibs.2006.07.007

Deng, Z., Norseen, J., Wiedmer, A., Riethman, H., & Lieberman, P. M. (2009). TERRA RNA binding to TRF2 facilitates heterochromatin formation and ORC recruitment at telomeres. *Mol Cell, 35*(4), 403-413. doi: 10.1016/j.molcel.2009.06.025

Denninger, V., Fullbrook, A., Bessat, M., Ersfeld, K., & Rudenko, G. (2010). The FACT subunit TbSpt16 is involved in cell cycle specific control of VSG expression sites in Trypanosoma brucei. *Mol Microbiol, 78*(2), 459-474. doi: 10.1111/j.1365-2958.2010.07350.x

Dobson, R., Stockdale, C., Lapsley, C., Wilkes, J., & McCulloch, R. (2011). Interactions among Trypanosoma brucei RAD51 paralogues in DNA repair and antigenic variation. *Mol Microbiol, 81*(2), 434-456. doi: 10.1111/j.1365-2958.2011.07703.x

Doksani, Y., Wu, J. Y., de Lange, T., & Zhuang, X. (2013). Super-resolution fluorescence imaging of telomeres reveals TRF2-dependent T-loop formation. *Cell, 155*(2), 345-356. doi: 10.1016/j.cell.2013.09.048

Dorn, P. L., Aman, R. A., & Boothroyd, J. C. (1991). Inhibition of protein synthesis results in super-induction of procyclin (PARP) RNA levels. *Mol Biochem Parasitol, 44*(1), 133-139.

Dreesen, O., & Cross, G. A. (2006). Consequences of telomere shortening at an active VSG expression site in telomerase-deficient Trypanosoma brucei. *Eukaryot Cell, 5*(12), 2114-2119. doi: 10.1128/EC.00059-06

Dreesen, O., & Cross, G. A. (2008). Telomere length in Trypanosoma brucei. *Exp Parasitol, 118*(1), 103-110. doi: 10.1016/j.exppara.2007.07.016

Dreesen, O., Li, B., & Cross, G. A. (2005). Telomere structure and shortening in telomerase-deficient Trypanosoma brucei. *Nucleic Acids Res, 33*(14), 4536-4543. doi: 10.1093/nar/gki769

Dreesen, O., Li, B., & Cross, G. A. (2007). Telomere structure and function in trypanosomes: a proposal. *Nat Rev Microbiol, 5*(1), 70-75. doi: 10.1038/nrmicro1577

Duraisingh, M. T., Voss, T. S., Marty, A. J., Duffy, M. F., Good, R. T., Thompson, J. K., . . . Cowman, A. F. (2005). Heterochromatin silencing and locus repositioning linked to regulation of virulence genes in Plasmodium falciparum. *Cell, 121*(1), 13-24. doi: 10.1016/j.cell.2005.01.036

Fairall, L., Chapman, L., Moss, H., de Lange, T., & Rhodes, D. (2001). Structure of the TRFH dimerization domain of the human telomeric proteins TRF1 and TRF2. *Mol Cell, 8*(2), 351-361.

Fairlamb, A. H. (2003). Chemotherapy of human African trypanosomiasis: current and future prospects. *Trends Parasitol, 19*(11), 488-494.

Fairlamb, A. H., Henderson, G. B., & Cerami, A. (1989). Trypanothione is the primary target for arsenical drugs against African trypanosomes. *Proc Natl Acad Sci U S A, 86*(8), 2607-2611.

Ferguson, M. A. (1999). The structure, biosynthesis and functions of glycosylphosphatidylinositol anchors, and the contributions of trypanosome research. *J Cell Sci, 112 (Pt 17)*, 2799-2809.

Figueiredo, L. M., & Cross, G. A. (2010). Nucleosomes are depleted at the VSG expression site transcribed by RNA polymerase I in African trypanosomes. *Eukaryot Cell, 9*(1), 148-154. doi: 10.1128/EC.00282-09

Figueiredo, L. M., Janzen, C. J., & Cross, G. A. (2008). A histone methyltransferase modulates antigenic variation in African trypanosomes. *PLoS Biol, 6*(7), e161. doi: 10.1371/journal.pbio.0060161

Frederiks, F., van Welsem, T., Oudgenoeg, G., Heck, A. J., Janzen, C. J., & van Leeuwen, F. (2010). Heterologous expression reveals distinct enzymatic activities of two DOT1 histone methyltransferases of Trypanosoma brucei. *J Cell Sci, 123*(Pt 23), 4019-4023. doi: 10.1242/jcs.073882

Freitas-Junior, L. H., Hernandez-Rivas, R., Ralph, S. A., Montiel-Condado, D., Ruvalcaba-Salazar, O. K., Rojas-Meza, A. P., . . . Scherf, A. (2005). Telomeric heterochromatin propagation and histone acetylation control mutually exclusive expression of antigenic variation genes in malaria parasites. *Cell, 121*(1), 25-36. doi: 10.1016/j.cell.2005.01.037

Galati, A., Magdinier, F., Colasanti, V., Bauwens, S., Pinte, S., Ricordy, R., . . . Gilson, E. (2012). TRF2 controls telomeric nucleosome organization in a cell

cycle phase-dependent manner. *PLoS One, 7*(4), e34386. doi: 10.1371/journal.pone.0034386

Galati, A., Rossetti, L., Pisano, S., Chapman, L., Rhodes, D., Savino, M., & Cacchione, S. (2006). The human telomeric protein TRF1 specifically recognizes nucleosomal binding sites and alters nucleosome structure. *J Mol Biol, 360*(2), 377-385. doi: 10.1016/j.jmb.2006.04.071

Ganapathi, M., Palumbo, M. J., Ansari, S. A., He, Q., Tsui, K., Nislow, C., & Morse, R. H. (2011). Extensive role of the general regulatory factors, Abf1 and Rap1, in determining genome-wide chromatin structure in budding yeast. *Nucleic Acids Res, 39*(6), 2032-2044. doi: 10.1093/nar/gkq1161

Garcia-Salcedo, J. A., Gijon, P., Nolan, D. P., Tebabi, P., & Pays, E. (2003). A chromosomal SIR2 homologue with both histone NAD-dependent ADP-ribosyltransferase and deacetylase activities is involved in DNA repair in Trypanosoma brucei. *EMBO J, 22*(21), 5851-5862. doi: 10.1093/emboj/cdg553

Gibson, W. C., & Borst, P. (1986). Size-fractionation of the small chromosomes of Trypanozoon and Nannomonas trypanosomes by pulsed field gradient gel electrophoresis. *Mol Biochem Parasitol, 18*(2), 127-140.

Ginger, M. L., Blundell, P. A., Lewis, A. M., Browitt, A., Gunzl, A., & Barry, J. D. (2002). Ex vivo and in vitro identification of a consensus promoter for VSG genes expressed by metacyclic-stage trypanosomes in the tsetse fly. *Eukaryot Cell, 1*(6), 1000-1009.

Giresi, P. G., & Lieb, J. D. (2009). Isolation of active regulatory elements from eukaryotic chromatin using FAIRE (Formaldehyde Assisted Isolation of

Regulatory Elements). *Methods, 48*(3), 233-239. doi: 10.1016/j.ymeth.2009.03.003

Glover, L., & Horn, D. (2006). Repression of polymerase I-mediated gene expression at Trypanosoma brucei telomeres. *EMBO Rep, 7*(1), 93-99. doi: 10.1038/sj.embor.7400575

Glover, L., Jun, J., & Horn, D. (2011). Microhomology-mediated deletion and gene conversion in African trypanosomes. *Nucleic Acids Res, 39*(4), 1372-1380. doi: 10.1093/nar/gkq981

Glover, L., McCulloch, R., & Horn, D. (2008). Sequence homology and microhomology dominate chromosomal double-strand break repair in African trypanosomes. *Nucleic Acids Res, 36*(8), 2608-2618. doi: 10.1093/nar/gkn104

Gommers-Ampt, J. H., Van Leeuwen, F., de Beer, A. L., Vliegenthart, J. F., Dizdaroglu, M., Kowalak, J. A., . . . Borst, P. (1993). beta-D-glucosyl-hydroxymethyluracil: a novel modified base present in the DNA of the parasitic protozoan T. brucei. *Cell, 75*(6), 1129-1136.

Gottschling, D. E., Aparicio, O. M., Billington, B. L., & Zakian, V. A. (1990). Position effect at S. cerevisiae telomeres: reversible repression of Pol II transcription. *Cell, 63*(4), 751-762.

Grandin, N., Damon, C., & Charbonneau, M. (2001). Ten1 functions in telomere end protection and length regulation in association with Stn1 and Cdc13. *EMBO J, 20*(5), 1173-1183. doi: 10.1093/emboj/20.5.1173

Grandin, N., Reed, S. I., & Charbonneau, M. (1997). Stn1, a new Saccharomyces cerevisiae protein, is implicated in telomere size regulation in association with Cdc13. *Genes Dev, 11*(4), 512-527.

Gravel, S., Larrivee, M., Labrecque, P., & Wellinger, R. J. (1998). Yeast Ku as a regulator of chromosomal DNA end structure. *Science, 280*(5364), 741-744.

Greenwood, J., & Cooper, J. P. (2012). Non-coding telomeric and subtelomeric transcripts are differentially regulated by telomeric and heterochromatin assembly factors in fission yeast. *Nucleic Acids Res, 40*(7), 2956-2963. doi: 10.1093/nar/gkr1155

Greider, C. W., & Blackburn, E. H. (1987). The telomere terminal transferase of Tetrahymena is a ribonucleoprotein enzyme with two kinds of primer specificity. *Cell, 51*(6), 887-898.

Griffith, J. D., Comeau, L., Rosenfield, S., Stansel, R. M., Bianchi, A., Moss, H., & de Lange, T. (1999). Mammalian telomeres end in a large duplex loop. *Cell, 97*(4), 503-514.

Gruszynski, A. E., van Deursen, F. J., Albareda, M. C., Best, A., Chaudhary, K., Cliffe, L. J., . . . Bangs, J. D. (2006). Regulation of surface coat exchange by differentiating African trypanosomes. *Mol Biochem Parasitol, 147*(2), 211-223. doi: 10.1016/j.molbiopara.2006.02.013

Gunzl, A., Bruderer, T., Laufer, G., Schimanski, B., Tu, L. C., Chung, H. M., . . . Lee, M. G. (2003). RNA polymerase I transcribes procyclin genes and variant surface glycoprotein gene expression sites in Trypanosoma brucei. *Eukaryot Cell, 2*(3), 542-551.

Gupta, S. K., Kolet, L., Doniger, T., Biswas, V. K., Unger, R., Tzfati, Y., & Michaeli, S. (2013). The Trypanosoma brucei telomerase RNA (TER) homologue binds core proteins of the C/D snoRNA family. *FEBS Lett, 587*(9), 1399-1404. doi: 10.1016/j.febslet.2013.03.017

Hardy, C. F., Sussel, L., & Shore, D. (1992). A RAP1-interacting protein involved in transcriptional silencing and telomere length regulation. *Genes Dev, 6*(5), 801-814.

Hartley, C. L., & McCulloch, R. (2008). Trypanosoma brucei BRCA2 acts in antigenic variation and has undergone a recent expansion in BRC repeat number that is important during homologous recombination. *Mol Microbiol, 68*(5), 1237-1251. doi: 10.1111/j.1365-2958.2008.06230.x

Hazelrigg, T., Levis, R., & Rubin, G. M. (1984). Transformation of white locus DNA in drosophila: dosage compensation, zeste interaction, and position effects. *Cell, 36*(2), 469-481.

Hecht, A., Laroche, T., Strahl-Bolsinger, S., Gasser, S. M., & Grunstein, M. (1995). Histone H3 and H4 N-termini interact with SIR3 and SIR4 proteins: a molecular model for the formation of heterochromatin in yeast. *Cell, 80*(4), 583-592.

Hertz-Fowler, C., Figueiredo, L. M., Quail, M. A., Becker, M., Jackson, A., Bason, N.,Berriman, M. (2008). Telomeric expression sites are highly conserved in Trypanosoma brucei. *PLoS One, 3*(10), e3527. doi: 10.1371/journal.pone.0003527

Hockemeyer, D., Sfeir, A. J., Shay, J. W., Wright, W. E., & de Lange, T. (2005). POT1 protects telomeres from a transient DNA damage response and determines how human chromosomes end. *EMBO J, 24*(14), 2667-2678. doi: 10.1038/sj.emboj.7600733

Holmes, P. (2013). Tsetse-transmitted trypanosomes--their biology, disease impact and control. *J Invertebr Pathol, 112 Suppl*, S11-14. doi: 10.1016/j.jip.2012.07.014

Horn, D., & Barry, J. D. (2005). The central roles of telomeres and subtelomeres in antigenic variation in African trypanosomes. *Chromosome Res, 13*(5), 525-533. doi: 10.1007/s10577-005-0991-8

Horn, D., & Cross, G. A. (1995). A developmentally regulated position effect at a telomeric locus in Trypanosoma brucei. *Cell, 83*(4), 555-561.

Horn, D., & McCulloch, R. (2010). Molecular mechanisms underlying the control of antigenic variation in African trypanosomes. *Curr Opin Microbiol, 13*(6), 700-705. doi: 10.1016/j.mib.2010.08.009

Houghtaling, B. R., Cuttonaro, L., Chang, W., & Smith, S. (2004). A dynamic molecular link between the telomere length regulator TRF1 and the chromosome end protector TRF2. *Curr Biol, 14*(18), 1621-1631. doi: 10.1016/j.cub.2004.08.052

Hovel-Miner, G. A., Boothroyd, C. E., Mugnier, M., Dreesen, O., Cross, G. A., & Papavasiliou, F. N. (2012). Telomere length affects the frequency and mechanism of antigenic variation in Trypanosoma brucei. *PLoS Pathog, 8*(8), e1002900. doi: 10.1371/journal.ppat.1002900

Hsu, H. L., Gilley, D., Galande, S. A., Hande, M. P., Allen, B., Kim, S. H., . . . Chen, D. J. (2000). Ku acts in a unique way at the mammalian telomere to prevent end joining. *Genes Dev, 14*(22), 2807-2812.

Hughes, K., Wand, M., Foulston, L., Young, R., Harley, K., Terry, S., . . . Rudenko, G. (2007). A novel ISWI is involved in VSG expression site downregulation in African trypanosomes. *EMBO J, 26*(9), 2400-2410. doi: 10.1038/sj.emboj.7601678

Hughes, T. R., Evans, S. K., Weilbaecher, R. G., & Lundblad, V. (2000). The Est3 protein is a subunit of yeast telomerase. *Curr Biol, 10*(13), 809-812.

Iglesias, N., Redon, S., Pfeiffer, V., Dees, M., Lingner, J., & Luke, B. (2011). Subtelomeric repetitive elements determine TERRA regulation by Rap1/Rif and Rap1/Sir complexes in yeast. *EMBO Rep, 12*(6), 587-593. doi: 10.1038/embor.2011.73

Imai, S., Armstrong, C. M., Kaeberlein, M., & Guarente, L. (2000). Transcriptional silencing and longevity protein Sir2 is an NAD-dependent histone deacetylase. *Nature, 403*(6771), 795-800. doi: 10.1038/35001622

Janzen, C. J., Lander, F., Dreesen, O., & Cross, G. A. (2004). Telomere length regulation and transcriptional silencing in KU80-deficient Trypanosoma brucei. *Nucleic Acids Res, 32*(22), 6575-6584. doi: 10.1093/nar/gkh991

Jehi, S. E., Wu, F., & Li, B. (2014). Trypanosoma brucei TIF2 suppresses VSG switching by maintaining subtelomere stability. *Cell Res,* manuscript accepted.

Kabir, S., Sfeir, A., & de Lange, T. (2010). Taking apart Rap1: an adaptor protein with telomeric and non-telomeric functions. *Cell Cycle, 9*(20), 4061-4067.

Kamper, S. M., & Barbet, A. F. (1992). Surface epitope variation via mosaic gene formation is potential key to long-term survival of Trypanosoma brucei. *Mol Biochem Parasitol, 53*(1-2), 33-44.

Kanoh, J., & Ishikawa, F. (2001). spRap1 and spRif1, recruited to telomeres by Taz1, are essential for telomere function in fission yeast. *Curr Biol, 11*(20), 1624-1630.

Karlseder, J., Broccoli, D., Dai, Y., Hardy, S., & de Lange, T. (1999). p53- and ATM-dependent apoptosis induced by telomeres lacking TRF2. *Science, 283*(5406), 1321-1325.

Kawahara, T., Siegel, T. N., Ingram, A. K., Alsford, S., Cross, G. A., & Horn, D. (2008). Two essential MYST-family proteins display distinct roles in histone H4K10 acetylation and telomeric silencing in trypanosomes. *Mol Microbiol, 69*(4), 1054-1068. doi: 10.1111/j.1365-2958.2008.06346.x

Kennedy, P. G. (2004). Human African trypanosomiasis of the CNS: current issues and challenges. *J Clin Invest, 113*(4), 496-504. doi: 10.1172/JCI21052

Kennedy, P. G. (2006). Diagnostic and neuropathogenesis issues in human African trypanosomiasis. *Int J Parasitol, 36*(5), 505-512. doi: 10.1016/j.ijpara.2006.01.012

Kennedy, P. G. (2007). The Fatal Sleep. Edinburgh, United Kingdom:Luath Press Ltd.

Kennedy, P. G. (2008a). The continuing problem of human African trypanosomiasis (sleeping sickness). *Ann Neurol, 64*(2), 116-126. doi: 10.1002/ana.21429

Kennedy, P. G. (2008b). Diagnosing central nervous system trypanosomiasis: two stage or not to stage? *Trans R Soc Trop Med Hyg, 102*(4), 306-307. doi: 10.1016/j.trstmh.2007.11.011

Kennedy, P. G. (2013). Clinical features, diagnosis, and treatment of human African trypanosomiasis (sleeping sickness). *Lancet Neurol, 12*(2), 186-194. doi: 10.1016/S1474-4422(12)70296-X

Kieft, R., Stephens, N. A., Capewell, P., MacLeod, A., & Hajduk, S. L. (2012). Role of expression site switching in the development of resistance to human Trypanosome Lytic Factor-1 in Trypanosoma brucei brucei. *Mol Biochem Parasitol, 183*(1), 8-14. doi: 10.1016/j.molbiopara.2011.12.004

Kim, H. S., & Cross, G. A. (2010). TOPO3alpha influences antigenic variation by monitoring expression-site-associated VSG switching in Trypanosoma brucei. *PLoS Pathog, 6*(7), e1000992. doi: 10.1371/journal.ppat.1000992

Kim, H. S., & Cross, G. A. (2011). Identification of Trypanosoma brucei RMI1/BLAP75 homologue and its roles in antigenic variation. *PLoS One, 6*(9), e25313. doi: 10.1371/journal.pone.0025313

Kim, H. S., Park, S. H., Gunzl, A., & Cross, G. A. (2013). MCM-BP is required for repression of life-cycle specific genes transcribed by RNA polymerase I in the mammalian infectious form of Trypanosoma brucei. *PLoS One, 8*(2), e57001. doi: 10.1371/journal.pone.0057001

Kim, M. K., Kang, M. R., Nam, H. W., Bae, Y. S., Kim, Y. S., & Chung, I. K. (2008). Regulation of telomeric repeat binding factor 1 binding to telomeres by casein kinase 2-mediated phosphorylation. *J Biol Chem, 283*(20), 14144-14152. doi: 10.1074/jbc.M710065200

Kim, S. H., Kaminker, P., & Campisi, J. (1999). TIN2, a new regulator of telomere length in human cells. *Nat Genet, 23*(4), 405-412. doi: 10.1038/70508

Klobutcher, L. A., Swanton, M. T., Donini, P., & Prescott, D. M. (1981). All gene-sized DNA molecules in four species of hypotrichs have the same terminal sequence and an unusual 3' terminus. *Proc Natl Acad Sci U S A, 78*(5), 3015-3019.

Konig, E., Delius, H., Carrington, M., Williams, R. O., & Roditi, I. (1989). Duplication and transcription of procyclin genes in Trypanosoma brucei. *Nucleic Acids Res, 17*(21), 8727-8739.

Konig, P., Giraldo, R., Chapman, L., & Rhodes, D. (1996). The crystal structure of the DNA-binding domain of yeast RAP1 in complex with telomeric DNA. *Cell, 85*(1), 125-136.

Kooter, J. M., & Borst, P. (1984). Alpha-amanitin-insensitive transcription of variant surface glycoprotein genes provides further evidence for discontinuous transcription in trypanosomes. *Nucleic Acids Res, 12*(24), 9457-9472.

Kooter, J. M., van der Spek, H. J., Wagter, R., d'Oliveira, C. E., van der Hoeven, F., Johnson, P. J., & Borst, P. (1987). The anatomy and transcription of a telomeric expression site for variant-specific surface antigens in T. brucei. *Cell, 51*(2), 261-272.

Kyrion, G., Boakye, K. A., & Lustig, A. J. (1992). C-terminal truncation of RAP1 results in the deregulation of telomere size, stability, and function in Saccharomyces cerevisiae. *Mol Cell Biol, 12*(11), 5159-5173.

Kyrion, G., Liu, K., Liu, C., & Lustig, A. J. (1993). RAP1 and telomere structure regulate telomere position effects in Saccharomyces cerevisiae. *Genes Dev, 7*(7A), 1146-1159.

Laemmli, U. K. (1970). Cleavage of structural proteins during the assembly of the head of bacteriophage T4. *Nature, 227*(5259), 680-685.

Landeira, D., Bart, J. M., Van Tyne, D., & Navarro, M. (2009). Cohesin regulates VSG monoallelic expression in trypanosomes. *J Cell Biol, 186*(2), 243-254. doi: 10.1083/jcb.200902119

Landeira, D., & Navarro, M. (2007). Nuclear repositioning of the VSG promoter during developmental silencing in Trypanosoma brucei. *J Cell Biol, 176*(2), 133-139. doi: 10.1083/jcb.200607174

Legros, D., Evans, S., Maiso, F., Enyaru, J. C., & Mbulamberi, D. (1999). Risk factors for treatment failure after melarsoprol for Trypanosoma brucei gambiense trypanosomiasis in Uganda. *Trans R Soc Trop Med Hyg, 93*(4), 439-442.

Lei, M., Baumann, P., & Cech, T. R. (2002). Cooperative binding of single-stranded telomeric DNA by the Pot1 protein of Schizosaccharomyces pombe. *Biochemistry, 41*(49), 14560-14568.

Lei, M., Podell, E. R., & Cech, T. R. (2004). Structure of human POT1 bound to telomeric single-stranded DNA provides a model for chromosome end-protection. *Nat Struct Mol Biol, 11*(12), 1223-1229. doi: 10.1038/nsmb867

Lenardo, M. J., Rice-Ficht, A. C., Kelly, G., Esser, K. M., & Donelson, J. E. (1984). Characterization of the genes specifying two metacyclic variable antigen types in Trypanosoma brucei rhodesiense. *Proc Natl Acad Sci U S A, 81*(21), 6642-6646.

Li, B., & de Lange, T. (2003). Rap1 affects the length and heterogeneity of human telomeres. *Mol Biol Cell, 14*(12), 5060-5068. doi: 10.1091/mbc.E03-06-0403

Li, B., Espinal, A., & Cross, G. A. (2005). Trypanosome telomeres are protected by a homologue of mammalian TRF2. *Mol Cell Biol, 25*(12), 5011-5021. doi: 10.1128/MCB.25.12.5011-5021.2005

Li, B., Oestreich, S., & de Lange, T. (2000). Identification of human Rap1: implications for telomere evolution. *Cell, 101*(5), 471-483.

Liu, C., Mao, X., & Lustig, A. J. (1994). Mutational analysis defines a C-terminal tail domain of RAP1 essential for Telomeric silencing in Saccharomyces cerevisiae. *Genetics, 138*(4), 1025-1040.

Loayza, D., & De Lange, T. (2003). POT1 as a terminal transducer of TRF1 telomere length control. *Nature, 423*(6943), 1013-1018. doi: 10.1038/nature01688

Loayza, D., Parsons, H., Donigian, J., Hoke, K., & de Lange, T. (2004). DNA binding features of human POT1: a nonamer 5'-TAGGGTTAG-3' minimal binding site, sequence specificity, and internal binding to multimeric sites. *J Biol Chem, 279*(13), 13241-13248. doi: 10.1074/jbc.M312309200

Luke, B., Panza, A., Redon, S., Iglesias, N., Li, Z., & Lingner, J. (2008). The Rat1p 5' to 3' exonuclease degrades telomeric repeat-containing RNA and promotes telomere elongation in Saccharomyces cerevisiae. *Mol Cell, 32*(4), 465-477. doi: 10.1016/j.molcel.2008.10.019

Lustig, A. J., Kurtz, S., & Shore, D. (1990). Involvement of the silencer and UAS binding protein RAP1 in regulation of telomere length. *Science, 250*(4980), 549-553.

Maicher, A., Kastner, L., Dees, M., & Luke, B. (2012). Deregulated telomere transcription causes replication-dependent telomere shortening and promotes cellular senescence. *Nucleic Acids Res, 40*(14), 6649-6659. doi: 10.1093/nar/gks358

Mair, G., Shi, H., Li, H., Djikeng, A., Aviles, H. O., Bishop, J. R., . . . Tschudi, C. (2000). A new twist in trypanosome RNA metabolism: cis-splicing of pre-mRNA. *RNA, 6*(2), 163-169.

Marcand, S., Gilson, E., & Shore, D. (1997). A protein-counting mechanism for telomere length regulation in yeast. *Science, 275*(5302), 986-990.

Marcello, L., & Barry, J. D. (2007). Analysis of the VSG gene silent archive in Trypanosoma brucei reveals that mosaic gene expression is prominent in antigenic variation and is favored by archive substructure. *Genome Res, 17*(9), 1344-1352. doi: 10.1101/gr.6421207

Martinez, P., Thanasoula, M., Carlos, A. R., Gomez-Lopez, G., Tejera, A. M., Schoeftner, S.,Blasco, M. A. (2010). Mammalian Rap1 controls telomere function

and gene expression through binding to telomeric and extratelomeric sites. *Nat Cell Biol, 12*(8), 768-780. doi: 10.1038/ncb2081

Matthews, K. R. (2005). The developmental cell biology of Trypanosoma brucei. *J Cell Sci, 118*(Pt 2), 283-290. doi: 10.1242/jcs.01649

Matthews, K. R., Ellis, J. R., & Paterou, A. (2004). Molecular regulation of the life cycle of African trypanosomes. *Trends Parasitol, 20*(1), 40-47.

McCulloch, R. (2004). Antigenic variation in African trypanosomes: monitoring progress. *Trends Parasitol, 20*(3), 117-121. doi: 10.1016/j.pt.2003.12.004

McCulloch, R., & Barry, J. D. (1999). A role for RAD51 and homologous recombination in Trypanosoma brucei antigenic variation. *Genes Dev, 13*(21), 2875-2888.

McElligott, R., & Wellinger, R. J. (1997). The terminal DNA structure of mammalian chromosomes. *EMBO J, 16*(12), 3705-3714. doi: 10.1093/emboj/16.12.3705

Melville, S. E., Gerrard, C. S., & Blackwell, J. M. (1999). Multiple causes of size variation in the diploid megabase chromosomes of African tyrpanosomes. *Chromosome Res, 7*(3), 191-203.

Melville, S. E., Leech, V., Gerrard, C. S., Tait, A., & Blackwell, J. M. (1998). The molecular karyotype of the megabase chromosomes of Trypanosoma brucei and the assignment of chromosome markers. *Mol Biochem Parasitol, 94*(2), 155-173.

Melville, S. E., Leech, V., Navarro, M., & Cross, G. A. (2000). The molecular karyotype of the megabase chromosomes of Trypanosoma brucei stock 427. *Mol Biochem Parasitol, 111*(2), 261-273.

Mitchell, J. R., Cheng, J., & Collins, K. (1999). A box H/ACA small nucleolar RNA-like domain at the human telomerase RNA 3' end. *Mol Cell Biol, 19*(1), 567-576.

Moazed, D., Kistler, A., Axelrod, A., Rine, J., & Johnson, A. D. (1997). Silent information regulator protein complexes in Saccharomyces cerevisiae: a SIR2/SIR4 complex and evidence for a regulatory domain in SIR4 that inhibits its interaction with SIR3. *Proc Natl Acad Sci U S A, 94*(6), 2186-2191.

Morcillo, G., Barettino, D., Carmona, M. J., Carretero, M. T., & Diez, J. L. (1988). Telomeric DNA sequences differentially activated by heat shock in two Chironomus subspecies. *Chromosoma, 96*(2), 139-144.

Moretti, P., Freeman, K., Coodly, L., & Shore, D. (1994). Evidence that a complex of SIR proteins interacts with the silencer and telomere-binding protein RAP1. *Genes Dev, 8*(19), 2257-2269.

Moretti, P., & Shore, D. (2001). Multiple interactions in Sir protein recruitment by Rap1p at silencers and telomeres in yeast. *Mol Cell Biol, 21*(23), 8082-8094. doi: 10.1128/MCB.21.23.8082-8094.2001

Mowatt, M. R., & Clayton, C. E. (1987). Developmental regulation of a novel repetitive protein of Trypanosoma brucei. *Mol Cell Biol, 7*(8), 2838-2844.

Mowatt, M. R., & Clayton, C. E. (1988). Polymorphism in the procyclic acidic repetitive protein gene family of Trypanosoma brucei. *Mol Cell Biol, 8*(10), 4055-4062.

Moyzis, R. K., Buckingham, J. M., Cram, L. S., Dani, M., Deaven, L. L., Jones, M. D.,Wu, J. R. (1988). A highly conserved repetitive DNA sequence, (TTAGGG)n,

present at the telomeres of human chromosomes. *Proc Natl Acad Sci U S A, 85*(18), 6622-6626.

Mugasa, C. M., Adams, E. R., Boer, K. R., Dyserinck, H. C., Buscher, P., Schallig, H. D., & Leeflang, M. M. (2012). Diagnostic accuracy of molecular amplification tests for human African trypanosomiasis--systematic review. *PLoS Negl Trop Dis, 6*(1), e1438. doi: 10.1371/journal.pntd.0001438

Nakamura, T. M., Morin, G. B., Chapman, K. B., Weinrich, S. L., Andrews, W. H., Lingner, J.,Cech, T. R. (1997). Telomerase catalytic subunit homologs from fission yeast and human. *Science, 277*(5328), 955-959.

Narayanan, M. S., Kushwaha, M., Ersfeld, K., Fullbrook, A., Stanne, T. M., & Rudenko, G. (2011). NLP is a novel transcription regulator involved in VSG expression site control in Trypanosoma brucei. *Nucleic Acids Res, 39*(6), 2018-2031. doi: 10.1093/nar/gkq950

Navarro, M., Cross, G. A., & Wirtz, E. (1999). Trypanosoma brucei variant surface glycoprotein regulation involves coupled activation/inactivation and chromatin remodeling of expression sites. *EMBO J, 18*(8), 2265-2272. doi: 10.1093/emboj/18.8.2265

Navarro, M., & Gull, K. (2001). A pol I transcriptional body associated with VSG mono-allelic expression in Trypanosoma brucei. *Nature, 414*(6865), 759-763. doi: 10.1038/414759a

Negrini, S., Ribaud, V., Bianchi, A., & Shore, D. (2007). DNA breaks are masked by multiple Rap1 binding in yeast: implications for telomere capping and telomerase regulation. *Genes Dev, 21*(3), 292-302. doi: 10.1101/gad.400907

Nergadze, S. G., Farnung, B. O., Wischnewski, H., Khoriauli, L., Vitelli, V., Chawla, R., . . . Azzalin, C. M. (2009). CpG-island promoters drive transcription of human telomeres. *RNA, 15*(12), 2186-2194. doi: 10.1261/rna.1748309

Ng, L. J., Cropley, J. E., Pickett, H. A., Reddel, R. R., & Suter, C. M. (2009). Telomerase activity is associated with an increase in DNA methylation at the proximal subtelomere and a reduction in telomeric transcription. *Nucleic Acids Res, 37*(4), 1152-1159. doi: 10.1093/nar/gkn1030

Nugent, C. I., Hughes, T. R., Lue, N. F., & Lundblad, V. (1996). Cdc13p: a single-strand telomeric DNA-binding protein with a dual role in yeast telomere maintenance. *Science, 274*(5285), 249-252.

O'Sullivan, R. J., Kubicek, S., Schreiber, S. L., & Karlseder, J. (2010). Reduced histone biosynthesis and chromatin changes arising from a damage signal at telomeres. *Nat Struct Mol Biol, 17*(10), 1218-1225. doi: 10.1038/nsmb.1897

Odiit, M., Coleman, P. G., Liu, W. C., McDermott, J. J., Fevre, E. M., Welburn, S. C., & Woolhouse, M. E. (2005). Quantifying the level of under-detection of Trypanosoma brucei rhodesiense sleeping sickness cases. *Trop Med Int Health, 10*(9), 840-849. doi: 10.1111/j.1365-3156.2005.01470.x

Ogawa, Y., Sun, B. K., & Lee, J. T. (2008). Intersection of the RNA interference and X-inactivation pathways. *Science, 320*(5881), 1336-1341. doi: 10.1126/science.1157676

Okamoto, K., & Shinkai, Y. (2009). TRFH domain is critical for TRF1-mediated telomere stabilization. *Cell Struct Funct, 34*(2), 71-76.

Pandey, R. R., Mondal, T., Mohammad, F., Enroth, S., Redrup, L., Komorowski, J.,Kanduri, C. (2008). Kcnq1ot1 antisense noncoding RNA mediates lineage-specific transcriptional silencing through chromatin-level regulation. *Mol Cell, 32*(2), 232-246. doi: 10.1016/j.molcel.2008.08.022

Pandya, U. M., Sandhu, R., & Li, B. (2013). Silencing subtelomeric VSGs by Trypanosoma brucei RAP1 at the insect stage involves chromatin structure changes. *Nucleic Acids Res, 41*(16), 7673-7682. doi: 10.1093/nar/gkt562

Pardo, B., & Marcand, S. (2005). Rap1 prevents telomere fusions by nonhomologous end joining. *EMBO J, 24*(17), 3117-3127. doi: 10.1038/sj.emboj.7600778

Pauler, F. M., Koerner, M. V., & Barlow, D. P. (2007). Silencing by imprinted noncoding RNAs: is transcription the answer? *Trends Genet, 23*(6), 284-292. doi: 10.1016/j.tig.2007.03.018

Payer, B., & Lee, J. T. (2008). X chromosome dosage compensation: how mammals keep the balance. *Annu Rev Genet, 42*, 733-772. doi: 10.1146/annurev.genet.42.110807.091711

Pays, E., Hanocq-Quertier, J., Hanocq, F., Van Assel, S., Nolan, D., & Rolin, S. (1993). Abrupt RNA changes precede the first cell division during the differentiation of Trypanosoma brucei bloodstream forms into procyclic forms in vitro. *Mol Biochem Parasitol, 61*(1), 107-114.

Pays, E., Lips, S., Nolan, D., Vanhamme, L., & Perez-Morga, D. (2001). The VSG expression sites of Trypanosoma brucei: multipurpose tools for the

adaptation of the parasite to mammalian hosts. *Mol Biochem Parasitol, 114*(1), 1-16.

Pays, E., Vanhamme, L., & Perez-Morga, D. (2004). Antigenic variation in Trypanosoma brucei: facts, challenges and mysteries. *Curr Opin Microbiol, 7*(4), 369-374. doi: 10.1016/j.mib.2004.05.001

Pedram, M., Sprung, C. N., Gao, Q., Lo, A. W., Reynolds, G. E., & Murnane, J. P. (2006). Telomere position effect and silencing of transgenes near telomeres in the mouse. *Mol Cell Biol, 26*(5), 1865-1878. doi: 10.1128/MCB.26.5.1865-1878.2006

Platt, J. M., Ryvkin, P., Wanat, J. J., Donahue, G., Ricketts, M. D., Barrett, S. P., Johnson, F. B. (2013). Rap1 relocalization contributes to the chromatin-mediated gene expression profile and pace of cell senescence. *Genes Dev, 27*(12), 1406-1420. doi: 10.1101/gad.218776.113

Polotnianka, R. M., Li, J., & Lustig, A. J. (1998). The yeast Ku heterodimer is essential for protection of the telomere against nucleolytic and recombinational activities. *Curr Biol, 8*(14), 831-834.

Poulet, A., Pisano, S., Faivre-Moskalenko, C., Pei, B., Tauran, Y., Haftek-Terreau, Z., . . . Giraud-Panis, M. J. (2012). The N-terminal domains of TRF1 and TRF2 regulate their ability to condense telomeric DNA. *Nucleic Acids Res, 40*(6), 2566-2576. doi: 10.1093/nar/gkr1116

Proudfoot, C., & McCulloch, R. (2005). Distinct roles for two RAD51-related genes in Trypanosoma brucei antigenic variation. *Nucleic Acids Res, 33*(21), 6906-6919. doi: 10.1093/nar/gki996

Raper, J., Fung, R., Ghiso, J., Nussenzweig, V., & Tomlinson, S. (1999). Characterization of a novel trypanosome lytic factor from human serum. *Infect Immun, 67*(4), 1910-1916.

Reichenbach, P., Hoss, M., Azzalin, C. M., Nabholz, M., Bucher, P., & Lingner, J. (2003). A human homolog of yeast Est1 associates with telomerase and uncaps chromosome ends when overexpressed. *Curr Biol, 13*(7), 568-574.

Rifkin, M. R. (1978). Identification of the trypanocidal factor in normal human serum: high density lipoprotein. *Proc Natl Acad Sci U S A, 75*(7), 3450-3454.

Roditi, I., Furger, A., Ruepp, S., Schurch, N., & Butikofer, P. (1998). Unravelling the procyclin coat of Trypanosoma brucei. *Mol Biochem Parasitol, 91*(1), 117-130.

Roditi, I., Schwarz, H., Pearson, T. W., Beecroft, R. P., Liu, M. K., Richardson, J. P., . . . et al. (1989). Procyclin gene expression and loss of the variant surface glycoprotein during differentiation of Trypanosoma brucei. *J Cell Biol, 108*(2), 737-746.

Rudenko, G. (2011). African trypanosomes: the genome and adaptations for immune evasion. *Essays Biochem, 51*, 47-62. doi: 10.1042/bse0510047

Rudenko, G., & Van der Ploeg, L. H. (1989). Transcription of telomere repeats in protozoa. *EMBO J, 8*(9), 2633-2638.

Ruepp, S., Furger, A., Kurath, U., Renggli, C. K., Hemphill, A., Brun, R., & Roditi, I. (1997). Survival of Trypanosoma brucei in the tsetse fly is enhanced by the expression of specific forms of procyclin. *J Cell Biol, 137*(6), 1369-1379.

Rusche, L. N., Kirchmaier, A. L., & Rine, J. (2002). Ordered nucleation and spreading of silenced chromatin in Saccharomyces cerevisiae. *Mol Biol Cell, 13*(7), 2207-2222. doi: 10.1091/mbc.E02-03-0175

Sandell, L. L., Gottschling, D. E., & Zakian, V. A. (1994). Transcription of a yeast telomere alleviates telomere position effect without affecting chromosome stability. *Proc Natl Acad Sci U S A, 91*(25), 12061-12065.

Sandhu, R., Sanford, S., Basu, S., Park, M., Pandya, U. M., Li, B., & Chakrabarti, K. (2013). A trans-spliced telomerase RNA dictates telomere synthesis in Trypanosoma brucei. *Cell Res, 23*(4), 537-551. doi: 10.1038/cr.2013.35

Sarthy, J., Bae, N. S., Scrafford, J., & Baumann, P. (2009). Human RAP1 inhibits non-homologous end joining at telomeres. *EMBO J, 28*(21), 3390-3399. doi: 10.1038/emboj.2009.275

Schoeftner, S., & Blasco, M. A. (2008). Developmentally regulated transcription of mammalian telomeres by DNA-dependent RNA polymerase II. *Nat Cell Biol, 10*(2), 228-236. doi: 10.1038/ncb1685

Schwede, A., & Carrington, M. (2010). Bloodstream form Trypanosome plasma membrane proteins: antigenic variation and invariant antigens. *Parasitology, 137*(14), 2029-2039. doi: 10.1017/S0031182009992034

Shampay, J., Szostak, J. W., & Blackburn, E. H. (1984). DNA sequences of telomeres maintained in yeast. *Nature, 310*(5973), 154-157.

Shore, D. (1994). RAP1: a protean regulator in yeast. *Trends Genet, 10*(11), 408-412.

Shaw, P. (2004). Economics of African Trypanosomiasis. In: Maudlin I, Holmes PH, Miles MA, editors. The Trypanosomiases. Wallingford, UK: CABI Publishing. 369–402.

Simarro, P. P., Diarra, A., Ruiz Postigo, J. A., Franco, J. R., & Jannin, J. G. (2011). The human African trypanosomiasis control and surveillance programme of the World Health Organization 2000-2009: the way forward. *PLoS Negl Trop Dis, 5*(2), e1007. doi: 10.1371/journal.pntd.0001007

Simarro, P. P., Jannin, J., & Cattand, P. (2008). Eliminating human African trypanosomiasis: where do we stand and what comes next? *PLoS Med, 5*(2), e55. doi: 10.1371/journal.pmed.0050055

Singer, M. S., & Gottschling, D. E. (1994). TLC1: template RNA component of Saccharomyces cerevisiae telomerase. *Science, 266*(5184), 404-409.

Snow, B. E., Erdmann, N., Cruickshank, J., Goldman, H., Gill, R. M., Robinson, M. O., & Harrington, L. (2003). Functional conservation of the telomerase protein Est1p in humans. *Curr Biol, 13*(8), 698-704.

Solovei, I., Gaginskaya, E. R., & Macgregor, H. C. (1994). The arrangement and transcription of telomere DNA sequences at the ends of lampbrush chromosomes of birds. *Chromosome Res, 2*(6), 460-470.

Song, K., Jung, D., Jung, Y., Lee, S. G., & Lee, I. (2000). Interaction of human Ku70 with TRF2. *FEBS Lett, 481*(1), 81-85.

Stanne, T. M., Kushwaha, M., Wand, M., Taylor, J. E., & Rudenko, G. (2011). TbISWI regulates multiple polymerase I (Pol I)-transcribed loci and is present at

Pol II transcription boundaries in Trypanosoma brucei. *Eukaryot Cell, 10*(7), 964-976. doi: 10.1128/EC.05048-11

Stanne, T. M., & Rudenko, G. (2010). Active VSG expression sites in Trypanosoma brucei are depleted of nucleosomes. *Eukaryot Cell, 9*(1), 136-147. doi: 10.1128/EC.00281-09

Takai, H., Smogorzewska, A., & de Lange, T. (2003). DNA damage foci at dysfunctional telomeres. *Curr Biol, 13*(17), 1549-1556.

Teo, H., Ghosh, S., Luesch, H., Ghosh, A., Wong, E. T., Malik, N., . . . Tergaonkar, V. (2010). Telomere-independent Rap1 is an IKK adaptor and regulates NF-kappaB-dependent gene expression. *Nat Cell Biol, 12*(8), 758-767. doi: 10.1038/ncb2080

Truc, P., Lejon, V., Magnus, E., Jamonneau, V., Nangouma, A., Verloo, D., . . . Buscher, P. (2002). Evaluation of the micro-CATT, CATT/Trypanosoma brucei gambiense, and LATEX/T b gambiense methods for serodiagnosis and surveillance of human African trypanosomiasis in West and Central Africa. *Bull World Health Organ, 80*(11), 882-886.

Van der Ploeg, L. H., Cornelissen, A. W., Barry, J. D., & Borst, P. (1984). Chromosomes of kinetoplastida. *EMBO J, 3*(13), 3109-3115.

Van der Ploeg, L. H., Cornelissen, A. W., Michels, P. A., & Borst, P. (1984). Chromosome rearrangements in Trypanosoma brucei. *Cell, 39*(1), 213-221.

van Leeuwen, F., Dirks-Mulder, A., Dirks, R. W., Borst, P., & Gibson, W. (1998). The modified DNA base beta-D-glucosyl-hydroxymethyluracil is not found in the tsetse fly stages of Trypanosoma brucei. *Mol Biochem Parasitol, 94*(1), 127-130.

van Leeuwen, F., Taylor, M. C., Mondragon, A., Moreau, H., Gibson, W., Kieft, R., & Borst, P. (1998). beta-D-glucosyl-hydroxymethyluracil is a conserved DNA modification in kinetoplastid protozoans and is abundant in their telomeres. *Proc Natl Acad Sci U S A, 95*(5), 2366-2371.

van Steensel, B., & de Lange, T. (1997). Control of telomere length by the human telomeric protein TRF1. *Nature, 385*(6618), 740-743. doi: 10.1038/385740a0

van Steensel, B., Smogorzewska, A., & de Lange, T. (1998). TRF2 protects human telomeres from end-to-end fusions. *Cell, 92*(3), 401-413.

Vanhamme, L., Poelvoorde, P., Pays, A., Tebabi, P., Van Xong, H., & Pays, E. (2000). Differential RNA elongation controls the variant surface glycoprotein gene expression sites of Trypanosoma brucei. *Mol Microbiol, 36*(2), 328-340.

Vickerman, K. (1985). Developmental cycles and biology of pathogenic trypanosomes. *Br Med Bull, 41*(2), 105-114.

Vodenicharov, M. D., Laterreur, N., & Wellinger, R. J. (2010). Telomere capping in non-dividing yeast cells requires Yku and Rap1. *EMBO J, 29*(17), 3007-3019. doi: 10.1038/emboj.2010.155

Vojtek, A. B., Hollenberg, S. M., & Cooper, J. A. (1993). Mammalian Ras interacts directly with the serine/threonine kinase Raf. *Cell, 74*(1), 205-214.

Wang, F., Podell, E. R., Zaug, A. J., Yang, Y., Baciu, P., Cech, T. R., & Lei, M. (2007). The POT1-TPP1 telomere complex is a telomerase processivity factor. *Nature, 445*(7127), 506-510. doi: 10.1038/nature05454

Wang, Q. P., Kawahara, T., & Horn, D. (2010). Histone deacetylases play distinct roles in telomeric VSG expression site silencing in African trypanosomes. *Mol Microbiol, 77*(5), 1237-1245. doi: 10.1111/j.1365-2958.2010.07284.x

Weiden, M., Osheim, Y. N., Beyer, A. L., & Van der Ploeg, L. H. (1991). Chromosome structure: DNA nucleotide sequence elements of a subset of the minichromosomes of the protozoan Trypanosoma brucei. *Mol Cell Biol, 11*(8), 3823-3834.

Wickstead, B., Ersfeld, K., & Gull, K. (2004). The small chromosomes of Trypanosoma brucei involved in antigenic variation are constructed around repetitive palindromes. *Genome Res, 14*(6), 1014-1024. doi: 10.1101/gr.2227704

Wirtz, E., Leal, S., Ochatt, C., & Cross, G. A. (1999). A tightly regulated inducible expression system for conditional gene knock-outs and dominant-negative genetics in Trypanosoma brucei. *Mol Biochem Parasitol, 99*(1), 89-101.

Wotton, D., & Shore, D. (1997). A novel Rap1p-interacting factor, Rif2p, cooperates with Rif1p to regulate telomere length in Saccharomyces cerevisiae. *Genes Dev, 11*(6), 748-760.

Xin, H., Liu, D., Wan, M., Safari, A., Kim, H., Sun, W., . . . Songyang, Z. (2007). TPP1 is a homologue of ciliate TEBP-beta and interacts with POT1 to recruit telomerase. *Nature, 445*(7127), 559-562. doi: 10.1038/nature05469

Yang, D., Xiong, Y., Kim, H., He, Q., Li, Y., Chen, R., & Songyang, Z. (2011). Human telomeric proteins occupy selective interstitial sites. *Cell Res, 21*(7), 1013-1027. doi: 10.1038/cr.2011.39

Yang, Q., Zheng, Y. L., & Harris, C. C. (2005). POT1 and TRF2 cooperate to maintain telomeric integrity. *Mol Cell Biol, 25*(3), 1070-1080. doi: 10.1128/MCB.25.3.1070-1080.2005

Yang, X., Figueiredo, L. M., Espinal, A., Okubo, E., & Li, B. (2009). RAP1 is essential for silencing telomeric variant surface glycoprotein genes in Trypanosoma brucei. *Cell, 137*(1), 99-109. doi: 10.1016/j.cell.2009.01.037

Yarragudi, A., Parfrey, L. W., & Morse, R. H. (2007). Genome-wide analysis of transcriptional dependence and probable target sites for Abf1 and Rap1 in Saccharomyces cerevisiae. *Nucleic Acids Res, 35*(1), 193-202. doi: 10.1093/nar/gkl1059

Zhong, Z., Shiue, L., Kaplan, S., & de Lange, T. (1992). A mammalian factor that binds telomeric TTAGGG repeats in vitro. *Mol Cell Biol, 12*(11), 4834-4843.

Zhou, J., Hidaka, K., & Futcher, B. (2000). The Est1 subunit of yeast telomerase binds the Tlc1 telomerase RNA. *Mol Cell Biol, 20*(6), 1947-1955.

Zomerdijk, J. C., Kieft, R., & Borst, P. (1992). A ribosomal RNA gene promoter at the telomere of a mini-chromosome in Trypanosoma brucei. *Nucleic Acids Res, 20*(11), 2725-2734.